SURFACE PROPERTIES AND INTERACTIONS OF
P. AERUGINOSA AND *B. SUBTILIS*
WITH STAINLESS STEEL SS316
AND THEIR RELATION IN BIOFILM DEVELOPMENT

ARDIYAN HARIMAWAN

(*B. Eng (Hons.), ITB; M. Eng, TUT*)

A THESIS SUBMITTED

FOR THE DEGREE OF DOCTOR OF PHILOSOPHY

DEPARTMENT OF CHEMICAL AND BIOMOLECULAR ENGINEERING

NATIONAL UNIVERSITY OF SINGAPORE

2011

ACKNOWLEDGEMENTS

TABLE OF CONTENTS

SUMMARY

Biofilms are ubiquitously found in a broad range of areas, such as in the food, environmental, and biomedical fields. It might be formed and developed in almost every environment when viable microorganism is present. Biofilms can be used for constructive purposes but can also be detrimental, and it estimated to be involved in over 65% of all human bacterial infections and costs industries, cities, and hospitals in excess of $500 billion each year. In this thesis, several issues related to adhesion interactions between bacteria and stainless steel surfaces in biofilm formation are addressed. These include: (i) characterization of biofilm formation using *Pseudomonas aeruginosa* and *Bacillus subtilis* as model organisms which are commonly found in industries, (ii) investigating the adhesion interaction of bacteria on stainless steel surface and its relationship with surface energy and force measurement, (iii) investigating the interaction and influence of spore adhesion to stainless steel on biofilm formation, and (iv) investigating the composition and adhesive properties of extracellular polymeric substances (EPS) produced by *Pseudomonas aeruginosa* and *Bacillus subtilis.*

Both bacterial strains formed biofilms within 24 hours. However, SEM and biofilm dry weight observation showed that biofilm formed by *P. aeruginosa* NRRL-B3509 were denser and formed more rapidly compared to *B. subtilis* NRRL-NRS762. This was due to higher specific growth rate of the former, its lower surface charge, and higher protein accumulation on the surfaces. Since both strains are commonly found in the industries, concerns with biofilm formation would be higher for *P. aeruginosa*, as initial attachment is the crucial step of the biofilm formation. This study also showed the likelihood of *P. aeruginosa* and *B. subtilis* to establish biofilm and become persistent in the environment.

Higher affinity was shown by *P. aeruginosa* when the adhesion force was measured using AFM. These higher forces has been found to be correlated with higher hydrophobicity and lower electrostatic repulsion interactions as explained by physicochemical analyses and DLVO and extended DLVO theories. Higher production of biosurfactant by *P. aeruginosa*, which is common for Gram-negative bacteria, also increases the overall hydrophobicity thus increasing the adhesion of these bacteria on SS316 surfaces.

B. subtilis sporulates under severe environmental conditions, which pose significant impact when biofilm is formed. Physicochemical analyses revealed that *B. subtilis* spores have higher hydrophobicity than the vegetative cells due to significant protein layers on their surfaces. Stronger affinity of *B. subtilis* spores toward SS316 surfaces were also corroborated by force measurement using AFM. The presence of spores during adhesion causes biofilm control to become more problematic due to stronger attachment and its persistence under severe environmental condition.

Elucidation of extracellular polymeric substances (EPS) produced by both bacterial strains during growth and biofilm formation provided further insight on surface properties that influence the adhesion process. It was established that EPS produced by the two different species were chemically dissimilar. More proteinaceous compounds, such as γ-PGA and peptidoglycan, were present or available for interaction in EPS from *B. subtilis*. Conversely, EPS from *P. aeruginosa* were characterized by greater carbohydrate components like lipopolysaccharides, alginate, Pel and Psl polysaccharides. However, the relative proportions of polysaccharides and/or proteins constituents and associated functional group chemistry varied with the growth mode of the bacteria. AFM was then used to probe the adhesive nature of EPS produced by the bacteria by using Single Molecule Force Spectroscopy (SMFS). Comparison of the two bacterial species indicated that the presence of polysaccharides in the EPS layer promoted the adhesion strength of the EPS. Proteins in EPS had lesser adherence effects. On the other hand, comparison of the two growth modes for the same bacterial strain indicated that greater EPS production and enhanced cellular adhesion are associated with biofilm growth.

LIST OF TABLES

LIST OF FIGURES

LIST OF SYMBOLS

A   absorbance

AFM   atomic force microscopy

BATH   bacterial adhesion to hydrocarbon

CAM   contact angle measurement

CFU   colony forming unit

CIP   Cleaning-in-place

DLVO   Derjaquin-Landau-Vervey-Overbeck

E   emulsification index

EPS   extracellular polymeric substances

FTIR   Fourier-transform-infra red

GPC   gel permeation chromatography

H   separation distance between cell and surface

MALDI-   matrix-assisted laser desorption ionization time-of-flight mass
TOF-MS   spectroscopy

OD   optical density

PBS   phosphate buffer saline

PUM   phosphate-urea-manganese

R   hydrodynamic radius

SAT   salt aggregation test

SEM   scanning electron microscopy

SMFS   single-molecule force spectroscopy

XPS   x-ray photoelectron spectroscopy

λ decay length pertaining to water molecule

A_{123} effective Hamaker constant for the system contains bacteria (1), surface (2), and medium (3)

l_0 minimum equilibrium distance between two parallel flat layers

γ_L surface tension of the liquid

γ_S surface energy of the solid

γ_{SL} solid/liquid interfacial energy

γ_i surface energy

γ_i^- electron donor sub-component of surface energy

γ_i^+ electron acceptor sub-component of surface energy

γ_i^{AB} Lewis acid-base polar component

γ_i^{LW} Lifshitz-van der Waals apolar component of surface energy

ΔG_{13} absolute hydrophobicity based on surface energy

ΔG^{AB} interaction energy of Lewis Acid-Base

ΔG^{BR} interaction energy of bacteria due to Brownian motion

ΔG^{EL} interaction energy of electrostatic double layer

ΔG^{LW} interaction energy of Lifshitz-van der Waals

ΔG^{TOT} total free interaction energy

ε electrical permittivity of the medium

κ Debye-Hûckel parameter

φ electrical surface potential

CHAPTER 1

INTRODUCTION

1. 1 Background

Reported more than 60 years ago (Zobell, 1943), the field of biofilm continues to be actively studied and researched. Whether useful or problematic, biofilm is ubiquitously found in a broad range of area, such as in food, environmental, and biomedical fields (Simoes et al., 2010). Biofilms might be formed and developed in almost every environment when viable microorganisms are present. A biofilm is defined as a functional consortium of microorganisms attached to a surface and is embedded in the extracellular polymeric substances (EPS) produced by the microorganism (Costerton *et al.*, 1987).

Biofilm formation is a dynamic process and involves a series of steps (Kumar and Anand, 1998). It starts with conditioning of surfaces where nutrients along with the bacteria are absorbed on the surface to form a conditioning film. The process then continues with the adhesion of microorganisms to the conditioned surface. After the microorganisms are firmly attached to the surface, they will grow and divide using the nutrients present in the conditioning film and the surrounding fluid environment. This will lead to the formation of microcolonies when the microorganisms start to produce extracellular polymeric substances (EPS). The continuous attachment of the bacterial cells to the surface and its subsequent growth along with EPS production will form a mature biofilm. As the biofilm ages, the attached bacteria must be able to detach and disperse from the biofilm in order to survive and colonize a new niche.

Biofilms can be used for constructive purposes, such as in water treatment plants, sand filters on the lake or rivers, fermentation, petroleum cleanup in marine

environment, and bioleaching. However, biofilms can also be detrimental. Biofilms in cooling/ heating water systems are known to reduce the heat transfer and operating efficiency (Characklis et al., 1981). Biofilms in marine engineering systems, such as pipelines of the offshore oil and gas industry can lead to substantial corrosion problems. Corrosion is mainly due to abiotic factors; however, at least 20% of corrosion is caused by microorganisms that are attached to the metal subsurface (i.e., microbially-influenced corrosion) (Schwermer et al., 2008). The attachment of the bacteria to food products or food contact surfaces may lead to serious hygienic problems and economic losses due to food spoilage (Poulsen, 1999). In water distribution systems, biofilm formation may not be inhibited by high levels of residual chlorines, and they can increase energy consumption by increasing drag and pump power, mechanical blockage and accelerated corrosion of metal surfaces (Kumar and Anand, 1998). In the medical field, biofilm formation on medical implants is a source of pathogen transfer and subsequent infections (Francolini and Donelli, 2010). Biofilms are estimated to be involved in over 65% of all human bacterial infections and costs industries, cities, and hospitals in excess of $500 billion each year.

Since biofilms are generally considered a major problem in industries, it is important to determine the factors that influence cell adhesion, as it is the most important step on biofilm formation. Factors influencing adhesion can be addressed from different points of view, such as studying the cell-surface interaction during adhesion, elucidating the properties of the cells, and also quantifying the force involved during adhesion. Understanding these factors would provide useful knowledge on the mechanism of cell adhesion to surface. Furthermore, control of biofilms would be more effective when the factors involved during the adhesion are better understood.

Prevention of biofilm formation can be performed by routine cleaning and disinfection. Other preventive strategies attempted to identify materials that do not promote or can even suppress biofilm formation. In food industries, cleaning and disinfection are an essential part of routine production, since the efficiency of these operations will affect the final product. However, disinfectants should be chosen carefully so that they are safe and easy to rinse off, leaving no toxic residues that can affect the product quality. The use of enzyme-based detergents as bio-cleaners can serve as a viable option to overcome biofilm problems in the food industry. Mixtures of enzymes may be necessary for sufficient biofilm degradation. A good understanding of the cell–cell signaling phenomenon (quorum sensing) of bacteria can also be used to control the biofilm formation process by the identification of products that can act as quorum sensing antagonists. This property can lead to the development of new and efficient natural products for biofilm control.

Interaction between the cell and the surface can be described by Derjaquin-Landau-Vervey-Overbeck (DLVO) theory due to their colloidal particle's dimension. This theory accounts for the interaction of two surfaces as sum of three major interactions, which are van der Waals, electrostatic, and acid-base interactions. This theory can be applied to study the interaction between microorganisms and metal surface (van Loosdrecht *et al.*, 1990). In addition to the DLVO interaction, hydrophobicity interaction is also considered an important factor influencing cell adhesion. Microbial surface hydrophobicity has been noted as a dominant factor influencing its adhesion on surfaces. In biological systems, hydrophobic interactions are usually the strongest of all long range non-covalent interactions and can be defined as the attraction between apolar or slightly polar molecules, particles or cells, when immersed in water (Van Oss, 1997).

Properties of microbial cells also hold significant influence on cell adhesion. Some microorganisms such as *Bacillus spp.* form spores on the surface as a dormant mode when encountering harsh environment such as nutrient deprivation or extreme conditions of temperature, pH, and moisture. The spores will germinate when the environment becomes favorable. Bacterial spores are well known to constitute a major problem in food and drug industries (Husmark and Ronner, 1990; Clement et al., 1993). Microorganisms also produce extracellular polymeric substances (EPS). EPS on bacterial surfaces themselves have long been recognized for their roles in mediating cellular recognition and bacterial adhesion (Costerton et al., 1999; Ubbink and Schär-Zammaretti, 2005). Their role in biofilm formation includes inducing genetic changes, enhancing the resilience of cells to antibiotics and disinfectant, and also causing corrosion to surfaces (Abu-Lail and Camesano, 2002).

Cell adhesion on surfaces play a vital role in biofilm development, and understanding the molecular basis of this phenomenon requires knowledge of the molecular interactions at the cell surface. Recently, the use of Atomic Force Microscopy (AFM) has been broadened to elicit information about cell adhesion by measuring the force acting between the AFM tip and a sample, by means of force-distance analysis. This measurement can provide new insights into the structure-function relationship of microbial surfaces and cells-surface interactions.

Force measurements with an AFM tip functionalized with bacterial cells (i.e. a cell probe) allow the probing of interfacial phenomena at the nanoscale, including specific and nonspecific interactions that are involved in the attachment, and molecular recognition events between cell-solid and cell-cell surfaces (Lower et al., 2001; Wright and Armstrong, 2006; Müller and Dufrêne, 2008). AFM cantilevers or tips with a single immobilized microorganism have been used to study a variety of

surfaces (Benoit et al., 2000; Bowen et al., 2001; Sheng et al., 2007). However, the technique utilizing gluteraldehyde has been found to denature the bacterial surface and inactivate cells glued onto the cantilever tip. An improved protocol was recently reported; a bioinspired polydopamine wet adhesive technique was successfully utilized to glue a single cell onto an AFM cantilevers without affecting its viability throughout the duration of force measurement (Kang and Elimelech, 2009).

1. 2 Gaps arising from Previous Study

Many research studies of bacterial biofilms have focused on characterizing the specific interactions during biofilm formation, especially during the adhesion step. A wide range of techniques has been applied to investigate the various stages of biofilm development either in the laboratory or in the field.

However, the majority of the techniques are qualitative and do not reveal the actual interactions that occur between the cells and substrates. Moreover, mechanisms of biofilm formation are not well understood. Hence, in this environment, specific gaps are described below:

1. The mechanism of adhesion interaction involving adhesion forces between bacterial cell and surface is not yet clearly understood. Adhesion forces previously studied were derived from qualitative characterization based on microscopic and spectroscopic study. These studies do not reveal the actual forces between the cell and the substrate

2. While biofilm formed by vegetative cells have been well reported, the adhesion interaction between bacterial spore and metal surface related to biofilm formation remains unexplored. There is currently no publication in this area.

3. Understanding bacterial adhesion to surfaces requires knowledge of EPS produced on the bacterial surface as well as their conformational properties.

Although much progress has been made in elucidating the EPS, their adhesive and conformational properties are poorly understood at the molecular level. Hence, studying their spatial organization and conformational properties at the molecular level remains a challenge.

1. 3 Objectives and Scopes of this Study

The main aim of this study is to investigate the surface properties and the interactions that occur between bacteria (both vegetative cells and spores) and a metal substrate related to the adhesion process during biofilm formation.

The specific objectives of this research were to:

1. Characterize biofilm formation using *Pseudomonas aeruginosa* and *Bacillus subtilis* as model organisms which are commonly found in food industries.

2. Investigate the adhesion interaction of bacteria on stainless steel surface and its relationship with surface energy and force measurement.

3. Investigate the interaction and influence of spore adhesion to stainless steel on biofilm formation.

4. Investigate the composition and adhesive properties of extracellular polymeric substances (EPS) produced by *Pseudomonas aeruginosa* and *Bacillus subtilis*.

The results of this study are expected to improve our understanding of both the cell surface properties and the structure-function relationship between bacteria and metal surface during the adhesion process by incorporating force quantification during bacteria-metal interactions and analyses of various physico-chemical properties that are involved in cell adhesion.

This thesis focused on investigating biofilm formation between food-borne bacteria and stainless steel, using *Pseudomonas aeruginosa* and *Bacillus subtilis* as model organisms. Biofilm formation consists of several steps, but only the adhesion

step is considered in this study. The other steps are not discussed in the study since adhesion is considered as the most crucial step in biofilm formation.

The next chapter (Chapter 2) presents an overview of biofilms in general, and describes specific cell-surface interaction which occurs during biofilm formation. Properties of cells and their influence on cell adhesion, and use of Atomic Force Microscopy (AFM) to study bacterial adhesion forces, are also discussed. The materials and methodologies used to conduct the experiments are described in Chapter 3. Chapter 4 presents characterization of biofilm formed by both model bacteria on SS316 surfaces. Chapter 5 discusses the role of surface and interaction energies on adhesion mechanisms of both model bacteria. Research findings on the quantification of spore adhesion on SS 316 during adhesion are given in Chapter 6. Chapter 7 discusses the investigation of extracellular polymeric substance (EPS) properties of both model bacteria and their role in biofilm formation. Finally, conclusions are drawn and future research works proposed are presented in Chapter 8.

CHAPTER 2

LITERATURE REVIEW

2. 1 Biofilms

Microorganism may attach to solid surfaces which are conditioned with nutrients, ions, and other organic material to support their growth. These microorganisms initially are deposited on the surfaces, and subsequently attach, grow and actively multiply to form a colony of cells. In this regard, secretion of extracellular polymeric substances (EPS) is essential for colonization by microorganisms. These mass of cells further become large enough to entrap organic and inorganic debris, nutrients and other microorganisms, thereby leading to the formation of a microbial biofilm (Allison and Sutherland, 1987).

2. 1. 1 Definition of Biofilm

The term biofilm refers to the biologically active matrix of cells and extracellular substances in association with a solid surface (Bakke et al., 1984). A biofilm is a functional consortium of microorganisms attached to a surface and is embedded in the EPS produced by the microorganism (Costerton et al., 1987).

'Biofilm' and 'biofouling' are two terms used to describe a surface accumulation of organisms. 'Biofilm' is a generic term for both positive and negative implications of microbial adhesion, while the term 'biofouling' describes instances where biologically active films are considered deleterious. Biofilms can be formed by all types of microorganisms, including spoilage and pathogenic microorganisms,

under suitable conditions. Biofilms can also be formed on all types of surfaces in most ecosystems.

2. 1. 2 Mechanism of Biofilm Formation

Biofilms may form and develop almost in every environment when viable microorganisms are present (Kumar and Anand, 1998). Bacteria tend to form biofilms under starvation conditions, adverse environmental condition, or when the nutrients from the surroundings are limited (Kim et al., 2000; Knoshaug et al., 2000). Biofilm formation is a dynamic process and involves a series of steps, as depicted in Figure 2.1.
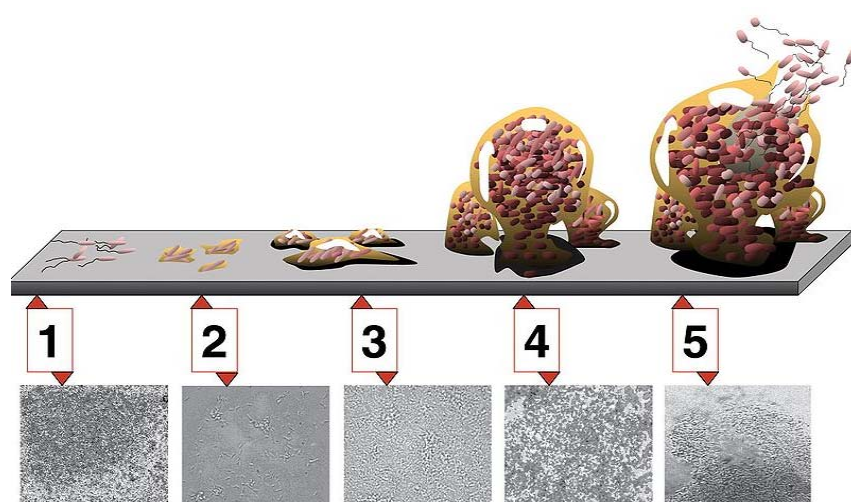
Figure 2.1 Mechanism of Biofilm Formation (Monroe, 2007)

Before bacteria attachment occurs, organic molecules present in the bulk fluid are carried by diffusion, turbulent flow, or gravitational forces to the surface and absorbed onto the surface to form a conditioning film. This accumulation of molecules can lead to a higher concentration of nutrients at the surface compared to the bulk fluid phase. This conditioning layer alters the physiochemical properties of

the surface, such as surface free energy, hydrophobicity and electrostatic charges (Dickson and Koohmaraie, 1989). These changes determine how bacterial cells attach to surfaces, either serving to inhibit or initiate biofilm development. For example, milk components such as casein and β-lacto globulin reduce the attachment of *L. monocytogenes* and *S. typhimurium* to stainless steel (Helke et al., 1993). The proteins in the bulk fluid phase may have acted as competition for binding sites on the surface of the stainless steel, thereby reducing the ability of the bacteria to attach. In other cases, it was reported that stainless steel and rubber surfaces treated with either lactose protein or whey protein components showed an increase in the attachment of milk-associated bacteria (Speers and Gilmour, 1985). In biofilms for waste water treatment, it was shown that absorption of organic polymers in particular improve biofilm growth (Lazarova and Manem, 1995).

When biofilm development is initiated, free-floating bacteria cells will attach reversibly to the pre-conditioned surface via non-specific long-distance interactions. These include Van der Waals and electrostatic interactions. Mechanisms by which bacteria are transported to a surface can include Brownian motion, sedimentation due to differences in specific gravity between the bacteria and the bulk liquid, or convective mass transport by movement of the bulk fluid (Palmer et al., 2007). Following initial association with a substratum, the bacterial cells then undergo a cascade of physiological changes, which leads to a series of events. Surface growth, replication, and further attachment of planktonic cells from the bulk fluid phase, micro-colony formation and production of EPS take place. The production of these substances further strengthens the attachment of the bacteria to the surface and ultimately irreversible cell attachment will result. This happens when various short-range forces such as dipole-dipole, hydrophobic, ion-dipole, ion-ion, covalent bonds

and hydrogen interactions come into play. The outcome is the formation of a mature biofilm (Hood and Zottola, 1995; Hall-Stoodley and Stoodley, 2002; Trachoo, 2003). Quorum sensing as a communication means between bacterial cells also plays important role in this stage. There is evidence that in some bacteria, biofilm formation is a carefully orchestrated process controlled by quorum sensing. The use of bacterial strains with mutations in genes involved in the production of signaling molecules and the analysis of temporal differential gene expression in biofilms have yielded information on the molecular mechanisms of biofilm formation and the role of quorum sensing. Knowledge of the chemical structures of different types of signaling molecules allows the identification of compounds that can be used to modulate quorum sensing-related processes, including biofilm formation (Davies et al., 1998b).

With time, some bacteria cells will eventually detach themselves from the mature biofilm and return to the bulk fluid as planktonic cells to colonize new surfaces elsewhere. The detachment of individual cells from the mature biofilm may involve enzymatic cleavage of the matrix polymers, or sloughing via fluid dynamic forces of a turbulent liquid environment or grazing with particles, or by passage through an air/liquid interface (Eginton et al., 1995). Factors such as biofilm thickness, fluid shear stress, nutrient availability and fluid velocity can affect the detachment process (Trachoo, 2003).

2. 1. 3 Advantages and Problems with Biofilm

Reported more than 60 years ago (Zobell, 1943), the field of biofilms continues to be actively studied and researched. Whether useful or problematic, biofilms are ubiquitously found in a broad range of areas, such as in the food, environmental, and biomedical fields (Simoes et al., 2010).

Biofilms can be used for constructive purposes. For example, many sewage treatment plants include a treatment stage in which waste water passes over biofilms grown on filters, which extract and digest organic compounds. In such biofilms, bacteria are mainly responsible for removal of organic matter, while protozoa and rotifers are mainly responsible for removal of suspended solids, including pathogens and other microorganisms (Lazarova and Manem, 1995). Slow sand filters rely on biofilm development in the same way to filter surface water from lake, spring or river sources for drinking purposes (El Masry et al., 1995). Biofilms can help eliminate petroleum oil from contaminated oceans or marine systems. The oil is eliminated by the hydrocarbon-degrading activities of microbial communities, in particular by a remarkable recently-discovered group of specialists, the so-called hydrocarbonoclastic bacteria (HCB) (Al-Awadhi et al., 2003). Biofilms are also useful in extraction of precious metal, called bio-leaching, which is more environmental friendly than conventional chemical leaching (Sand et al., 1995).

However, biofilms can also be detrimental. Biofilm in cooling/ heating water systems are known to reduce the heat transfer and operating efficiency (Characklis et al., 1981). Biofilms in marine engineering systems, such as pipelines of the offshore oil and gas industry can lead to substantial corrosion problems. Corrosion is mainly due to abiotic factors; however, at least 20% of corrosion is caused by microorganisms that are attached to the metal subsurface (i.e., microbially-influenced corrosion) (Schwermer et al., 2008). The attachment of the bacteria to food product or the food contact surfaces may leads to serious hygienic problems and economic losses due to food spoilage (Poulsen, 1999). In water distribution systems, biofilm formation may not be inhibited by high level of residual chlorines, and they can increase energy consumption by increasing drag and pump power, mechanical blockage and

accelerate corrosion of metal surfaces (Kumar and Anand, 1998). In the medical field, biofilm formation on medical implants becomes the source of pathogen transfer and subsequent infections (Francolini and Donelli, 2010).

The composition of a biofilm is usually heterogeneous and is dependent on the particular environment. Examples of genera of microorganisms producing biofilm commonly found in various fields are given in Table 2.1.

Since the existence of biofilms has numerous consequences, research into the mechanism of microbial biofilm formation is important and has become an actively researched field in recent years. Various analyses of biofilm formation have been carried out with different technologies, providing theoretical bases for implementing new strategies to eliminate and control biofilm.

In this study, *P. aeruginosa* and *B. subtilis* were used as model microorganisms. Their adhesion properties were observed during attachment on stainless steel SS-316 surfaces. These two bacteria were chosen to be used in this study because of several reasons. First, these bacteria are two common genus found in many biofilm systems, such as in the food industry, medical environments, and in the petroleum industry. Second, *Pseudomonas* and *Bacillus* represent two different classes of bacteria, i.e. Gram-negative and Gram-positive, respectively. Third, *B. subtilis* has the unique property of producing spores during unfavorable conditions. And finally, these two bacteria are classified as safe to be used for the lab-work. Since these bacteria are ubiquitously found in the environment, research into their adhesion properties is important in order to understand their interaction with surfaces as this will be beneficial for biofilm control and removal.

2. 1. 4 Control Strategies of Biofilm

Biofilms are estimated to be involved in over 65% of all human bacterial infections and costs industries, cities, and hospitals in excess of $500 billion each year. Therefore, prevention and control of biofilms are very important not only for process improvement but also for cost reduction. However, biofilm control is not an easy task. Compared to individual cells grown in suspension, bacterial biofilms exhibit an increased resistance to antimicrobial treatments. This resistance has been widely observed and is attributed to the varied properties associated with the biofilm including reduced diffusion, physiological change due to reduced growth rates and the production of enzymes degrading antimicrobial substances.

A characteristic feature of microbial biofilms is the presence of an EPS matrix embedded with the component cells. This matrix may act to various degrees as a diffusion barrier, molecular sieve and adsorbent (Boyd and Chakrabarty, 1995). Therefore, the production of excess amounts of EPS by the bacteria during biofilm formation and growth may protect the innermost cells by binding with antimicrobial substances and quenching their effect as the substance diffuse through it.

Furthermore, antimicrobial agents are far more effective against actively growing cells. It means that the best disinfectants for planktonic cells are not necessarily the suitable ones for biofilm cells. This implies that the bacteria within biofilms exhibit a varied physiological pattern and show nutrient and oxygen gradients across the biofilm. In addition, in cases of biofouling, thick biofilms are formed which may include many metabolically dormant and/ or dead cells. These states of the bacterial cells of the biofilm may have an altered growth rate and physiology, resulting in increase resistance to antimicrobial agents. Resistance against

various disinfectants is more severe in older biofilms that in the young ones (Anwar et al., 1990).

Table 2.1 Summary biofilm forming microorganisms in various fields

Field	Genus	Reference
Wastewater Treatment	*Nitrospira*	Daims et al., 2001
	Nitrosomonas	Egli et al., 2003
	Thiobacillus	Ito et al., 2004
Petroleum Treatment	*Pseudomonas*	Al-Zahrani and Idris, 2010
	Acetinobacter	Marin et al., 1996
	Rhodococcus	Kuyukina et al., 2009
Fermentation	*Rhizopus*	Cao et al., 1997
	Aspergilus	Villena et al., 2009
	Lactobacillus	Chan-Blanco et al., 2003
Bioleaching	*Leptospirillum*	Ziegler et al., 2009
	Proteobacter	Bond et al., 2000
	Sulfobacillus	Bosecker, 1997
Biocorrosion	*Desulfovibrio*	Sheng et al., 2007
	Citrobacter	Beech and Gaylarde, 1999
	Thiobacillus	Coetser and Cloete, 2005
Food Industries	*Listeria*	Blackman and Frank, 1996
	Pseudomonas	Hood and Zottola, 1997
	Bacillus	Ankolekar and Labbe, 2009
Medical	*Pseudomonas*	Ernst et al., 1999
	Staphylococcus	Cramton et al., 1999
	Candida	Li et al., 2003

Resistance to antibiotics by the bacteria is caused by the production of antibiotic-degrading enzymes. Such enzymes degrade and inactivate the antibiotics as they permeate through the cell envelope to their target sites. In adherent biofilms, many of the similar hydrolytic enzymes are produced and they become trapped and

concentrated within the biofilm matrix, exhibiting enhanced protective properties (Anwar et al., 1992).

Prevention of biofilm formation is performed by routine cleaning and disinfection (Midelet and Carpentier, 2004). Biofilm detectors have also been developed to monitor the surface colonization by bacteria and allow the control of biofilms in the early stages of development (Pereira et al., 2008). Such sensors are also able to detect the presence of cleaning products on a surface, and identify when it was biologically and chemically cleaned, and measure the rate of cleaning. Other preventive strategies attempted to identify materials that do not promote or can even suppress biofilm formation. A study reportedly ranked different materials according to their biofilm growth propensity, and concluded that there is hardly any material that does not allow biofilm formation (Rogers et al., 1994).

Several attempts have been made to avoid biofilm formation by the incorporation of antimicrobial products into the surface of materials (Weng et al., 1999; Park et al., 2004), by coating surfaces with antimicrobials (Tsibouklis and Stone, 2000; Gottenbos et al., 2002b; Thouvenin et al., 2003) or by modifying the surfaces physicochemical properties (Whitehead et al., 2004; Rosmaninho et al., 2007). It is also reported that surface pre-conditioning with surfactant also has potential to prevent bacterial adhesion (Cloete and Jacobs, 2001; Splendiani et al., 2006).

In food industries, cleaning and disinfection are the essential part of routine production, since the efficiency of these operations will affect the final product (Bremer et al., 2006). However, a disinfectant should be chosen carefully so that it is safe and easy to rinse off, leaving no toxic residues that can affect the product quality. Selection of disinfectants in food industries depends on the material of the processing

equipment used and on the adhering microorganisms. Chemicals such as alhdehyde-based biocides, caustic products, chlorine, and isothiazolinones are commonly used as disinfectant in food industries (Dosti et al., 2005; Bremer et al., 2006).

Newer control strategies in biofilm control are required since most disinfection processes are only effective on planktonic cells and can be highly ineffective when applied to control biofilm. The use of enzyme-based detergents as bio-cleaners can serve as a viable option to overcome biofilm problem in the food industry. Mixture of enzymes may be necessary for sufficient biofilm degradation (Augustin et al., 2004). Enzymes and detergents have also been used together to improve disinfectant efficacy (Parkar et al., 2004). However, the specificity in the enzyme mode of action makes it a complex technique, increasing the difficulty of identifying enzymes that are effective against all the different types of biofilms. Formulations containing several different enzymes seem to be fundamental for a successful biofilm control strategy (Meyer, 2003)

The existence of multiple interspecies interactions can interfere with biofilm formation and development (Carpentier and Chassaing, 2004; Kives et al., 2005). The discovery that many bacteria use quorum sensing as a communication way to form biofilms makes it an attractive target for their control (Dunstall et al., 2005; Rasmussen et al., 2005). It is conceivable that quorum sensing inhibition may represent a natural antimicrobial strategy with significant impact on biofilm formation (Dong et al., 2002). A good understanding of the cell–cell signaling phenomenon of bacteria can be used to control the biofilm formation process by the identification of products that can act as quorum sensing antagonists (Smith et al., 2004). This property can lead to the development of new and efficient natural products for biofilm control.

2. 2 Cell-Surface Interactions during Biofilm Formation

Adhesion of bacteria onto surfaces consists of initial attraction of the cells to the surface followed by adsorption and attachment (Rijnaarts et al., 1995). Bacteria move to a material surface through and by the effects of physical forces, such as Brownian motion, van der Waals attraction forces, gravitational forces, and the effect of surface electrostatic charges, and hydrophobic interactions (Gottenbos et al., 2002a). The physical interactions are further classified as long-range interactions and short range interactions (Gottenbos et al., 2002a). The long-range interactions between cells and surfaces (non specific, distance>50 nm) are described by mutual forces, which are a function of distance and free energy. Short-range interactions become effective when the cell and the surface come into close contact (<5 nm); these can be separated into chemical bonds (such as hydrogen bonding), ionic and dipole interactions, and hydrophobic interactions (Mayer et al., 1999). Bacteria are transported to the surface by the long-range interactions and upon closer contact, short range interactions become more dominant. This initial attachment of bacteria to surfaces is the beginning of adhesion, causing the molecular or cellular phase of adhesion possible (Katsikogianni and Missirlis, 2004).

During the second phase of adhesion, molecular-specific reactions between bacterial surface structures and substratum surfaces become predominant. Firmer adhesion of bacteria to a surface occur by the selective-bridging function of bacterial surface polymeric structures, which include capsules, fimbriae, or pili and slime (Katsikogianni and Missirlis, 2004).

Once the microorganisms reach the proximity of a surface, attachment is determined by physical and chemical interactions, which may be attractive or repulsive, depending on the complex interplay of the chemistry of bacterial and

substratum surfaces, and the aqueous phase. Theoretical approaches have been used to understand forces that determine adhesion. The most established model is the Derjaguin-Landau-Verwey-Overbeek (DLVO) theory, which characterize total interaction energy between cells and surfaces as a balance between van der Waals interaction (generally attractive) and electrostatic double layer (generally repulsive) (Brant and Childress, 2002).

However, the DLVO theory alone often fails to accurately describe cell-surface interaction, particularly when the separation distance is small (Molina-Bolivar et al., 1999; Chin et al., 2002). Discrepancies between DLVO predictions and experimental observations have been attributed to various surface properties and additional interactions such as surface roughness, chemical and morphologic heterogeneities, and short-range non-DLVO forces such as hydrophobic effects and hydration pressure (Ducker et al., 1991; Pashley et al., 1998; Brant and Childress, 2002).

Hydrophobic and hydration effects are considered to play a significant role in surface interactions in polar media (Butt et al., 1995; Christenson and Claesson, 2001; Van Oss, 2006). These polar interactions are then generally referred as Lewis acid base interaction (Van Oss, 1993) which are based on electron acceptor-electron donor interactions between polar moieties in a polar media (e.g., water). Consideration of these additional interactions has resulted in an extended DLVO (xDLVO) approach for characterizing surface interactions (Van Oss, 2006). In this approach, acid base interactions are accounted for in addition to electrostatic and van der Waals interactions.

In this study, DLVO theory was used to calculate the interaction energies and explain the adhesion interaction between model bacteria (*P. aeruginosa* and *B.*

subtilis) and stainless steel SS-316 surfaces. Extended DVLO (xDLVO) will also be incorporated to quantify the significance of polar interactions in these bacteria-metal interactions. Both of these theories will then be compared with adhesion force obtained by Atomic Force Microscopy (AFM) (discussed in later subchapter) to obtain deeper understanding of the factors influencing the attachment of microorganism onto surfaces.

2. 3 Calculations of Surface Energy Components and Free Interaction Energies based on DLVO and xDLVO theories

2. 3. 1 Surface Energy Calculations

Calculating the free energy of adhesion requires the values of surface tension components. Since the 1970s, researchers have begun correlating microbial adhesion with surface free energy of the substratum and the hydrophobicity of surfaces. These studies have shown the effectiveness of modifying substratum surfaces in order to reduce biofilm growth (Vladkova, 2009).

Bacteria adhesion occurs if there is a decrease in the free energy of the system. It can be described by Young's equation:

$$\gamma_L cos\theta = \gamma_S - \gamma_{SL} \qquad (1)$$

where γ_L is the surface tension value of the liquid, θ is is the contact angle, γ_S is the surface energy of the solid and γ_{SL} is the solid/liquid interfacial energy. In order to obtain the solid surface free energy γ_S, an estimate of γ_{SL} has to be obtained.

Acid-base theory for surface energy calculation has been developed (Van Oss, 1993). The surface energy is seen as the sum of a Lifshitz-van der Waals apolar component (γ_i^{LW}) and a Lewis acid-base polar component (γ_i^{AB}).

$$\gamma_i = \gamma_i^{LW} + \gamma_i^{AB} \qquad\qquad (2)$$

The acid-base polar component γ_i^{AB} can be further subdivided by using specific terms for an electron donor (γ_i^-) and an electron acceptor subcomponent (γ_i^+).

$$\gamma_i^{AB} = 2\sqrt{\gamma_i^- \cdot \gamma_i^+} \qquad\qquad (3)$$

The solid/liquid interracial energy is then given by:

$$\gamma_{SL} = \gamma_S + \gamma_L - 2(\sqrt{\gamma_S^{LW} \cdot \gamma_L^{LW}} + \sqrt{\gamma_S^+ \cdot \gamma_L^-} + \sqrt{\gamma_S^- \cdot \gamma_L^+}) \qquad\qquad (4)$$

Combining this with the Young equation, a relation between contact angle, and the solid and liquid surface free energy terms can be obtained:

$$\gamma_L(1 + cos\theta) = 2(\sqrt{\gamma_S^{LW} \cdot \gamma_L^{LW}} + \sqrt{\gamma_S^+ \cdot \gamma_L^-} + \sqrt{\gamma_S^- \cdot \gamma_L^+}) \qquad\qquad (5)$$

This equation is also known as the van Oss-Chaudhury-Good (OCG) equation. In order to determine the three surface tension energy components (γ_S^{LW}, γ_S^+ and γ_S^-) of a solid, three equations are required. Therefore the contact angle values of three liquids (one apolar and two polar liquids) with known surface tension components (γ_L^{LW}, γ_L^+ and γ_L^-) have to be determined (Liu and Zhao, 2005)

2. 3. 2 Calculations of Hamaker Constant

The Hamaker constant (A) is the property of two surfaces that identify their interaction strength in the medium and depends on the dielectric properties of the surface, medium, and the cell in the case of microbial adhesion (Hermansson, 1999). Hamaker constant is determined with contact angle measurement using apolar fluid

on the cell lawn to produce the surface tension component γ_{LW}. This surface tension is related to the Hamaker constant using following equation:

$$A_{ii} = 24\pi l_0 \gamma_i^{LW} \qquad (6)$$

where l_0 represent the minimum equilibrium distance between two parallel flat layers. In our calculation we use the value of 0.157 nm which has been generally accepted for a large range of materials. The effective Hamaker constant for the system containing bacteria (1), surface (2), and medium (3) is given by:

$$A_{123} = \left(\sqrt{A_{11}} - \sqrt{A_{33}}\right)\left(\sqrt{A_{22}} - \sqrt{A_{33}}\right) \qquad (7)$$

Combining equation (6) and (7) the Hamaker constant becomes:

$$A_{123} = 24\pi l_0^2 \left(\sqrt{\gamma_1^{LW}} - \sqrt{\gamma_3^{LW}}\right)\left(\sqrt{\gamma_2^{LW}} - \sqrt{\gamma_3^{LW}}\right) \qquad (8)$$

2. 3. 3 Calculation of Absolute Hydrophobicity based on Surface Energy

Absolute hydrophobicity of any given substances can be determined through the use of the surface tension components. Van Oss (Van Oss, 1995) expressed the free interaction energy between bacteria (1) and water (3) using following expression:

$$\Delta G_{13} = -2\left(\sqrt{\gamma_1^{LW}} - \sqrt{\gamma_3^{LW}}\right)^2 - 4\left(\sqrt{\gamma_1^+ \gamma_1^-} + \sqrt{\gamma_3^+ \gamma_3^-} - \sqrt{\gamma_1^+ \gamma_3^-} - \sqrt{\gamma_1^- \gamma_3^+}\right) \qquad (9)$$

According to Van Oss, when the value of $\Delta G_{13} < 0$ the bacteria is classified as hydrophobic, while when $\Delta G_{13} > 0$, it is classified as hydrophilic.

2. 3. 4 Calculation of Free Interaction Energies

Bacterial adhesion involves a reversible and subsequently irreversible process. DLVO theory is commonly used to predict colloidal stability and cell adhesion, and

describes the interaction between cell and surfaces as a net result from the Lifshitz-van der Waals (LW) attractions and electrostatic double layer (EL) repulsions. Van Oss proposed an extended DLVO theory that include a Lewis acid-base (AB) component and Brownian motion (Br) component (Van Oss, 2006). The total free interaction energy between a particle and a solid surface can be written as the sum of these corresponding interaction terms:

$$\Delta G^{TOT} = \Delta G^{LW} + \Delta G^{EL} + \Delta G^{AB} + \Delta G^{Br} \qquad (10)$$

This theory suggested that the balance between all possible interaction determine whether or not bacteria will attach on the surface. Adhesion will take place when ΔG^{TOT} is negative (i.e., total interaction force is attractive) (Oliveira, 1997; Azeredo et al., 1999).

Lifshitz-van der Waals Interaction Energy (ΔG^{LW})

Interaction energy of Lifshitz-van der Waals between a bacteria of radius R and a flat surface can be calculated using the following equation:

$$\Delta G^{LW} = -\frac{A.R}{6.H} \qquad (11)$$

where H is the separation distance between cell and surface, R is the cell hydrodynamic radius, and A is the Hamaker constant which is calculated from equation (8). Combininq equation (8) with equation (11) results in:

$$\Delta G^{LW} = -\frac{24\pi l_0^2 \left(\sqrt{\gamma_1^{LW}} - \sqrt{\gamma_3^{LW}}\right)\left(\sqrt{\gamma_2^{LW}} - \sqrt{\gamma_3^{LW}}\right).R}{6.H} \qquad (12)$$

Electrostatic Double Layer Interaction Energy ($\Delta \boldsymbol{G^{EL}}$)

Interaction energy of Electrostatic double layer between a bacteria and a flat surface at constant surface potential φ is given by following equation (Liu and Zhao, 2005):

$$\Delta G^{EL} = \varepsilon \pi R \{ (\varphi_1 + \varphi_2)^2 \ln[1 + \exp(-\kappa H)] + (\varphi_1 - \varphi_2)^2 \ln[1 - \exp(-\kappa H)] \}$$

(13)

where φ_1 and φ_2 are the electrical surface potential of the cell and the flat surface respectively; R is the cell hydrodynamic radius; ε is the electrical permittivity of the medium (7.082 x 10^{-10} for water at 25°C) and κ is the Debye-Hûckel parameter ($1/\kappa = 1.1$ nm). The $1/\kappa$ is obtained by assuming that the background electrolyte concentration of 0.01M PBS was used (Myers and Meyers, 1991). Since surface potential cannot be determined experimentally, it is usually replaced by zeta potential.

Lewis Acid-Base Interaction Energy ($\Delta \boldsymbol{G^{AB}}$)

Interaction energy of Lewis Acid-Base between bacteria and flat surface is given by following equation:

$$\Delta G^{AB} = 2\pi R \lambda \Delta G_{132}^{AB} \exp\left(\frac{l_o - H}{\lambda}\right) \qquad (14)$$

where λ is the decay length pertaining to water molecule (estimated value (Van Oss, 2006) of 0.6 nm), l_0 is the equilibrium distance, and H is the separation distance between cell and surface. ΔG_{132}^{AB} is a function of the electrodonor (γ^-) and electroacceptor (γ^+) parameters of the polar component (γ^{AB}) of the surface tension of interacting bodies which is given by:

$$\Delta G_{132}^{AB} = 2[\sqrt{\gamma_3^+}.\left(\sqrt{\gamma_1^-} + \sqrt{\gamma_2^-} - \sqrt{\gamma_3^-}\right) + \sqrt{\gamma_3^-}.\left(\sqrt{\gamma_1^+} + \sqrt{\gamma_2^+} - \sqrt{\gamma_3^+}\right) -$$
$$\sqrt{\gamma_1^+.\gamma_2^-} - \sqrt{\gamma_1^-.\gamma_2^+}]$$

(15)

Brownian Motion Interaction Energy (ΔG^{BR})

Corresponding free interaction energy of bacteria adhering to surface caused by Brownian motion equals to 0.414×10^{-20} J (1 kT) (Liu and Zhao, 2005).

2. 4 Cell Surface Properties and its Influence on Cell Adhesion

2. 4. 1 Cell Hydrophobicity

Microbial adhesion to surface is regarded as the most crucial step in biofilm development. Adhesion is a complex process and involving several factors, including physico-chemical properties of the cell surface. Cell surface properties, along with factors such as the influence of surface-active compounds secreted by microorganisms, the hydrodynamic of surrounding environments, surface roughness, nutrient availability, and shear rate, profoundly affects the final structure of the biofilm and biofilm-associated microbial diversity (Basson et al., 2008) and play an important role in of opportunistic pathogens to integrate in the food biofilm.

One important aspect on physico-chemical properties of the cell surface is cell hydrophobicity. Hydrophobicity of bacteria is a term used to describe the hydrophobic properties conferred on bacterial cells by their outermost cell surfaces. The main role of bacterial hydrophobicity in adhesion is to remove the water film between interacting surfaces, thereby enabling short-range interaction to occur (Mozes et al., 1991).

Hydrophobicity interaction has been suggested as being responsible for a wide range of adherence phenomena, and several methods have been widely used to determine cell surface hydrophobicity. One common method is salt aggregation test (SAT). This technique is based on the theory that, as hydrophobicity increases, the more likely the cells are to precipitate out of solution at lower concentrations of salting-out agents. In this method, the bacteria are suspended in a dilute buffer solution and ammonium sulfate is added until aggregation occurs (Lindahl et al., 1981).

Another method based on adhesion is referred to bacterial adhesion to hydrocarbon (BATH). In this method, a hydrocarbon such as hexadecane or xylene is mixed with a suspension of bacterial cells. Hydrophobic cells will adhere to the hydrocarbon; hence the decrease in absorbance of the bacterial suspensions can be measured (Obuekwe et al., 2007).

Contact angle measurement (CAM) is the other method to measure cell surface hydrophobicity. Basically, when a droplet of water is placed on a surface (a lawn of bacteria), the contact angle is proportional to the hydrophobicity of the surface (Fletcher and Marshall, 1982). Typical contact angles of water on surfaces is shown on Figure 2.2

hydrophilic
$0^o < \alpha < 30^o$

hydrophobic
$\alpha > 90^o$

strong hydrophobic
$\alpha > 150^o$
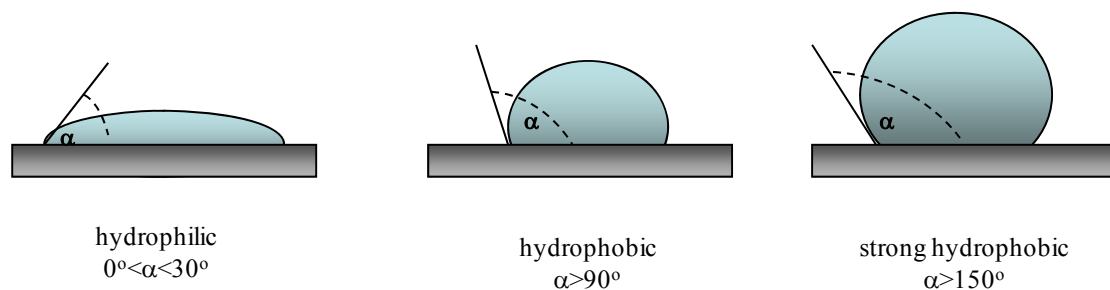
Figure 2.2 Typical contact angles of water on surfaces

2. 4. 2 Properties of Spore Surfaces

Spores are the dormant stage of bacteria which are highly resistant to severe environmental conditions. Spores are formed in response to nutrient deprivation or extreme condition, such as temperature, pH, and moisture. When nutrients become available, spores returns to vegetative growth via the process of germination (Chen et al., 2010).
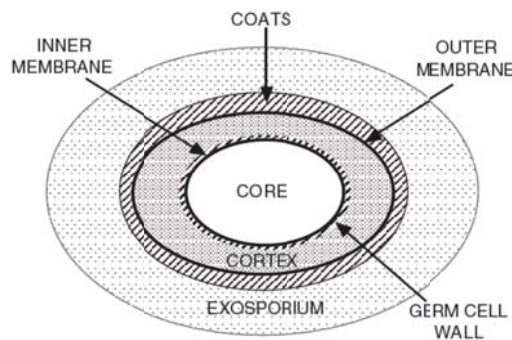
Figure 2.3 Structures of Spores (Setlow, 2006)

Spore resistance is mainly influenced by its structure and chemical composition. Figure 2.3 shows the general structure of spores. Starting from the outside and proceeding inward the spore layers include the exosporium, coats, outer membrane, cortex, germ cell wall, inner membrane, and central core (Setlow, 2006).

Bacterial spores are well known to constitute a major problem in food and drug industries (Husmark and Ronner, 1992; Clement et al., 1993). Adhesion of spores to surfaces has been identified as an important virulence factor for some species of *Bacillus,* such as *B. cereus* and *B. subtilis.* High adhesion of these bacteria has been correlated with food poisoning symptoms (Anderson et al., 1995; Granum and Benjamin, 2003; Jullien et al., 2003). Spore adhesion is a significant problem in the dairy industry, especially in pipelines where they may multiply and resporulate. Once present, spores may initiate food infection because of their extraordinary

resistance against common food preservation (Anderson *et al.*, 1995; Scheldeman *et al.*, 2005).

Bacillus spores show hydrophobic characteristic, resulting in firm adhesion to surface frequently used for food processing material like stainless steel (Peng et al., 2001; Faille et al., 2002; Tauveron et al., 2006). Adhesion of cells and spores may initiate biofilm formation (Ryu and Beuchat, 2005) which can cause cross-contamination in the product (Flint *et al.*, 2001) and subsequently decrease its shelf life (Giffel *et al.*, 2002). Since adhesion of spores onto metal surfaces has also been considered significant in biofilm formation, it is important to study the interaction between spores and metal and vegetative cells during the adhesion process. In order to inhibit and control spore and cell adhesion on surfaces, it is important to understand the adhesion mechanism onto surfaces. Interaction forces between spores and various surfaces has been studied, such as between fungal spores and fiber surface in examining the efficiency of filtration of spores (Bowen *et al.*, 2000), between bacillus spores and hydrophobic coated glass surface (Bowen *et al.*, 2002), and also between dormant fungal spores and the germinating ones to investigate their differences in terms of adhesion force (Dufrene *et al.*, 1999).

To date, the chemical basis of spore adhesion to surfaces is still poorly understood. Adhesion interactions between spores and metal surfaces, especially in the food specific environments and related to biofilm formation, has not been sufficiently studied. Therefore this study will differentiate vegetative cells and spores of the model bacteria, *Bacillus subtilis*. This study will investigate the surface properties of spores as well as their adhesion behavior on stainless steel surfaces. By understanding the interactions involved during adhesion, more effective biofilm control and removal techniques can be developed.

2. 4. 3 Microbial Cell Wall and Extracellular Polymeric Substances (EPS)

Microbial cell walls support various key functions, such as protecting the cytoplasm, maintaining the pressure inside cell, imparting the shape of microorganism, and controlling molecular recognition (Beveridge and Graham, 1991; Mozes et al., 1991). The mechanical strength of bacterial wall is provided by layers of peptidoglycan which are cross-linked by short peptide chains. As shown in Figure 2.4, in Gram-positive bacteria, peptidoglycan bind to anionic polymers, while in Gram-negative bacteria, it is overlaid by an outer membrane, which is an asymmetrical bilayer of phospholipids and lipopolysaccharides containing membrane protein (Alsteens et al., 2008).
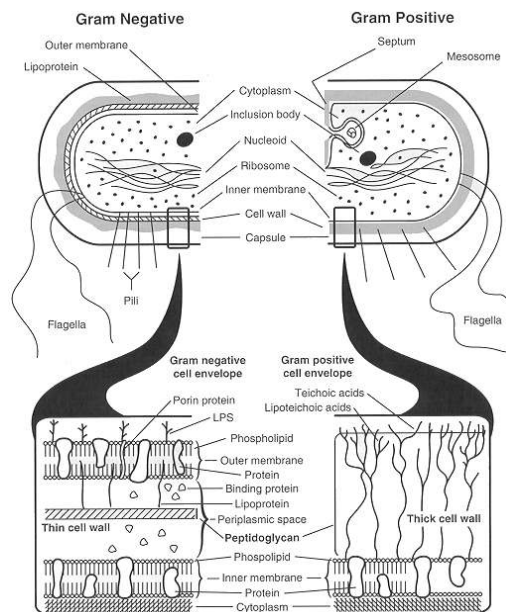
Figure 2.4 Schematic Diagram of Gram-negative and Gram-positive bacteria
(http://gsbs.utmb.edu)

Extracellular polymeric substances (EPS) is a term used to describe separate classes of organic macromolecules such as polysaccharides, proteins, nucleic acids, lipids and other polymeric compounds found both on the outer surface of cell walls and in the interior of microbial aggregates (biofilm matrix) (Wingender et al., 1999).

EPS associated with the outermost surface layers of bacteria cells often exist as boundary structures, for instance, capsules or sheaths (Costerton et al., 1995).

EPS production in the biofilm poses several important functions. EPS matrix acts as a diffusion barrier to antimicrobial agents and offers protection against unfavorable environmental conditions. Therefore, biofilm cells exhibit enhanced resilience unlike planktonic cells, and are more difficult to completely eliminate (Abu-Lail and Camesano, 2003a; Meyer, 2003). EPS that coats a cell also alters the physiochemical characteristics of the cell such as surface charge, hydrophobicity and polymeric properties. These changes mediate cellular recognition and promote initial cell adhesion and aggregation (Tsuneda et al., 2003). It has been reported that EPS comprises carboxylate, phosphate and amine functional groups that contribute to bacterial adhesion onto surfaces (Leone et al., 2006a). Production of EPS acts as a trap to increase the availability of nutrients for growth. The polyanionic nature of EPS matrix allows it to concentrate nutrients from the surrounding fluid (Trachoo, 2003). EPS is also shown to be required for biofilm development and maintenance of biofilm structure. For instance, glucose and galactose-rich EPS produced by a rugose variant of *Vibrio cholerae* O1 E1 Tor was required for complex structural biofilm development (Hall-Stoodley and Stoodley, 2002; Abu-Lail and Camesano, 2003b). Recent developments also suggested a connection between EPS production and population density within biofilms via quorum sensing, which is the regulation of gene expression in response to fluctuations in cell population density (Branda et al., 2005). The initial recognition of a relationship between quorum sensing and biofilm architecture in *P. aeruginosa* provided direct evidence for the role of extracellular signaling in biofilm development. The dramatic effects on biofilm thickness and shape resulting from the inability to produce N-(3-oxododecanoyl)-L-homoserine

lactone signal suggested major alterations in the extracellular matrix (Davies et al., 1998a).

In order to obtain a comprehensive understanding of bacterial adhesion to surfaces, knowledge of the composition and conformational properties of EPS produced by bacteria during growth and biofilm formation is required. Earlier results show that EPS covers about 45% of the cell surface of Gram-negative bacteria and may protrude 30 nm or more into surrounding media (Jucker *et al.*, 1998). Many bacterial surfaces also have a layer of extracellular polysaccharides (Davies et al., 1998a). The compressibility and affinity of these polysaccharides for solids were thought to determine whether they enhanced or inhibited adhesion (Jucker *et al.*, 1998).

Although much progress has been made in elucidating the chemical structures of cell wall associated polysaccharides, their adhesive and conformational properties remain poorly understood at the molecular level (Camesano *et al.*, 2007; Dufrêne, 2008). Studying their spatial organization and conformational properties at the molecular level remains a challenge. In this study, composition and characteristic of EPS produced by *P. aeruginosa* and *B. subtilis* during growth and biofilm formation will be elucidated using several chemical analysis techniques. Furthermore, single molecule force spectroscopy (SMFS) using AFM will be used to relate the composition of EPS with their adhesive properties (as discussed in Section 2.5.4).

2. 5 Atomic Force Microscopy (AFM)

2. 5. 1 AFM as Emerging Technique for Bacterial Interaction Study

Invented in 1986, AFM is surface imaging technique that operates by sensing the force between a very sharp tip and the sample surface (Binnig *et al.*, 1986). The

force is monitored by attaching the probe to a flexible cantilever and measuring the deflection of the cantilever. AFM has been extensively used due to its capability of investigating microbial surface at high resolution. It also provides three dimensional images of the surface ultra-structure. Besides providing the topography of surfaces at the nanometer scale, AFM is may also be operated to study cells in air or liquid environment, obviating the need for any staining or the use of ultrahigh vacuum for sample analysis. A schematic diagram of AFM is presented on Figure 2.5.
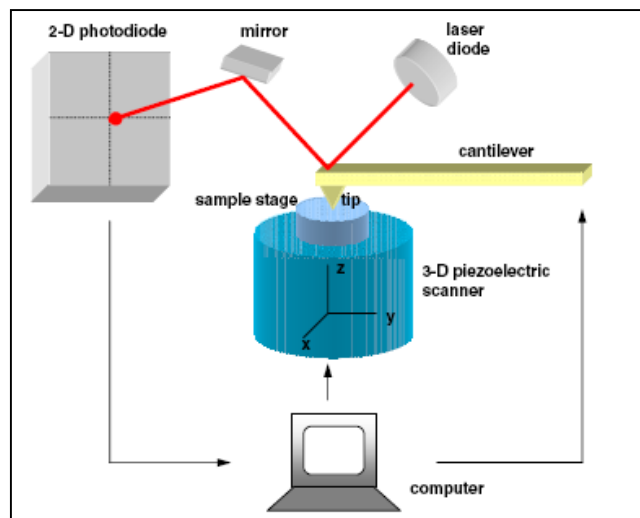
Figure 2.5 Schematic Diagram of Atomic Force Microscope (Lim et al., 2006)

2. 5. 2 Measurement of Force-Distance Curve using AFM

Recently, the use of AFM has been broadened to obtain experimental information about cell adhesion by measuring the force acting between the AFM tip and the sample, by means of force-distance analysis. Force distance curves are recorded by monitoring, at given x-y position, the cantilever deflection as a function of vertical displacement of the piezoelectric scanner. Different parts of force-distance curve can provide various information. The schematic diagram of idealized force-distance curve is shown in Figure 2.6.
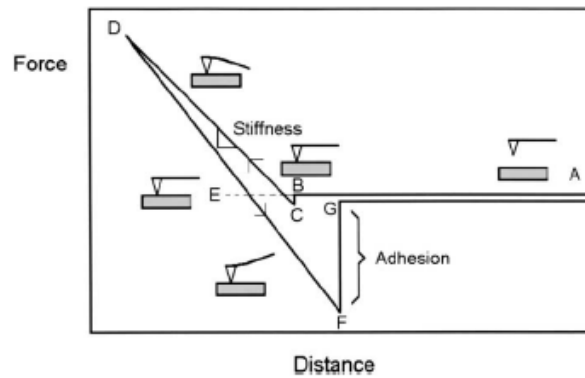
Figure 2.6 Schematic Diagram of Idealized AFM Force-Distance Curve (Beech et al., 2002)

At a far distance between the tip and the sample, the force experienced by the tip is zero (A-B). As the tip approaches the sample surface, the cantilever may bend upwards due to repulsive forces until it jumps into contact when the gradient of attractive forces exceeds the spring constant plus the gradient of repulsive forces (B-C). The approach portion of the force-distance curve can be use to estimate surface forces, including van der Waals and electrostatic, solvation, hydration, and steric/bridging forces. When the force is increased in the contact region (C-D), the shape of the approach curve may provide direct information on the elasticity of the sample. When the tip is retracted form the surface (D-E-F), the curve often shows a hysteresis (F-G) referred to as the adhesion force, which can be use to estimate the surface energy of solids or the binding forces between complementary molecules (Dufrene, 2002).

AFM continues to receive much interest, not only in biofilm research field but also in other research areas in microbiology. Besides its capability in capturing images at high resolution and providing three dimensional image of surface ultrastructure, force measurement with AFM can be used to probe the physical properties of the sample, such as molecular interaction, surface hydrophobicity, surface charges, and mechanical properties. These measurements can provide new

insight into the structure-function relationship of microbial surfaces and cells-surface interaction. Progress in research using AFM as force spectroscopy tools will be discussed briefly in Section 2.5.3.

2. 5. 3 Application of AFM in Force Measurement

Cell aggregation and adhesion towards surfaces plays a vital role in biofilm development. Understanding the molecular basis of these phenomena requires knowledge on the molecular interactions at the cell surface. Some approaches have been developed with the goal of probing molecular interaction and physicochemical properties by AFM. One attempt is the so called cell-probe method, where cells are attached directly to the AFM tip, and force-distance curve is recorded between the cell-coated tip and the surface. Using this method, forces between *E. coli* coated tip and various surfaces with different hydrophobicity have been measured (Ong *et al.*, 1999). The result revealed the role of hydrophobic interactions where behavior of both attractive forces and cell adhesion were promoted by surface hydrophobicity.

Force measurement using cell probes of different microorganisms causing corrosion on different metals had also been investigated (Sheng *et al.*, 2007). It was found that the bacterial adhesion force to metals is not only influenced by electrostatic force and metal surface hydrophobicity, but also by physiological properties of bacteria (i.e. surface charge and hydrophobicity). Further investigation revealed that interactions between bacteria and metal surfaces is influenced by nutrient, pH and the ionic strength of the solution (Sheng *et al.*, 2008). Cell-coated tip were also used in biomaterial research, where forces between *E. coli* and substrate coated with block copolymer was measured (Razatos *et al.*, 2000). Polymeric brush layers appeared not only to hinder the long-range attractive forces of interaction between bacteria and

substrates but also to introduce repulsive steric effects. Modification of the AFM tip with defined chemical groups had also been implemented. AFM tip has been functionalized by ionizable carboxyl groups to map the electrostatic properties for *S. cerevisiae*. Changes in adhesion forces and adhesion map contrasts were measured as a function of pH and shown to provide information on local isoelectric points (Ahimou *et al.*, 2002). In another study, a tip coated with *Staphylococcus epidermis* was used to study the differences in interaction between these bacteria to hydrophilic and hydrophobic surfaces (Boks *et al.*, 2008). A tip with immobilized *Streptococcus* bacteria was used in a study on its interaction with stainless steel to investigate the influence salivary conditioning film covering the metal surfaces (Mei et al., 2009). In both studies, the influence of hydrogen bonding has been observed. Hydrogen bonding interaction was decoupled from total interaction using Poisson analysis.

Force-distance curves have also been recorded between AFM tip and cells immobilized on solid substrate. The relative contribution of electrostatic and steric interactions associated with negatively charged bacterial strains were investigated. Forces were measured as a function of pH and ionic strength. The measured forces were represented well by an electrosteric repulsion model accounting for repulsion between the tip and bacterial polymers but were much larger in magnitude and extended over longer distance than predicted by DLVO theory. Varying the ionic strength did not affect the equilibrium length polymers nearly as much as pH (Camesano and Logan, 2000).

Immobilization of biomolecules onto an AFM tip has also been investigated to measure forces between individual ligands and receptors. Such studies have great potential in microbiology for mapping specific recognition sites at cell surfaces and new biomedical application (Zlatanova *et al.*, 2000).

Besides probing surface morphology and surface forces, AFM can also be used to characterize the local mechanical properties of the sample. One method that has been employed to measure local mechanical properties of bacteria was by force modulation microscopy (Fritz *et al.*, 1994). A strong contrast was observed in the force modulation images due to the presence of hard magnetosomes inside bacterial cells. This allowed discriminating between topological and local elasticity features in the AFM images. Another application is measuring elastic properties of proteinaceous sheath of archeon *Methanospirillum hungatei* GP1 in terms of the Young Modulus (Xu *et al.*, 1996). It was reported that the cell could withstand an internal pressure of 400 atm, beyond that needed for a eubacterial envelope to withstand turgor pressure.

Young Modulus of the cells has also been studied using nano indentation. In this method a micro bead attached to AFM cantilever is used to indent the surface of the cancer cells to measure its elasticity and investigate the corresponding sub-membrane cytockeletal structures (Li *et al.*, 2008).

Force measurement has also been used to observe changes in the mechanical properties of *P. chrysosporium* spores during germination. No significant deviation from linearity was seen from the contact region upon approach for dormant spores, whereas for germinating spores, a curvature was observed. This difference was consistent with the presence of proteinaceous layer on the surface of dormant spores and the absence of such layer in germinating spores (Dufrene *et al.*, 1999).

AFM force curves were obtained for different *Escherichia coli* strains, which were treated or untreated with gluteraldehyde, with the aim to probe the role of lipopolysaccharides in bacterial adhesion and cell elasticity (Velegol and Logan, 2004). Quantitative measurement of single biomolecules has also been studied by measuring the elongation force on the surface of germinating *A. oryzae* spores. These

forces were attributed to the stretching of cell surface polysaccharides (van der Aa *et al.*, 2001).

2. 5. 4 Single Molecule Force Spectroscopy using AFM

The distribution and adhesion properties of EPS on the cell surface can be probed with the use of AFM, using a technique known as single-molecule force spectroscopy (SMFS). Real-time AFM imaging only allows for visualization of cell ultra-structures. However, analysis of the conformational and nano-mechanical properties (adhesion and extension) of individual EPS or exopolymers on the microbial cell surface is made possible with the use of SMFS (Francius et al., 2008). In a typical SMFS experiment, adhesion properties are probed by measuring the interaction forces between the flexible AFM cantilever and the biopolymer by stretching the biopolymer (as shown by Figure 2.7a). Usually, a silicon nitride AFM tip or a functionalized AFM tip is used (Abu-Lail and Camesano, 2003a; Francius et al., 2009). Figure 2.7b illustrates the process that occurs during an AFM force measurement. This figure is different from Figure 2.6, where the adhesion peaks represent the rupture forces of the polymer and the separation distance represent the length of the polymer where the rupture occurs.

At location 1 (Figure 2.7b), no deflection is observed due to negligible or near zero forces experienced between the bacterial exopolymers and the AFM tip located far away. As the tip approaches the bacterial surface, the cantilever bends upwards due to induced repulsive forces. It jumps into contact when the gradient of the attractive forces exceeds the sum of the spring constant and the gradient of repulsive forces. This is given by location 2. Exopolymers on the bacterial surface will adsorbed onto the tip when contact is made. This portion of the force-distance curve can be used to estimate the types of interaction forces present. When the force is

further increased in this contact region, the shape of this portion of the force-distance curve can provide information on the elasticity of the sample.
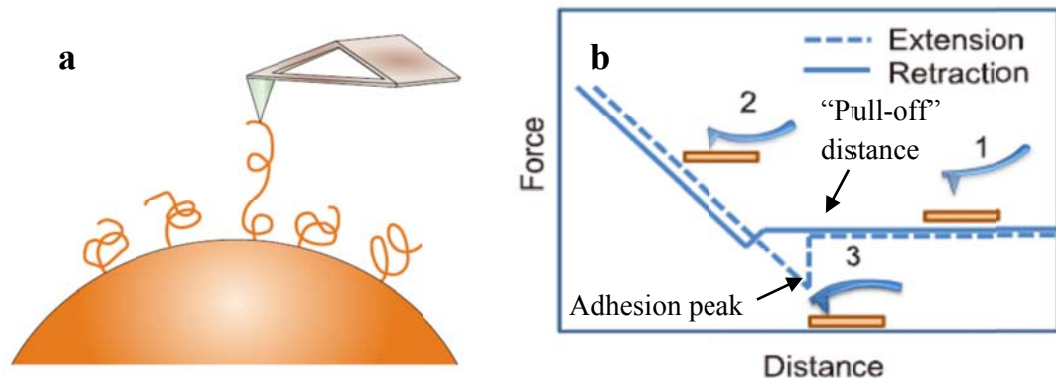
Figure 2.7 Illustrations of SMFS Experiments on Cell Surface with Corresponding AFM Force Distance Curve (Dufrene, 2004)

Upon retraction of the tip from the surface, attractive forces will cause the cantilever to bend downwards, as shown at location 3. A hysteresis effect will be experienced. The force required to pull the tip away from the surface is known as the "pull-off" force and the "pull-off" distance depends on the length of the polymer chain (Abu-Lail and Camesano, 2002; Jung et al., 2010). The adhesion peak observed indicates a rupture event where contact with molecules or molecules themselves break due to stretching and unfolding of molecules as the tip is retracted (Wright et al., 2010). Multiple adhesion peaks may also be observed, depending on the polymer type, polymer length, and whether one or multiple chains are adsorbed onto the tip. Even though different polymers portions or multiple polymers may have absorbed onto the tip, they will detach at different times. Therefore, each rupture event represents the adhesion of a single chain (Abu-Lail and Camesano, 2002; Jung et al., 2010).

Deflections of the AFM cantilever at given x, y locations as a function of the vertical displacements of the scanner will be recorded. The results can be transformed into force-distance graphs as shown in Figure 2.7b with appropriate corrections and

"zeroing" the force curves using the constant compliance regions. When multiple force-distance measurements are taken over a specified area, information on the distribution of elongation and adhesion events can be spatially resolved (Francius et al., 2009). In this way, microbial adhesion can be analyzed through mapping the nano-mechanical properties of EPS on the cell surface.

CHAPTER 3

MATERIALS AND METHODS

3. 1 Biofilm Characterization

3. 1. 1 Microbial Strains and Growth Condition

Pseudomonas aeruginosa NNRL-B3509 and *Bacillus subtilis* NNRL-NRS762 were obtained from Agricultural Research Service (ARS) Culture Collection, United States Department of Agriculture (USDA). Both bacteria were cultured in TGY medium containing 5 g/L tryptone, 5 g/L yeast extract, 1 g/L glucose, 1g/L K_2HPO_4 and pH 6.8 for 16-18 hours. Strains were grown in 300 ml Erlenmeyer flasks in an orbital shaker at 150 rpm and maintained at $30^{o}C$.

3. 1. 2 Optical Densities and Cell Enumeration

Batch cultures of 300 ml were routinely grown in conical flasks. Samples of 2 ml liquid medium were taken for measurement of optical density and colony forming units in the same time interval as the coupons. For optical density, absorbance of the cultures was measured using Biospec Mini UV-Vis Spectrophotometer at 600nm wavelength. For cell enumeration, serial dilution of liquid medium were made and 100μl of each dilution was spread onto TGY agar (similar composition with liquid TGY medium with addition of 20g/l agar) and colonies were enumerated after 24 hour incubation. In order to obtain optimum accuracy and reliability of a count, only colonies with total count of 30-300 were considered in this experiment.

To enumerate the viable cell on the biofilm, coupon samples were first washed with Phosphate Buffer Solution (PBS) and then immersed in 1 ml of fresh TGY medium in 10 ml vial. The vial containing coupon and medium was then sonicated in

a water bath for 3 minutes and 50 kHz to detach the sessile cells from the metal surface. Serial dilutions were then made on the medium containing the sessile cells and 100μl of each dilution was spread onto TGY agar and colonies were enumerated after 24 hour incubation at 37°C.

3. 1. 3 Stainless-steel Coupon Preparation

Stainless steel SS-316 coupons (10 mm diameter and 1 mm thickness) were polished using sand paper with various grit size (P400 to P2500), then with 0.3 micron alumina paste until a smooth finish was attained. Coupons were subsequently washed with copious amounts of water before being sonicated at 50 kHz for 5 minutes with acetone and finally rinsed with 70% ethanol. Cleaned and dried coupons were then stored in 70% ethanol prior to use.

3. 1. 4 Reactor System and Biofilm Development

Each overnight culture of bacteria was grown in a 500 ml Duran bottle with 300 ml working volume containing TGY medium for static biofilm development. Polished coupons were hung inside the bottle and subsequently withdrawn for biofilm analysis over a period of time. Schematic diagram of the biofilm reactor is shown in Figure 3.1.

3. 1. 5 Biofilm Dry Weight

Coupons were first washed with PBS solution to remove attached microorganisms and residual medium on the metal surface, and dried in an oven for at least 2 hours. Dry coupons were then weighed, followed by sonication using ethanol 70% for 5 minutes and 50 kHz to remove the biofilm from the metal surface. Coupons

were dried again inside the oven for at least 2 hours and their weight were measured. Biofilm dry weight was determined gravimetrically by weight difference.
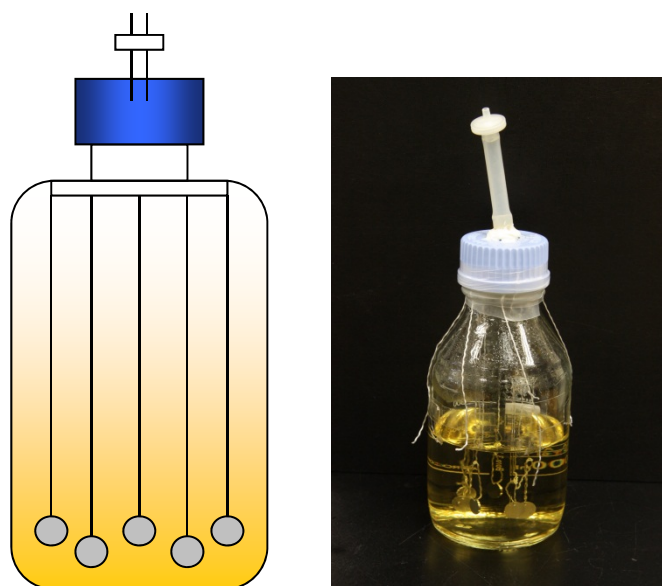
Figure 3.1 Schematic diagram of biofilm reactor

3. 1. 6 Scanning Electron Microscopy (SEM)

SEM analysis was conducted to observe the surface morphology. Samples were fixed with 3% gluteraldehyde (in PBS) for more than four hours, rinsed with PBS, and dehydrated with an ethanol gradient (25%, 50%, 70%, 90% and 99%) before final storage in desiccators. Prior to analysis, the coupons were coated with platinum at a voltage of 30 mV for 100 seconds. A scanning electron microscope (JEOL JSM-5600) with beam voltage 13-15 kV was used to visualize the morphology of the biofilm.

3. 2 Hydrophobicity Test

3. 2. 1 Salt Aggregation Test (SAT)

Overnight bacterial cultures were first harvested into 2 ml culture tubes, and centrifuged at 5500 rpm and 4°C for 10 minutes. Cell were then washed twice using

sodium phosphate buffer (0.002M, pH 6.8), and finally resuspended in the same buffer. Sodium phosphate buffer (0.002M, pH 6.8) was also used to dilute a solution of 4 M $(NH)_2SO_4$. Serial dilutions were made giving $(NH)_2SO_4$ concentration ranging from 4 M to 0.2 M, differing by 0.2 M per dilution. Bacterial suspensions of 25 μl were mixed with an equal volume of salt solution into 24 well tissue culture trays. The bacterial-salt mixtures were gently rocked for 2 minutes at 25^oC and a visual reading was performed against a black background. The results were expressed as the lowest molarity of ammonium sulphate causing bacterial aggregation. Experiments were done in triplicate on two separate occasions. The results were classified as follows: <0.1 M = highly hydrophobic, 0.1-1 M = hydrophobic, and >1 M = hydrophilic (Basson et al., 2008).

3. 2. 2 Bacterial Adhesion to Hydrocarbon (BATH)

Overnight bacterial cultures were first harvested into 2ml culture tubes and centrifuged at 5500 rpm and 4^oC for 10 minutes. The cells were washed twice with phosphate/urea/Mg (PUM) buffer (22.2 g/L K_2HPO_4, 7.26 g/L KH_2PO_4, 1.8 g/L Urea, and 0.2 g/L $MgSO_4.7H_2O$) and finally resuspended in the same buffer to obtain an absorbance of about 1.0 (A_o), measured at 600 nm on Shimadzu UV-Vis Spectrophotometer. 500μL of hexadecane was added to 5ml of microbial suspension and vortexed for 5 minutes. After standing for 15 minutes, the absorbance of the aqueous phase was measured (A_1). The degree of hydrophobicity was calculated as $[1-(A_1/A_o)]$ x 100%. The procedure was repeated in triplicate on two separate cultures (Pijanowska et al., 2007).

3. 2. 3 Contact Angle Measurement (CAM)

Contact angle measurement was made using the sessile drop method (1 μL sized liquid) using a VCA Optima goniometer (by AST Products Inc.). Approximately 30μl of concentrated overnight bacterial suspension was spread onto glass coverslips and left overnight to obtain thick cell lawns. The cell lawns then were collected and dried for at least 4 hours. Static liquid contact angles on cell lawns and SS-316 surfaces were measured at $25^{\circ}C$ and 60% relative humidity (van der Mei et al., 1987).

3. 2. 4 Emulsification Index (E)

The emulsifying capacity was evaluated by an emulsification index (E_{24}). The E_{24} of culture samples was determined by adding 2 ml of hexadecane to the same amount of culture, vortexing for 2 min and allowing the samples to stand for 24 h. E_{24} index is defined as the percentage of the height of the emulsified layer (mm) divided by the total height of the liquid column (mm). Measurements were also conducted with cell-free supernatants (Bento et al., 2005).

3. 3 Study of Cell Interaction

3. 3. 1 Zeta Potential and Equivalent Radius Measurement

Overnight samples of bacteria were harvested into 2ml tube and centrifuged at 8000 rpm for 15 minutes. After discarding the supernatant, the cells were washed three times using PBS solution (0.01M). The zeta potential of cells was analysed using Mavern Zetasizer Nano System. The same system was carried out to measure the equivalent radius of the bacteria using dynamic light scattering function of the

Zetasizer. The zeta potential of the stainless steel coupon was measured using the Adjustable Gap Cell of the SurPASS Electrokinetic Analyser (Anton Paar).

3. 4 Quantification of Spore Adhesion

3. 4. 1 Spore Growth and Staining

Overnight cell cultures were transferred to sporulation agar plates (Husmark and Ronner, 1990). The sporulation medium consisted of nutrient broth (8 g/L Difco), $MgSO_4$ (0.25 g/L), KCl (0.97 g/L), $CaCl_2$ (0.15 g g/L), $MnCl_2$ ($2x10^{-3}$ g/L), $FeSO_4$ ($0.3x10^{-3}$ g/L) and 3% Agar. The plates were left for 10 days at 25^oC. The spores were then harvested from the plates and washed by resuspension and centrifugation three times in 0.145 M NaCl, and stored in 4^oC.

Spore formation was confirmed by Schaeffer-Fulton staining technique. Two separate smears of the *B. subtilis* spore solution and cell solution on glass slides were stained with Malachite green and counter-stained with Safranin. The spores harvested would appear blueish-green while the vegetative cells would appear reddish-brown.

3. 4. 2 Atomic Force Microscopy (AFM) Imaging of Spores

AFM analysis was also conducted to observe the morphology of the spore. Dried in a dessicator, overnight *B. subtilis* spores on glass were used as samples in the AFM. All imaging was done in tapping mode using a Nanoscope IIIa Scanning Probe Microscope (Digital Instruments, Santa Barbara, California, USA) with a 'J' Scanner (AS-130, Digital Instruments). Both height and phase images were captured. The scan rate was 0.5 Hz.

3. 4. 3 Fourier-Transform Infra Red (FTIR) Spectroscopy

FTIR analysis was also conducted with FTIR 8400m (Shimadzu, Japan) to compare the infrared spectrum of the *B. subtilis* spores and cells. Dried in a dessicator, overnight *B. subtilis* spores and cells on glass slides were used as samples in the FTIR. Two consistent readings were taken for each sample for the region of wavenumber between 4000 and 500 cm^{-1} which holds characteristic bands that are suitable for the characterization of microorganisms.

3. 5 Atomic Force Microscopy (AFM) Force Measurement

3. 5. 1 Preparation of Cell Probe

A triangular shaped cantilever (Veecoprobes Nanofabrication Center, CA) with a spring constant of 0.12 ± 0.01 N/m (calibrated using thermal tune software) was exposed in UV chamber for 15 min. The silicon nitride cantilever tip was exposed to 4 mg/mL dopamine hydrochloride (99%, Sigma) in 10 mM TRIS buffer (pH 8.5) solution for 1 h to coat the inner surface of the tip with the polydopamine (Kang and Elimelech, 2009). The cantilever was then washed with DI water and dried under vacuum. To immobilize bacterial cells on the cantilever, 10 µL of prepared cell suspension was spread onto a polished stainless steel surface placed onto AFM piezoholder and active cells were then transferred to the end of the prepared AFM tip by slowly moving the tip holder downwards until it touches the cell suspensions, and holding for one minute to allow adhesion of the bacterial cell. The bacterial cell coated AFM tip was further confirmed by scanning electron microscopy.

3. 5. 2 Quantification of Force Measurement

All force curves were obtained using Multimode Picoforce AFM coupled to an upright microscope at room temperature using fluid cells buffered with PBS solution (pH 7.1). Cantilevers with spring constant 0.12 ± 0.01 N/m, determined using thermal tune module, were used in all the force measurements, where the cantilever was moved at a velocity of 500 nm/s with a piezo movement of 1000 nm at a resolution of 3584 data points. The duration of contact time between the cell probe and SS316 surface before the force measurements were taken (termed "surface delays") was varied between 0 and 60 seconds. Data were sampled more than 10 times at each of the three locations on the SS surface. The total experimental time did not exceed two hours to ensure the viability of the single cell at the end of each cantilever (Kang and Elimelech, 2009). Raw data were converted from cantilever deflection during the approach and retraction, into force versus distance curves using the software V613r1 (Nanoscope).

3. 5. 3 Single Molecule Force Spectroscopy (SMFS)

Prior to AFM probing, cells were immobilized by filtering concentrated cell suspension through a porous cellulose acetate membrane (Millipore) with 0.2μm pore size. The membrane was then carefully cut (1cm x 1cm square) and attached to a steel sample puck (Veeco Metrology Group) using double-sided adhesive tape. AFM tips were functionalized with polydopamine by exposure to 4mg/ml dopamine hydrochloride (99%, Sigma) in 10mM TRIS buffer (pH 8.5) for 1h.

AFM force-distance curves were recorded at room temperature (25°C) in PBS solution (pH 7.4) using a Nanoscope IV Multimode AFM (Veeco Metrology Group) and oxide-sharpened microfabricated silicon nitride tip cantilevers (Veecoprobe

Nanofabrication Centre, CA). The spring constant of the cantilever was measured using the thermal noise method (Picoforce, Veeco Metrology Group). SMFS measurements were performed using a constant approach and retraction speed of 1.0 μm/s. Mechanical properties were mapped by recording force-volume images consisting of arrays of 10 x 10 force curves.

3. 6 Study of Extracellular Polymeric Substances (EPS) Properties

3. 6. 1 Extraction of EPS from Cell Suspension

10 ml of bacterial suspension samples were taken and centrifuged at 5000 G and 4°C for 20 minutes. After the supernatant was separated, the concentrated biomass was then re-suspended in a 10ml of aqueous solution containing 0.85% NaCl and 0.22% formaldehyde at 80°C for 30 min for EPS extraction. The EPS dissolved in the formaldehyde solution was recovered by further centrifugation at 4°C, 15000 G for 30 min (Fang *et al.*, 2002).

3. 6. 2 Extraction of EPS from Biofilm

Biofilm-coated coupons were removed from each reactor after three days and immersed in PBS buffer. Biofilm was scrapped form each coupon using sonicator for 5 minutes and 50 kHz, and then centrifuged at 5000 G and 4°C for 20 minutes. The concentrated biomass was then re-suspended in a 10ml of aqueous solution containing 0.85% NaCl and 0.22% formaldehyde at 80°C for 30 min for EPS extraction. The EPS dissolved in the formaldehyde solution was recovered by further centrifugation at 4°C, 15000 G for 30 min (Fang *et al.*, 2002).

3. 6. 3 Chemical Composition Analysis based on ATR-FTIR

FTIR spectroscopy was performed with a Bio-rad FTS-3500ARX FTIR (Excalibur Series) in attenuated total reflection (ATR) mode, in the range of 400 – 4000 cm^{-1} with a 4cm^{-1} resolution and 64 scans per spectrum. Measurements were obtained using a trough-style sample holder with a ZnSe internal reflection element (IRE) subjected to a nominal incident beam angle of 45°. Noise from water was automatically filtered out. Pure EPS extracting solution containing 0.85% NaCl and 0.22% formaldehyde was used as background for all ATR spectra.

3. 6. 4 Carbohydrate Analysis

Anthrone test was used to determine the carbohydrate concentrations in the EPS samples. 0.1% anthrone solution is made up in 75% (v/v) sulphuric acid at least 2 h before use. This reagent was freshly prepared on each day of analysis. Glucose solution of 100 mg/l was used as a standard. 1ml of the sample and standard solution was transferred into Pyrex test tubes, followed by the addition of 1 ml of cold anthrone reagent. The test tubes were closed with rubber stoppers and immediately shaken. The test tubes were then placed in a water bath at 100°C for 14 minutes and cooled in a water bath at 5°C for 5 minutes. The absorbance of the samples and standards were then measured using a spectrophotometer at 625 nm (Ahimou et al., 2007b).

3. 6. 5 Protein Analysis

Lowry test was used to determine the protein concentration in the EPS samples. Stock solutions of reagent A containing 2.0% Na_2CO_3, 0.4% NaOH, 0.16% sodium tartrate and 1% SDS, and reagent B containing 4% $CuSO_4.5H_2O$ were prepared. These solutions were stable indefinitely when stored at room temperature.

On the day of use, Folin-Ciocalteu phenol reagent was diluted 1:1 with distilled water. 100 parts of reagent A were mixed with 1 part of reagent B to form reagent C, the alkaline copper reagent. A sample volume of 1 ml containing 10 to 100 pg of protein, plus sucrose or EDTA when indicated, was added to 3 ml of reagent C and incubated at room temperature for 10 to 60 min without change in the final absorbance. The samples were mixed vigorously with 0.3 ml of diluted phenol reagent and incubated for 45 min at room temperature. The absorbance of the samples on the spectrophotometer were then taken at 660 nm (Markwell *et al.*, 1978)

3. 6. 6 X-ray Photoelectron Spectroscopy (XPS) Analysis

XPS spectra of EPS extracted solutions were acquired using a KRATOS AXIS UltraDLD System Photoelectron Spectrometer. The data were gathered using a monochromatised Al Kα X-ray source (1486.71eV) at 15kV and 5mA. The takeoff angle between the substrate normal and the detector was fixed at 90°. 100μl of air-dried EPS extracted solution deposited on cleaned glass chips were mounted on standard sample studs using double-sided adhesive tape. Survey spectrum pass energy of 160eV for acquiring the wide spectrum and narrow scanning spectrum pass energy of 40eV for individual photoelectron lines were used. Binding energies were calibrated using the C 1s peak at 285.0eV.

3. 6. 7 Gel Permeation Chromatography (GPC)

Molecular weights of different components in the EPS extracted samples were chromatographed by GPC using a Waters HPLC system equipped with a model 2414 refractive index detector, a model 1515 isocratic HPLC pump and an Agilent PL aquagel-OH MIXED-M column (8μm, 7.5 x 300 mm). All measurements were done at 35 °C, using ultrapure water as an eluent at a flow rate of 1.0 ml/min and a sample

injection volume of 10μl. All samples were filtered with 0.45mm filters (Millipore) prior to injection. The molecular-mass range and retention characteristics of the column were calibrated with polystyrene standards.

3. 6. 8 MALDI-TOF Analysis

EPS extracted samples were analyzed via matrix-assisted laser desorption ionization time-of-flight mass spectroscopy (MALDI-TOF-MS) using an Autoflex II MALDI-TOF mass spectrometer (Bruker Daltonics). 0.5μl of matrix solution 2,5-Dihydroxybenzoic acid (2,5-DHA) and 0.5μl of analyte EPS extracted solution were mixed and spotted on a MALDI sample plate and air-dried at room temperature. The matrix solution is composed of 10mg/ml of α-cyano-4-hydroxycinnamic acid in 50% acetonitrile and 0.1% TFA.

CHAPTER 4

CHARACTERIZATION OF BIOFILM FORMED BY

P. AERUGINOSA AND *B. SUBTILIS* ON STAINLESS STEEL

A study of attachment processes in biofilm formation is important because it is considered as the crucial step in biofilm formation where it sets the foundation for mature biofilm formation. Attachment processes are affected by the chemical and physical environment to which the bacterial cell and the surface are exposed. The multiple factors involved in the cell attachment, such as temperature, nutrient limitation, or pH make it difficult to characterize the role and the overall importance of each factor in the attachment process.

In this chapter, the attachment process of bacterial biofilm formed by *Pseudomonas aeruginosa* NRRL-B3509 and *Bacillus subtilis* NRRL-NRS762 were investigated. Morphology of the biofilm was observed along with the characteristics of bacterial growth in the bulk phase and in the biofilm. FTIR spectroscopy was performed to analyze the changes on the surface of the stainless steel coupon. Zeta potentials were also measured to observe the effect of physicochemical properties on biofilm formation.

4. 1 Biofilm Morphology

Figure 4.1 and Figure 4.2 show that single culture biofilm was formed by both bacterial strains, showing rod shaped where *B. subtilis* NRRL- NRS762 was longer than *P. aeruginosa* NRRL-B3509. These SEM figures showed evidence that during biofilm development *P. aeruginosa* show no significant change in length size, which is around 1 to 2 micron, while for *B. subtilis* is around 2 to 8 micron. Size of both

bacteria found in this study is comparable with other studies, where *P. aeruginosa* are known to have length size 1-5 µm (Costerton and Anwar, 1994; Lederberg, 2000), while *B. subtilis* are 2.5-6.6 µm (Sargent, 1975).
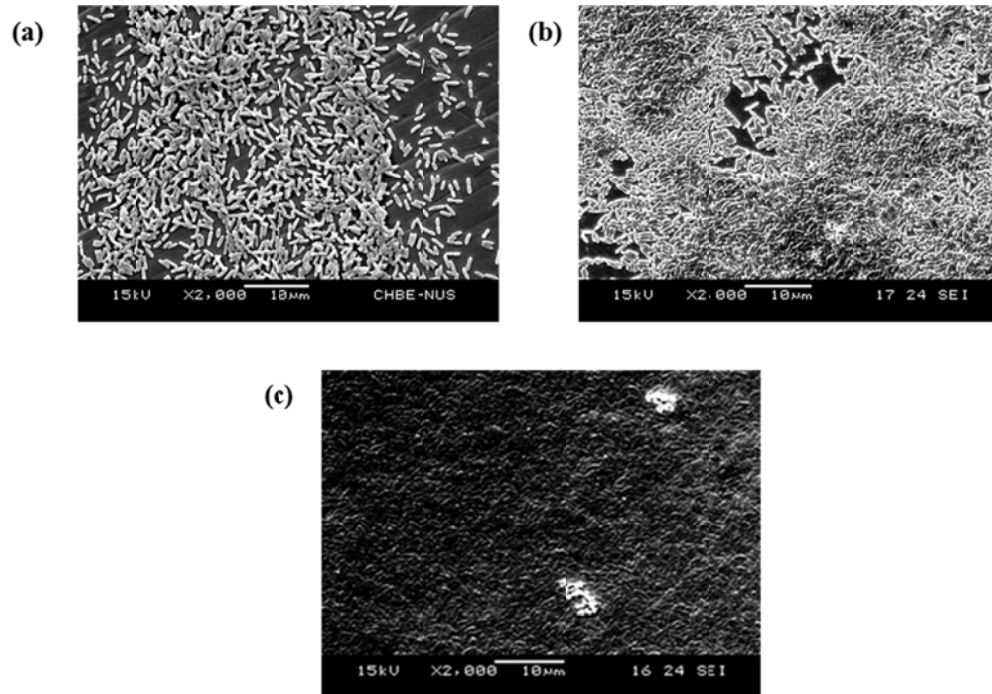
Figure 4.1 SEM observation of *P. aeruginosa* NRRL-B3509 during biofilm growth: (a) 1 hour; (b) 10 hours; and (c) 24 hours

Biofilms develope over time, beginning with the random attachment of bacteria, and becoming denser as the biofilm ages, and covering the metal surface. With bacterial growth, the bacteria were clumped together, forming thicker biofilms with decreasing coverage area. It is also evident that over time, the surface is covered by EPS which causes the structure of biofilm become denser and thicker.

Biofilm formation of *P. aeruginosa* occurs faster than *B. subtilis*. Comparing Figure 4.1a and Figure 4.2a, denser accumulation of *P. aeruginosa* was evident as early as 1 hour compared to *B. subtilis* where only sparse colonies were found on the metal surface.

It is also found that for *P. aeruginosa*, the biofilm coverage contracted from 10 to 24 hours, due to two reasons. First, as the biofilm ages, more of bacteria are

attached on the surface. However, some bacteria will also detach from the mature biofilm and return to the bulk phase as planktonic cells to colonize new surfaces causing reduction of biofilm coverage. Second, biofilm is not uniformly formed on the surface. In this experiment, at least three metal coupons were analysed for biofilm morphology (scanned using SEM) at each time of sampling. SEM image at 10h and 24h biofilm formation were taken from different coupons, hence a difference in biofilm coverage is observed. However, from these figures it can be concluded that the biofilm density increased over the time.

An interesting phenomenon was observed for the 10 hr biofilm of *B. subtilis*. With slow biofilm development, at 10 hours sample, it was shown that *B. subtilis* formed an orderly biofilm, with longer size (around 6 to 8 micron). During this time, the *Bacillus* is at the end of its exponential phase (at around 10 hours, see Figure 4.3 and Figure 4.4b). Over the time, however, the biofilm was covered by EPS which alters the biofilm structure. *B. subtilis* have been reported to typically grow up to a length from 2.5 to 6.6 micron, depending on the growth medium and various conditions, such as temperature, medium composition, and pH (Sargent, 1975). Such significantly longer *Bacillus* rods have not been previously reported elsewhere.
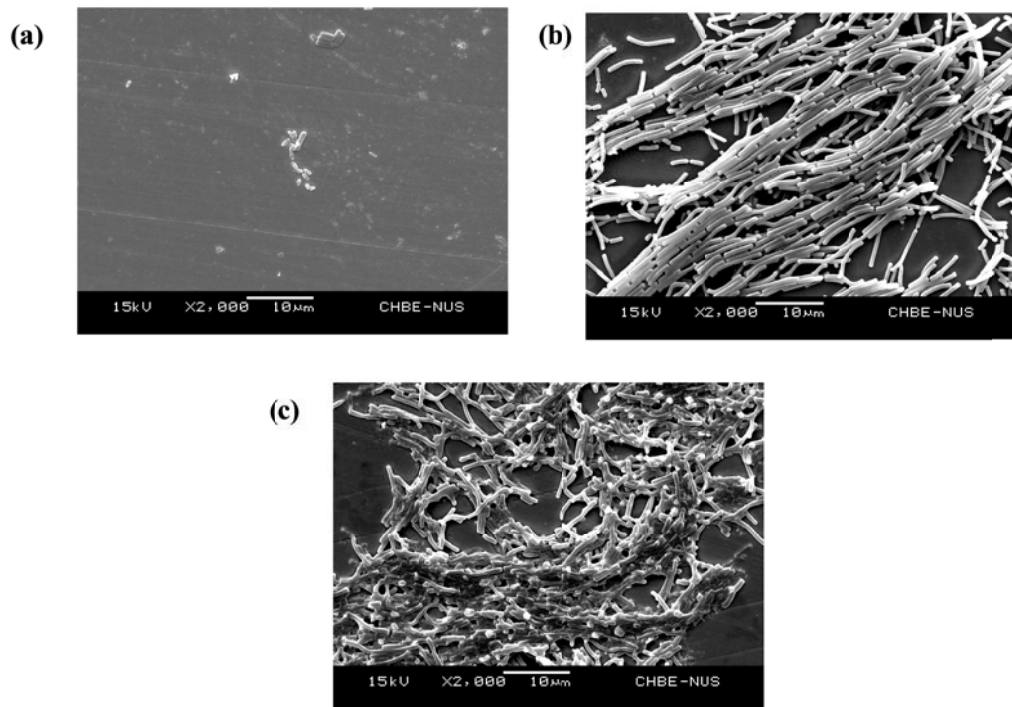
Figure 4.2 SEM observation of *B. subtilis* NRRL-NRS762 during biofilm growth: (a) 1 hour; (b) 10 hours; and (c) 24 hours

Initial attachment of microorganisms is reported to be dependent on the interaction between the cell wall and the underlying solid surface, and biofilm formation of bacteria were found to be related to the hydrophobic interaction between the bacteria and stainless steel surfaces (Blaschek et al., 2007).
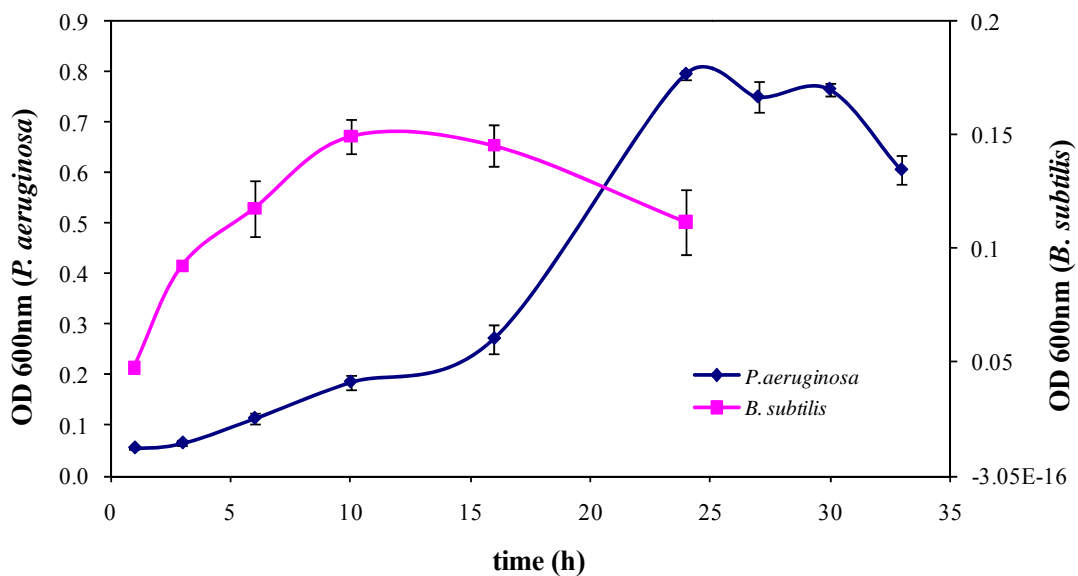
Figure 4.3 Comparison of Optical Density of *P. aeruginosa* and *B. subtilis* (at 600 nm)

4. 2 Bacterial Growth on Suspensions and Biofilm

Growth of both bacteria in the suspension (i.e., the planktonic cells) for the first hour of experiments showed similar trend (Figure 4.3) where the optical density (absorbance) at 600 nm was about 0.05. However, with time, *P. aeruginosa* exhibited a longer growth cycle. At 24 hours, *P. aeruginosa* reached the end of the exponential phase, while *B. subtilis* was already into the stationary phase. After 24 hour, *P. aeruginosa* entered the stationary phase until 33 hour when the death phase occurred.

An enumeration of colony forming unit (CFU) for both bacterial strains also revealed the same trend. Figure 4.4 shows *P. aeruginosa* reached higher CFU than *B. subtilis* early in the batch cycle and with exponential phase between 10 hours and 24 hours. The death phase occurred after 30 hours.
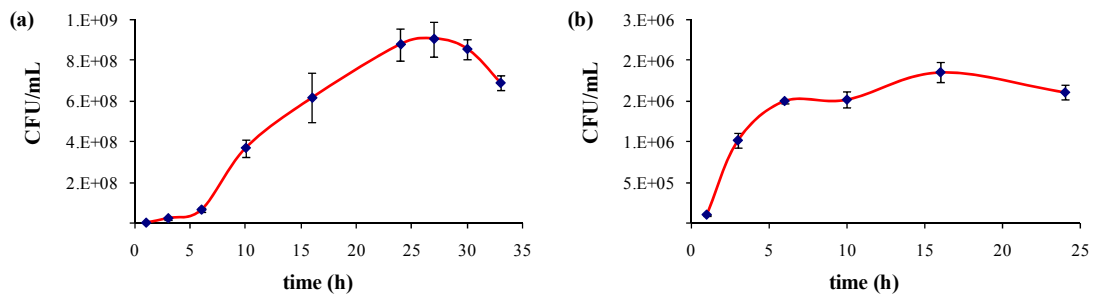
Figure 4.4 Comparison of CFU of planktonic cells: (a) *P. aeruginosa* and (b) *B. subtilis*

Maximum specific growth rate (μ_{max}) for *P. aeruginosa* and *B. subtilis* was found to be 0.108 h^{-1} and 0.069 h^{-1} for *B. subtilis* respectively. The growth rate of *P. aeruginosa* is consistent with other research, which reported that maximum growth rate of this strain is on the range of 0.05 to 0.3 h^{-1} (Wu and Livermore, 1990; Tamagnini and Gonzalez, 1997; Guina et al., 2003). However, for *B. subtilis*, the growth rate was significantly lower than other reported values, in the range of 0.5 to 2 h^{-1} (Sargent, 1975; Wu et al., 2000). One likely reason is the experimental condition;

in our experiments, the cultures were unshaken and unstirred (i.e., surface aeration) unlike other fully aerated reactors used by other researchers.

The growth of biofilm, as confirmed in SEM picture, was faster for *P. aerugionsa* strain compared to *B. subtilis*. Results from biofilm recultured by sonication followed by agar spread method showed that cell counts found in *P. aeruginosa* were of the order of six, while *B. subtilis* were of the order of three (Figure 4.5). *P. aeruginosa* also showed higher biofilm dry weight compared to *B. subtilis* (Figure 4.6), which further confirm higher density of the former bacterial biofilm as shown in the SEM picture (Figure 4.1and Figure 4.2)
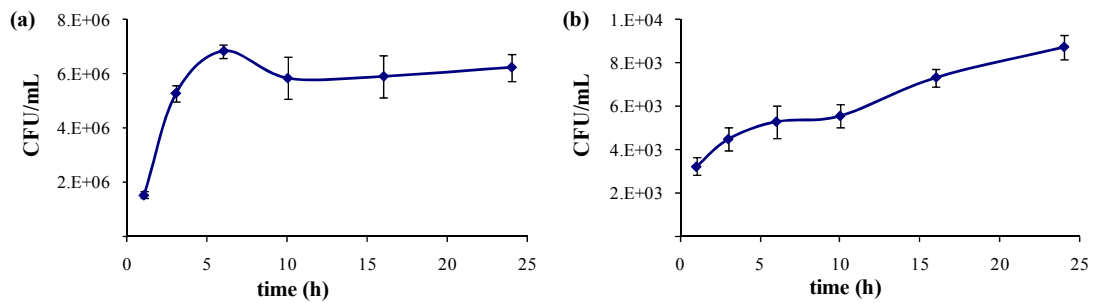
Figure 4.5 Comparison of CFU of bacteria in the sessile cells: (a) *P. aeruginosa* and (b) *B. subtilis*
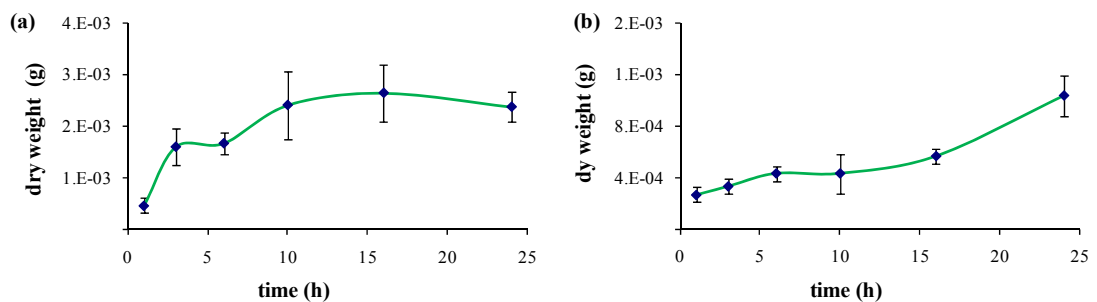
Figure 4.6 Biofilm dry weights of both bacterial strains: (a) *P. aeruginosa* and (b) *B. subtilis*

The more rapidly formed and denser biofilm by *P. aeruginosa* might be due to the higher maximum specific growth rate. Higher growth rates cause higher competition among bacteria on utilizing the nutrient in the medium. Since biofilm

formation is one of the defensive ways of microorganism surviving a lack of nutrient, more of such bacterial cells become sessile and form biofilm.

4. 3 Analysis of Surfaces

The FTIR spectra of biofilm development of *P. aeruginosa* and *B. subtilis* are illustrated in Figure 4.7 and Figure 4.8 respectively. It is evident from a comparison of these figure (over the wavenumber range of 900-1800 cm^{-1}) that *P. aeruginosa* exhibited significant changes compared to *B. subtilis*. The FTIR spectra also showed that the % transmittance of the bare metal on *B. subtilis* experiment is slightly higher than on *P. aeruginosa*. This might be due to differences in the infrared intensity on each experiment.

The amide I ($\sim$1650 cm^{-1}) and amide II ($\sim$1550 cm^{-1}) bands of the FTIR spectra are used as universal probes for proteins because the peptidic acid bond is a basic and repetitive functional group in proteins (Marcotte et al., 2007). The amide I band is generally more intense than amide II band, but some polysaccharides, such as alginate, give rise to an intense band associated with the C-O stretching vibrational mode located at 1610 cm^{-1} (Silverstein et al., 1991). The bands near 1640 cm^{-1} become more prominent during biofilm growth. This band correspond to amide I, (C=O) with different conformation. The intense bands near 1500 cm^{-1} correspond to the symmetric deformation of NH_3^+ absorbed onto the surface of the metal. The bands near 1410 cm^{-1} correspond to the symmetric stretches mode of carboxylate group, which manifest the interaction between –COO⁻ group and the metal surface.
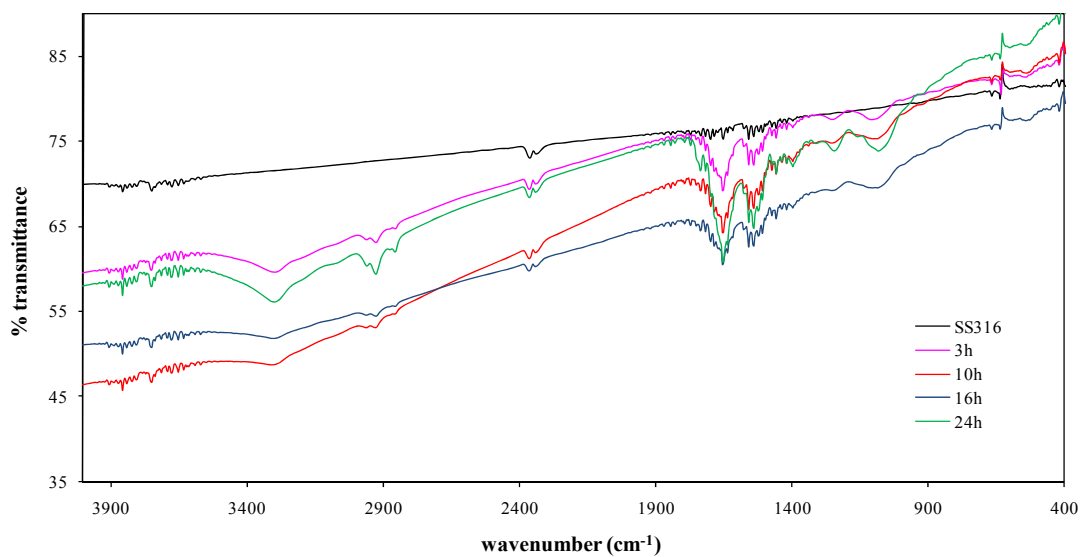
Figure 4.7 FTIR spectra of the biofilm developed by *P. aeruginosa* on SS316 at different time
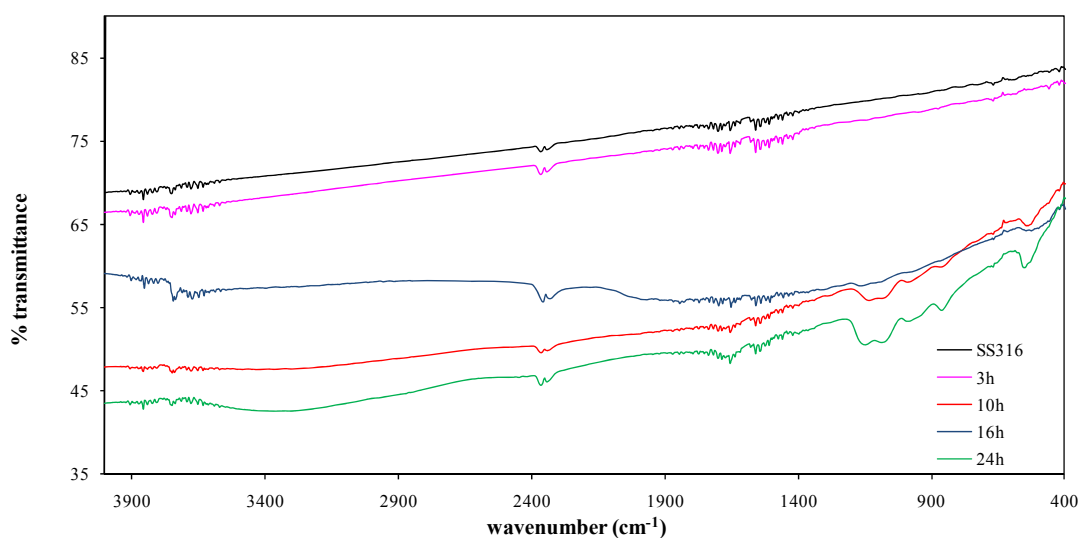
Figure 4.8 FTIR spectra of the biofilm developed by *B. subtilis* on SS316 surfaces at different time

The results suggest that the changes in chemical bonding with the surface atoms during the initial attachment of the biofilm involve COO^- and NH_3^+ interaction. These results are in general agreement with the findings of Fletcher and Marshall (1982), who suggested that proteins often function as adhesives in specific attachment mechanism.

B. subtilis showed no significant change in FTIR spectra in the same wavenumber range with *P. aeruginosa*, thus suggesting that this strain produced no significant amount of surface proteins as component of extracellular polymeric substances (EPS) during initial attachment of biofilm. Since EPS is considered as essential factor in biofilm maturation, this is consistent with our earlier observation that biofilm formation of *B. subtilis* was slower and not as thick as the biofilm of *P. aeruginosa* (as seen in Figure 4.1 and Figure 4.2).

4. 4 Effect of Surface Charge on Biofilm Formation

The electrostatic charge of the bacterial surface was inferred from zeta potential measurements at $37^{o}C$ in their respective TGY medium. Both strains were found to be negatively charged. As shown in Figure 4.9, the zeta potential of *P. aeruginosa* was in the range of -20 to -30 mV, while for *B. subtilis* was in the range of -30 to -38 mV. Meanwhile, the pH of both *P. aeruginosa* and *B. subtilis* are remained relatively constant at between 7.2 and 7.3.
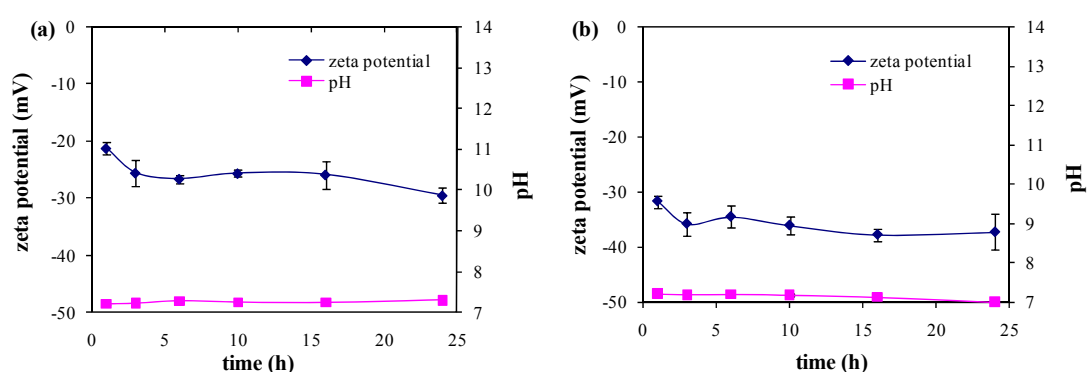
Figure 4.9 Zeta potential and pH during biofilm growth on: (a) *P. aeruginosa*; and (b) *B. subtilis*

Most bacteria possess negative surface charges which originate from the lipopolysaccharides of the cell envelope and/or acidic functional groups on the

proteins of the pili (Bayer and Sloyer Jr, 1990; Dorobantu et al., 2008). Since *B. subtilis* shows a more negative zeta potential than *P. aeruginosa*, it suggests that the stability of *B. subtilis* in the medium suspensions is higher than *P. aeruginosa*, which renders it is more unlikely for this bacteria to attach to the metal surface. This is confirmed by CFU count and dry weight measurement of the biofilm, which were found to be lower for *B. subtilis* as shown in Figure 4.4 and Figure 4.5 respectively.

Result from this experiment suggests that biofilm would be more likely to occur in the presence of *P. aeruginosa* strain. Since both strains are commonly found in industries, concerns about biofilm formation would be higher on *P. aeruginosa* presence, as initial attachment is the crucial step in biofilm formation. This experiment also showed the likelihood of *P. aeruginosa* and *B. subtilis* to establish biofilm and become persistent in the environment.

However, in order to observe the mechanism of biofilm development of these bacterial strains, it is important to study further the interactions that occur between bacterial and substrate surfaces during the adhesion process. In addition to the interactions, properties of interacting surfaces also play important role in the mechanism of biofilm formation. Details of study investigating the surface properties and interactions between bacteria and SS316 related to adhesion process are discussed in Chapter 5.

4. 5 Summary

In this study, initial attachment of microorganism on biofilm formation of *P. aeruginosa* and *B. subtilis* on SS316 surfaces has been monitored. Both model bacteria are found to form biofilm within 24 hours with denser and more rapid formation from former bacteria which is indicated in the SEM images, biofilm cell count, and biofilm dry weight calculations.

Rapid biofilm formation by *P. aeruginosa* was caused by its higher growth rate, inducing sessile cells growth due to stronger competition for nutrients. Higher surface protein contents on *P. aeruginosa*, as indicated in FTIR spectra, also lead to denser biofilm formation. Protein as a component in extracellular polymeric substances (EPS), will enhance the attachment of the bacteria onto the metal surfaces. In addition, rapid attachment of this bacteria is also influenced by lower stability in the medium (indicated by surface charge) where the bacteria will likely to be attached on the metal surfaces. This study shows the likelihood of *P. aeruginosa* and *B. subtilis* to establish biofilm and become persistent in the environment, where biofilm would be more likely to occur in the presence of *P. aeruginosa.*

CHAPTER 5

ROLE OF SURFACE AND INTERACTION ENERGIES ON ADHESION MECHANISM OF *P. AERUGINOSA* AND *B. SUBTILIS* ON STAINLESS STEEL

Adhesion forces are dependent on the surface property of bacteria, such as hydrophobicity and surface charge. They are also dependent on the physicochemical properties of the solid surface, such as surface energy. When a surface is immersed in an aqueous solution, molecules or atoms at the surface will interact with molecules or ions in the solution, and the type of forces and interactions will depend on the chemistry of both solid and liquid. Therefore the surface energy of a solid surface gives a direct measure of the intermolecular or interfacial attractive forces (Liu and Zhao, 2005).

In this chapter the adhesion interactions between the two model bacteria, *P. aeruginosa* and *B. subtilis* and stainless steel SS316 were investigated. A theoretical approach using DLVO and extended DLVO (xDLVO) theories was used to calculate the interaction energies between the bacteria and the metal surfaces. The effect of surface energies on bacterial adhesion has been elucidated using this approach in conjunction with the direct force measurement using AFM force spectroscopy.

5. 1 Influence of Physico-Chemical Properties on Bacteria-Metal Interaction

To determine free surface energy components for the three solid surfaces (SS316 and two bacterial surfaces), measurement of contact angles using three different liquids are required to solve equation 5 (Section 2.3.1). Table 5.1

summarizes the various surface energy components of the three liquids used to determine the contact angles (Van Oss, 1993; Liu and Zhao, 2005). Both water and ethylene glycol are polar components, showed by non-zero values of γ^+ and γ^-, showing electron donor-acceptor interactions, while hexadecane has zero value for both γ^+ and γ^-, indicating non-polar properties. Measuring contact angles of stainless steel and cell lawn using these three different liquids and calculation of surface energy by using equation 5 (Section 2.3.1) will yield the surface energy components for each surface as shown in Table 5.2. Comparable values of surface energy components the three surfaces have been reported in other studies (Grasso et al., 1996; Liu and Zhao, 2005; Chen et al., 2010). Measurement of surface energy component for both bacteria revealed negligible value of γ^+ and sizeable value of γ^-. This shows the monopolarity properties of the hydrophilic surface which leads to the tendency to favor electron donation and hence result in strong acid base repulsion (Van Oss, 1993).

Table 5.1 Surface energy components of the liquids used in contact angle measurement (Van Oss, 1993; Liu and Zhao, 2005)

Surface Tension (mJm^{-2})	γ_L	γ_L^{LW}	γ_L^{AB}	γ_L^+	γ_L^-
Water (W)	72.8	21.8	51.0	25.5	25.5
Hexadecane (HD)	27.47	27.47	0	0	0
Ethylene Glycol (EG)	48.0	29.0	19.0	1.92	47.0

Acid base interaction is also related to the differences in the value between γ^+ and γ^- of the particles and that of water. For both bacteria, values of γ^+ were lower than water while values of γ^- were higher than water. This indicates the surfaces have stronger affinity towards water, resulting in hydrophilic repulsive interaction with SS316 surfaces (Van Oss, 2006). As shown in Table 5.2, values of γ^+ and γ^- of

Bacillus subtilis is higher than *Pseudomonas aeruginosa*. From this data, we can expect that hydrophilic repulsion interaction is more pronounced for *Bacillus subtilis*. However, both bacteria and metal have higher value of γ^{LW} compared to water. This would result in attraction interaction between the two surfaces (Van Oss, 2006). It means that adhesion might still occur between bacteria and metal surface.

Table 5.2 Contact angles, zeta potential, and surface energy component of stainless steel and bacteria

Surface	Contact angle θ (°)			Zeta Potential ζ (mV)	Surface energy components (mJm^{-2})				
	θ^w	θ^{HD}	θ^{EG}		γ^+	γ^-	γ^{LW}	γ^{AB}	γ^{TOT}
SS316	86.8 ± 6.1	14.6 ± 7.4	59.7 ± 9.6	-337 ± 4	0.65	4.16	26.59	3.28	34.68
P. aeruginosa	47.9 ± 8.7	0	47.2 ± 5.4	-12.4 ± 0.8	0.15	46.43	27.47	5.25	79.30
B. subtilis	29.8 ± 8.9	32.2 ± 5.8	44.7 ± 8.7	-18.9 ±0.7	0.22	72.67	23.41	7.95	104.25

Table 5.2 also shows surface potential of stainless steel and both bacteria in terms of zeta potential, which were found to be negative for all surfaces, with stainless steel having the highest negative value. Zeta potential of stainless steel was measured over the range pH 4 to 9 using Surpass Electrokinetic Analyzer (Figure 5.1), with a value of -337 ± 4 mV at pH 6.8. Such a high value of zeta potential for stainless steels has earlier been reported (Sheng et al., 2007, 2008).
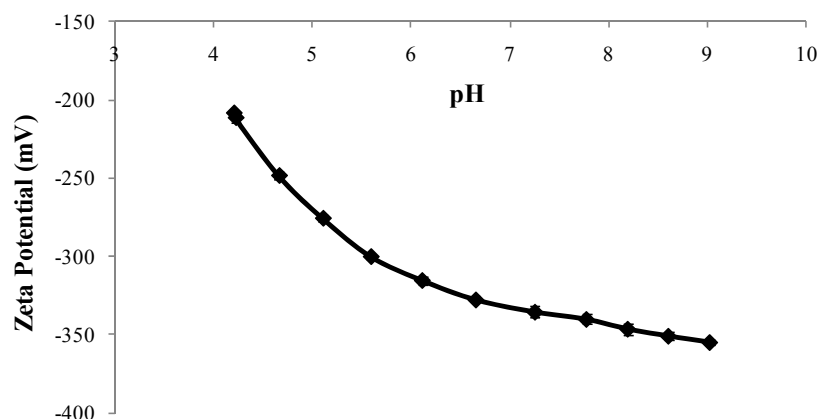
Figure 5.1 Zeta potential of SS316 measured by AGC Surpass Elektrokinetic
Analyzer

Most bacteria possess negative surface charges, which originates from the lipopolysaccharides of the cell envelope and/or acidic functional groups on the proteins of the pili (Bayer and Sloyer Jr, 1990; Dorobantu et al., 2008). Negative charges for both bacteria and metal surfaces will result in electrostatic repulsion interaction. However, since *P. aeruginosa* has lower zeta potential than *B. subtilis*, the former shows less repulsive force of interaction than the latter. Despite both surfaces being negatively charged, electrostatic attraction can still occur. When a charged particle (such as bacteria) approaches a charged-conducting material (such as SS316), a so-called image-charge will develop in the conducting material. This image-charge will be opposite in sign to the charge of the approaching particle and will form or disappears by charge rearrangement in the conducting materials upon approach or retract of the charged particle from the surface, respectively. Upon contact, the attractive force between the negatively charged particle and its image charge is maximal, hence the interactions with the image charges cause an additional attraction between SS316 and the negatively charged bacteria (Mei et al., 2009).

Hamaker constant (A) is the property of two surfaces that identify their interaction strength in the medium and depends on the dielectric properties of the surface, medium, and the cell in the case of microbial adhesion (Hermansson, 1999). For both the model organisms examined, A is positive (Table 5.3) which results in negative interaction potential, i.e. attraction interaction (Malmsten, 2003). Positive value of A for aqueous media has also been reported elsewhere (Norde and Lyklema, 1989). Since the Hamaker constant of *P. aeruginosa* is higher than *B. subtilis,* the attraction interaction between *P. aeruginosa* and stainless steel is greater than *B. subtilis*.

Table 5.3 Hamaker constant and equivalent radius of bacteria

Bacteria	Hamaker Constant (A)* $(J \times 10^{20})$	Equivalent Radius R (μm)
P. aeruginosa	5.18	0.74 ± 0.1
B. subtilis	1.54	2.07 ± 0.6

*between bacteria and SS316 in water

5. 2 Effect of Hydrophobicity on Cell Adhesion

Hydrophobicity of bacteria is assessed using contact angle measurement (CAM), Salt Aggregation Test (SAT), Bacterial Adhesion to Hydrocarbon (BATH) test (as described in Section 3.2), as well as the calculation of the absolute hydrophobicity (ΔG_{13}) based on surface energy components by using equation 9 (Section 2.3.3). Experiments on contact angle measurements (CAM) provide a more direct comparison of hydrophobicity between the two bacteria. Theoretically, CAM should give a definitive overall hydrophobicity value of the microbial cell surface. Both bacteria were found to be hydrophilic; water contact angle value for *P.*

aeruginosa was found to be 47.85 ± 8.7, while that for *B. subtilis* was 29.78 ± 8.9 (Table 5.2), confirming the stronger hydrophobicity of the former.

Tests on SAT and BATH (Table 5.4) further confirm that both bacteria are hydrophilic. SAT values in this study are found to be higher than reported by other researchers. The minimum concentration of ammonium sulfate aggregated by *P. aeruginosa* and various species of *Bacillus* are reported to be in the range of 1.6-1.8 M (Pruthi and Cameotra, 1997), although others have also reported higher values at 3.4 M (Obuekwe et al., 2007). SAT value ranging from 0-4 M for *P. aeruginosa*, which shows a wide range of hydrophobicity level of this bacteria has also been reported (Vanhaecke et al., 1990).

Table 5.4 Hydrophobicity assessments of bacteria

Bacteria	SAT (M)	BATH (%)	ΔG_{13} (mJ/m^2)
P. aeruginosa	2-4	12.29 ± 0.8	32.27
B. subtilis	2.2-4	4.98 ± 0.8	63.65

On BATH test, partition of *P. aeruginosa* on hexadecane averages 12% while for *B. subtilis* it averages 5%. It shows that *P. aeruginosa* exhibits stronger hydrophobicity. Tests using hexadecane and octadecane shows BATH value of 7-89% (Vanhaecke et al., 1990), while that for *B. subtilis*, ranged from 1.6-6% (Doyle et al., 1984; Ahimou et al., 2001). However, it should be noted that BATH test were carried out at pH of the growth medium (i.e., pH 6.8) where at this pH the test may also measure the complicated interplay of long-range van der Waals and electrostatic forces and of various short range interactions (Busscher et al., 1995; van der Mei et al., 1995).

Surface hydrophobicity is recognized as a dominant factor influencing microbial adhesion on surfaces. In biological systems, hydrophobic interactions are usually the strongest of all long range non-covalent interactions and can be defined as the attraction between apolar or slightly polar molecules, particles or cells, when immersed in water (Van Oss, 1997). Hydrophobic groups on the microbial cells play a major role in removing water films from between the interacting surfaces, enabling adhesion to occur. Despite both model bacteria being found to be hydrophilic in nature, net hydrophobic attraction can still be formed on the surface of the microorganisms (Van Oss, 2006). Certain areas such as tips of appendages of bacteria contain hydrophobic components (Hermansson, 1999). Calculation of absolute hydrophobicity interaction between bacteria and water using equation 9 (Section 2.3.3) is shown in Table 5.4. Since ΔG_{13} for both bacteria are greater than zero, this calculation also revealed that these bacteria are hydrophilic. However, *P. aeruginosa* has smaller value of ΔG_{13}, as much as half of *B. subtilis*, suggesting higher hydrophobicity and better adhesion interaction.

Higher hydrophobicity of *P. aeruginosa* can be also correlated to biosurfactant production. Biosurfactants produced by bacteria reportedly increase the cell hydrophobicity and its ability to degrade hydrocarbons (Zhang and Miller, 1994). The emulsifying capacity evaluated using the emulsification index (E) (methodology explained in Section 3.2.4) at different time periods of 24, 48 and 72 hours was higher in *P. aeruginosa* as compared to *B. subtilis* (Table 5.5). This suggests that the biosurfactant production of the Gram-negative bacteria *P. aeruginosa* is higher than Gram-positive bacteria *B. subtilis*. Higher production of biosurfactant, which mainly contains polysaccharides and lipoprotein (Desai and Banat, 1997), leads to higher uptake of hexadecane as the carbon source (Zhong et al., 2007).

Table 5.5 Emulsification index of bacteria for 24-72 hours

Bacteria	Emulsification Index (%)		
	E_{24}	E_{48}	E_{72}
P. aeruginosa	44.79 ± 3.6	48.96 ± 1.8	48.96 ± 1.8
B. subtilis	11.46 ± 1.8	15.63 ± 0.0	16.67 ± 1.8

The surface thermodynamics of a bacterium is highly influenced by its outer membrane's characteristics (Van Oss, 2006). Gram-negative bacteria contain high lipid and low peptidoglycan content in their outer membrane, causing the surface properties to be easily influenced by moisture content of the surrounding environment. Gram-positive bacteria are high in peptidoglycan, making them more resistant to the surrounding environment (Hancock and Poxton, 1988; Nikaido, 2003). The hydrophilicity of Gram-negative bacteria increases significantly with a decrease of surrounding moisture content, while the hydrophilicity of Gram-positive bacteria is relatively stable (Strevett and Chen, 2003).

5. 3 Microbial-Metal Interactions based on DLVO and xDLVO theories

Microbial-metal interactions during adhesion can be interpreted based on the classical DLVO and extended DLVO theories in terms of free interaction energies versus separation distance between bacteria and a metal surface. Comparisons of each component of free interaction energies for both bacteria are presented in Figure 5.2. The profile of van der Waals free interaction energy is displayed in Figure 5.2a, which shows that both bacteria have negative ΔG^{LW} implying attractive interaction. At short separation distance *B. subtilis* has slightly lower attractive interaction energy compared to *P. aeruginosa*, but then the intensity of attractive interaction decays with separation distance and reach almost zero at above 8 nm.

Figure 5.2b describes free interaction energy based on electrostatic force (ΔG^{EL}). It appears that for separation distance lower than 2 nm, the electrostatic repulsion of *B. subtilis* is much higher than *P. aeruginosa*. It was also found that *B. subtilis* has a higher energy barrier than *P. aeruginosa*, and of the order of more than 1×10^3 kT, which subsequently decayed at larger separation distance, and reached almost zero at distance greater than 6 nm.
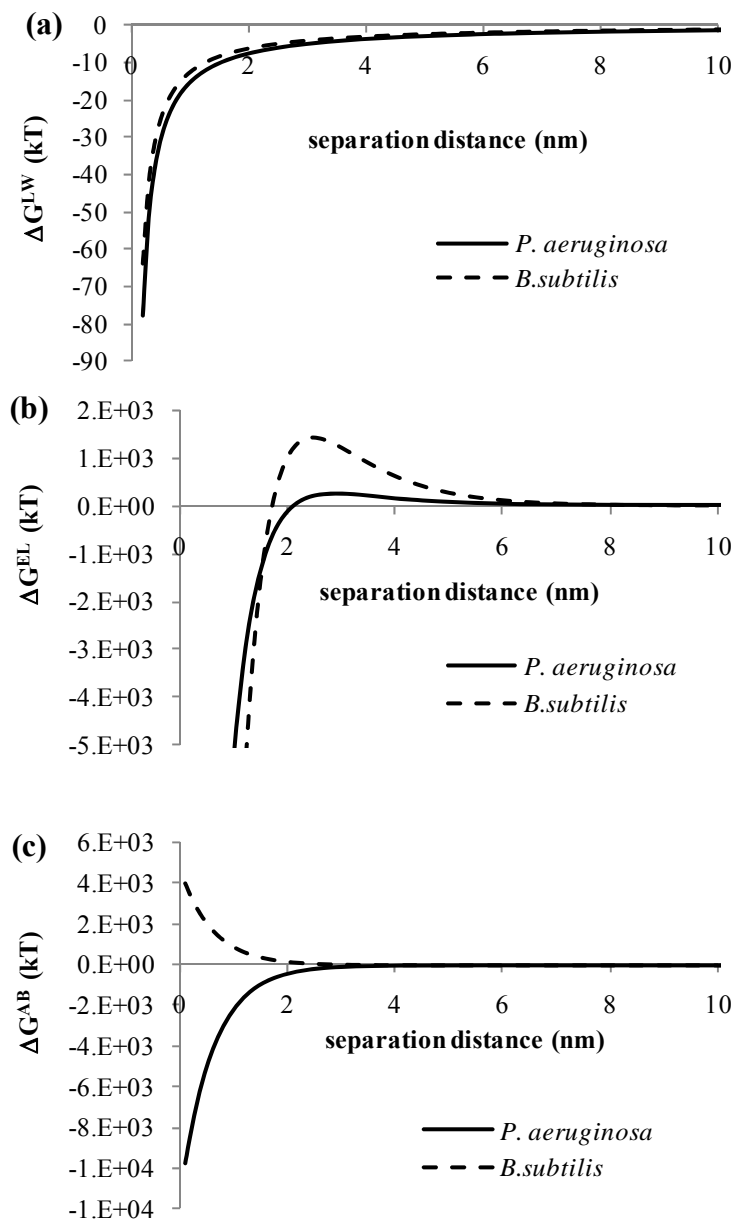
Figure 5.2 Free Interaction Energies for *P. aeruginosa* and *B. subtilis*: (a) van der Waals interactions, (b) electrostatic interactions, and (c) acid-base interactions

Figure 5.2c shows free interaction energy based on acid-base interaction (ΔG^{AB}). On the very short range separation distance (below 2 nm) it was shown that ΔG^{AB} for *B. subtilis* was positive, indicating net repulsion, whereas for *P. aeruginosa*, it was negative, indicating net attraction. The influence of electrostatic interaction rapidly decreased with longer separation distance and reached almost zero at 3 nm.

The effect of each component of the interaction energies on the total energies based on DLVO and extended DLVO (xDLVO) for each bacteria are presented in Figure 5.3. In Figure 5.3a, it was shown that for *P. aeruginosa* the effect of electrostatic (EL) and acid-base (AB) are significant to total interaction energy, while for *B. subtilis* the total interaction energies is influenced mainly by electrostatic (EL) interaction only (Figure 5.3b). Electrostatic double layer interactions are brought about by the repulsion of the same charge particles in aqueous medium. When particles approach the surface (i.e. the equilibrium stage), the electrostatic interaction drop drastically due to the overlap of the diffused layers (Chen and Strevett, 2003). Stainless steel SS316 surface is more negatively charged than the bacteria surfaces (Table 5.2). This generates a net strong attraction at close distance (< 1 nm). As observed in Figure 5.2b and Figure 5.3, the electrostatic repulsion is a dominant contribution to the total energy barrier. This was especially so in the case of *B. subtilis* where the electrostatic interactions were of the same order of magnitude as the total interaction energy (Figure 5.3b). In the case of *P. aeruginosa*, the electrostatic effect was dampened by attraction acid-base interaction, thus giving lower total interaction energy (Figure 5.3a).
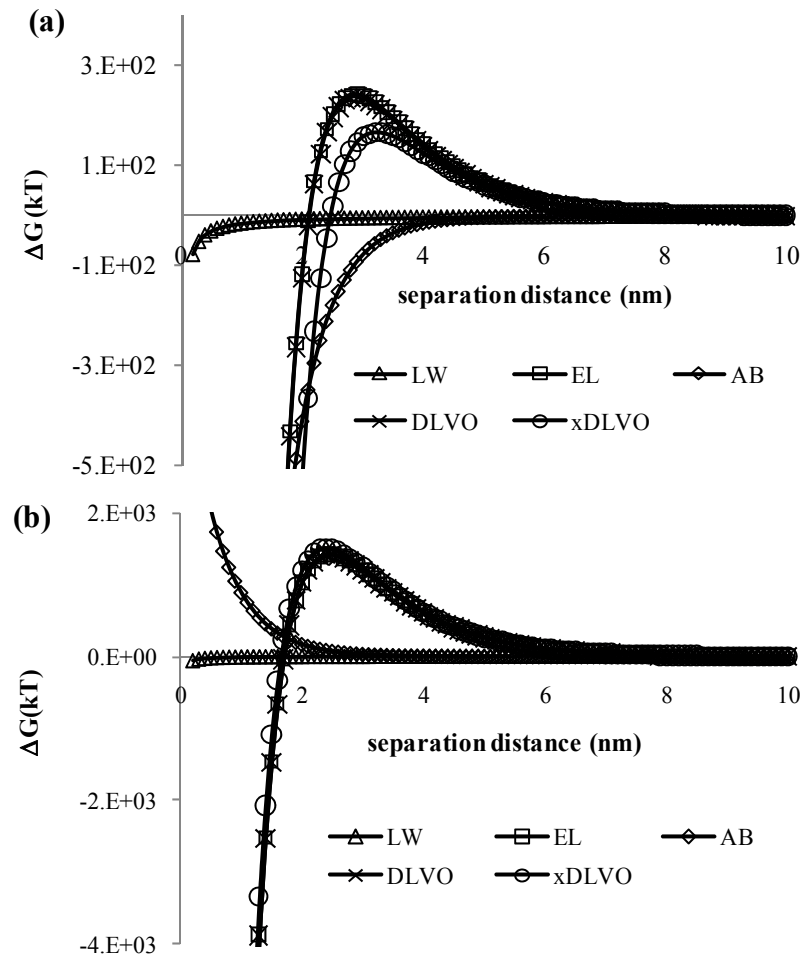
Figure 5.3 Components of total interaction energies for: (a) P. aeruginosa, (b) *B. subtilis*

Figure 5.4 compares the differences between the total interaction energies calculated from DLVO and extended DLVO (xDLVO) theories. It is observed that for the case of *B. subtilis*, both theories were in close agreement (Figure 5.4b). At large separation distances (>5 nm) both bacteria appear to have a similar total interaction energy calculated by DLVO and xDLVO theories. This was because interaction at large separation distance is due to van der Waals (LW) attraction between the bacteria and the surface. The secondary minimum for xDLVO theory was slightly lower for *B. subtilis* than DLVO (Figure 5.4b). The opposite was observed for *P. aeruginosa* where secondary minimum for xDLVO is significantly lower than DLVO (Figure 5.4a). Bacteria in the state of secondary minimum are reversibly attached to surface.

After moving closer to the surface, they must overcome a high energy barrier. Upon overcoming this barrier, the bacteria will fall into a deep primary minimum and become irreversibly attached to the surface (Hoek and Agarwal, 2006). Between both bacteria, *B. subtilis* has higher energy barrier than *P. aeruginosa*. This higher barrier means it was more difficult for these bacteria to be deposited into the primary minimum, which cause irreversible attachment. Thus *B. subtilis* was predicted by both theories to have less permanent attachment compared to *P. aeruginosa*.
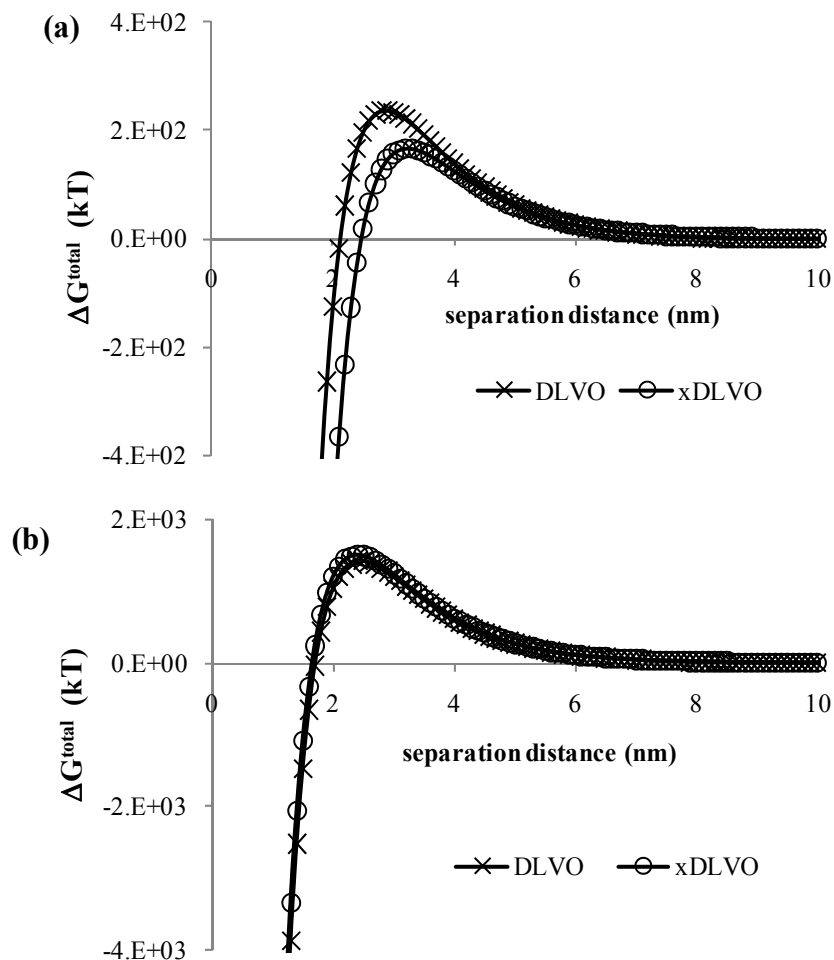
Figure 5.4 Total interaction energies for: (a) P. aeruginosa, (b) *B. subtilis*

The predicted energy barrier for *B. subtilis* from DLVO and xDLVO theories were very similar to each other (Figure 5.4b). This was due to the low value of ΔG^{AB}

for this bacteria. Thus the AB interactions have negligible effect on the total interaction energy. However, for *P. aeruginosa*, the xDLVO theory predicted smaller secondary minima and a smaller energy barrier than DLVO theory (Figure 5.4a). This was because the effect of ΔG^{AB} for this bacteria is very significant to the total interaction energy, where the interaction is attractive, thus reducing the total energy barrier for this bacteria. A smaller energy barrier means irreversible attachment is easier to be attained.

5. 4 Force Measurements of Bacterial-Metal Interactions using AFM Spectroscopy

Adhesion forces between each bacterium and SS316 surfaces was investigated using AFM force spectroscopy. Figure 5.5 shows SEM images of an AFM cell probe prepared using the polydopamine technique, with bacterial cells successfully coated on the cantilever tip. Unlike the gluteraldehyde immobilization technique, where cross-linking of proteins and amino acids in the exocellular polymeric layer significantly influences the interaction of gluteraldehyde-treated cells (Burks et al., 2003), this technique is noninvasive and can be performed for a wide range of application without affecting cell viability (Kang and Elimelech, 2009).

Results of the AFM force measurement are presented in Figure 5.6 and Table 5.6. Figure 5.6 shows examples the retraction force curves of the functionalized bare AFM tip (as control) and tip coated with *P. aeruginosa* and *B. subtilis* on the SS316 surfaces, which relate to their adhesion forces onto surfaces. With surface delays of up to 60 seconds, the adhesion forces increased gradually, followed by increasing separation distance. As seen in Figure 5.6a, the control experienced least adhesion forces within smallest separation distances as compared with tip coated with bacteria.
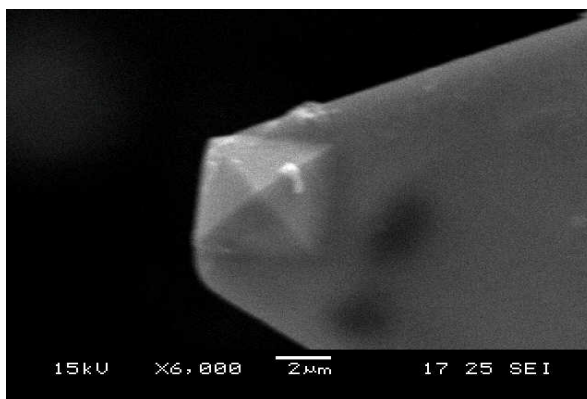
Figure 5.5. SEM images of the bacterial cell probe.

Average adhesion forces of bacterial cell probes on SS316 surfaces in 10mM PBS buffer (pH 7.2) with surface delays varying from 0 to 60 seconds are shown in Table 5.6. Compared with *B. subtilis* (a Gram positive bacterium), *P. aeruginosa* (Gram negative bacterium) shows significantly larger adhesion forces. These forces were also gradually increased with surface delay for all bacteria. Increasing surface delay will lead to bond maturation between the bacterial surface and the SS316 surface, and will give rise to removal of interfacial water, unfolding of bacterial surface structures or rotation of an entire particle to have its most favorable site opposing a substratum surface (i.e., rearrangement of microorganisms on the surface) (Busscher et al., 2010; Olsson et al., 2010). Increasing surface delay also increases the interaction of the protein structures on the bacterial surface through the electrostatic or hydrogen bonding forces between charged amino acid and metal surface charges which increase the overall adhesion forces (Dorobantu et al., 2008).
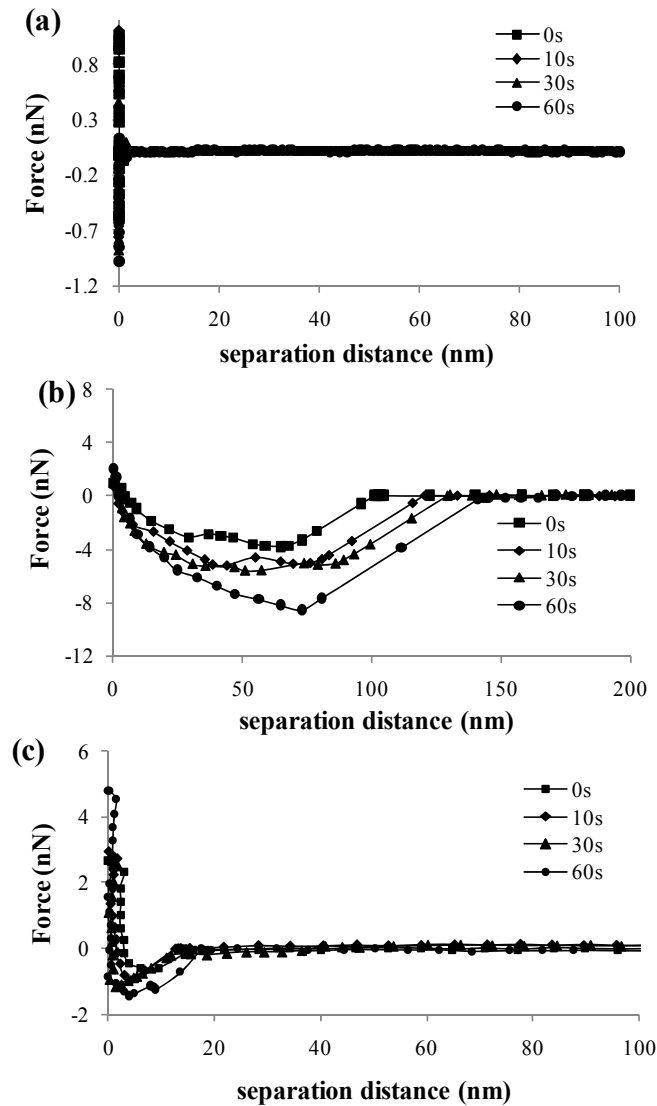
Figure 5.6. Examples of AFM retraction curves for: (a) functionalized bare AFM tip (control); (b) *P. aeruginosa*; and (c) *B. subtilis* with various surface delays

Table 5.6. Average adhesion forces between bacterial cell probes on SS 316 in 10 mM PBS buffer solution (pH 7.2)

No	Type of cell probe	Adhesion Force (nN)			
		Duration (s)			
		0	**10**	**30**	**60**
1	Control	0.59 ± 0.16	0.76 ± 0.28	0.88 ± 0.19	0.99 ± 0.24
2	*P. aeruginosa*	3.84 ± 0.28	5.31 ± 0.30	5.66 ± 0.68	8.53 ± 1.40
3	*B. subtilis*	0.65 ± 0.17	0.99 ± 0.16	1.16 ± 0.13	1.44 ± 0.21

($\pm$) represents the standard deviation over 30 adhesion forces from each type of cell probe

5. 5 Analysis of Biofilm Formation

In order to observe the ability of each bacterial strain to adhere to the metal surface, SS316 coupons were hung inside a biofilm reactor containing 10^8 cell/ml of each bacterial strain cultures. After 24 hours of growth, coupons were withdrawn and biofilm formed on the SS316 surfaces were then analyzed. Figure 5.7 shows evidence that after 24 hours of biofilm formation, *P. aeruginosa* formed denser biofilm than *B. subtilis*.
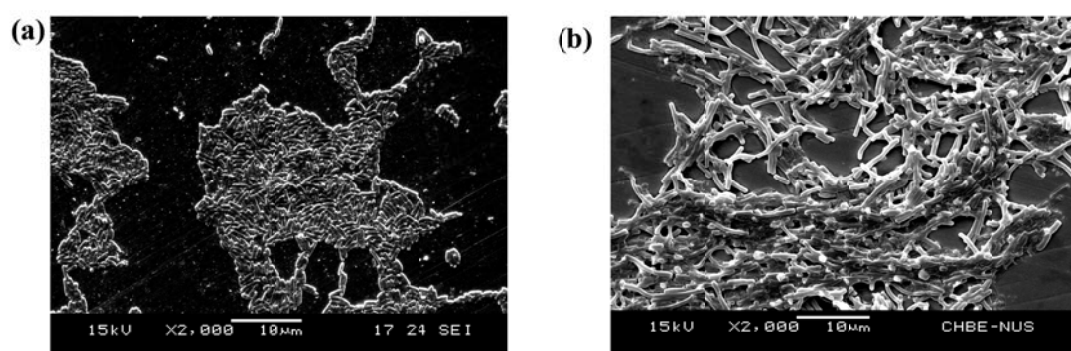
Figure 5.7. Examples of SEM images of the bacterial biofilm on SS 316 coupon surfaces: (a) *P. aeruginosa* and (b) *B. subtilis*

The surface properties of the biofilm formed after 24 hours were also analyzed using Fourier Transform-Infra Red (FTIR) Spectroscopy which has been successfully applied in the characterization of chemical composition of metabolites in bacterial samples (Verhoef et al., 2005). Figure 5.8 shows the FTIR spectra of 24 hour-biofilm formed by each bacterial strain with bare SS316 as control. The spectra were measured in the range of 4000–500 cm^{-1}, which would include the major characteristic bands pertinent for microorganism (Schmitt and Flemming, 1998).

In the presence of *P. aeruginosa*, broad peaks were noted in the range of 2900-3650 cm^{-1}, which may be assigned to adsorbed water molecule OH/NH group (Cornell and Schwertmann, 1996). This band can also be attributed to symmetric stretching of C-H from –CH$_3$, asymmetric C-H stretching from –CH$_2$, C-H vibration

of –CH$_3$ and –CH$_2$ functional groups dominated by fatty acid chains (e.g., phospholipids), and O-H stretching of hydroxyl group and N-H stretching (Fett et al., 1995; Beech et al., 2000).
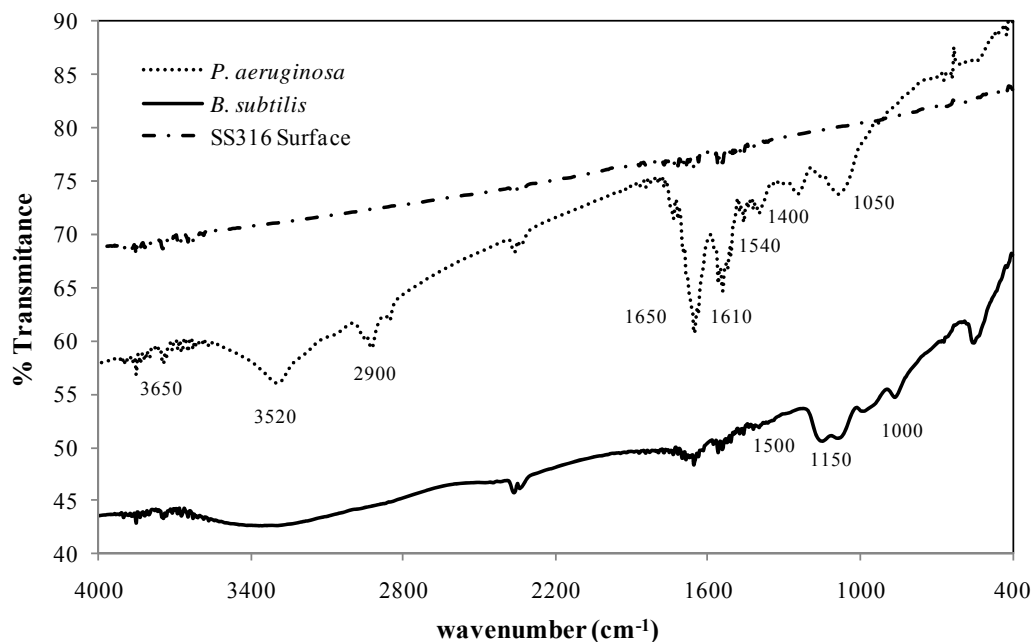
Figure 5.8. FTIR spectrum of bare SS-316 (control) and biofilm formed by *P. aeruginosa* and *B. subtilis*

The FTIR spectra also indicated the presence of proteins (1700 to 1500 cm^{-1}) as well as polysaccharides and nucleic acids (1200 to 900 cm^{-1}). During cell growth, both in planktonic and biofilm state, bacteria are known to produce varieties of polymeric materials such as proteins, lipopolysaccharides, oligosaccharides and possibly a variety of other polymers (Sheng et al., 2008). The protein amide I (C=O stretch strongly coupled with C-N stretch and N-H bending) and amide II (C-N stretch strongly coupled with N-H bending) regions are found at approximately 1650 and 1540 cm^{-1}, respectively. These amide bands can be used as universal probes for proteins because the peptidic acid bond is a basic and repetitive functional group in proteins (Marcotte et al., 2007). The amide I band is generally more intense than amide II band. However, Figure 5.8 also showed intense amide II bands due to some

polysaccharides, such as alginate, which give rise to an intense band associated with the C-O stretching vibrational mode (Silverstein et al., 1991) located at 1610 cm^{-1}.

The amide I bands near 1650 cm^{-1} is more prominent since it corresponded to C=O stretching with different conformation and C-N bending of protein and peptides amide. The intense small peaks near 1500 cm^{-1} can be attributed to the symmetric deformation of NH_3^+ absorbed onto stainless steel surfaces (Cheung et al., 2000; Socrates, 2004). The peaks near 1400 cm^{-1} represent the symmetric stretches mode of C=O and C-O bending from carboxylate group, which manifest the interaction between –COO$^-$ group and the metal surface (Helm and Naumann, 1995). In this range, FTIR confirms the presence of EPS (COO-, amide groups) secreted by the Gram negative bacteria on the metal surface (Jolley et al., 1988; Schreiber et al., 1990; Socrates, 2004). In the case of *B. subtilis,* FTIR peaks showed less intensity of C-O, and OH group compared to *P. aeruginosa.*

The bands in the polysaccharide region (1200-900 cm^{-1}) were attributed to C-OH stretching mode and C-O-C (1150 cm^{-1}), C-O ring vibrations of carbohydrates (oligo and polysaccharides), C-O-P and P-O-P in polysaccharides of the cell wall, and also symmetric stretching of P=O from PO^{2-} in nucleic acid (Fett et al., 1995; Beech et al., 2000).

Results from FTIR spectra showed that proteins and polysaccharides as components of extracellular polymeric substances (EPS) were produced by both bacteria during biofilm formation. The results, which suggest that the changes in chemical bonding with the surface atoms during the initial attachment of the biofilm involve COO$^-$ and NH_3^+ interaction, are in good agreement with the previous findings (Fletcher and Marshall, 1982) which suggested that proteins often function as adhesives in specific attachment mechanism.

However, based on the spectra, *B. subtilis* showed less intense peaks in the same wave number range than *P. aeruginosa*. This was due to less denser biofilm formed by this bacteria during the same 24 hour duration (as depicted in Figure 5.7). These results corroborate our previous findings that stronger adhesion forces were found on Gram-negative bacteria as compared to Gram-positive bacteria, thus creating greater attachment of bacteria onto the SS316 surfaces. In addition, FTIR spectra revealed that both bacterial strains produce extracellular polymeric substances (EPS); the denser biofilm formed by Gram-negative bacteria might be due to the fact that Gram negative bacteria secreted more EPS than Gram-positive bacteria (Anderson and Unger, 1983; Sutherland, 2001; Fang et al., 2002), which is a critical component in the structural integrity of biofilms (Costerton et al., 1987) since it serves to provide protection of the bacteria from dehydration and loss of nutrient (Konig et al., 1998).

5. 6 Summary

Direct approach via AFM force measurement and theoretical approach using surface interaction energies combined with DLVO and extended DLVO (xDLVO) theories has been used to interpret the interactions between two food-borne bacteria, *P. aeruginosa* NRRL-B3509 (Gram-negative) and *B. subtilis* NRRL-NRS762 (Gram-positive), and stainless steel SS316 surfaces during the adhesion process. As observed in the previous study, *P. aeruginosa* showed higher affinity towards SS316 and formed denser biofilm than *B. subtilis*.

This higher affinity was manifested when the adhesion force was measured using AFM. With the implementation of polydopamine coating on AFM tip to prepare viable cell probes, *P. aeruginosa* showed higher forces than *B. subtilis* when retracted

from SS316 surfaces. Due to bond maturation and protein interaction between metal and bacterial surfaces, stronger forces became prominent with longer surface delays.

Several factors have been found to cause higher interactions between *P. aeruginosa* and SS316 surfaces. Physicochemical analyses have revealed *P. aeruginosa* have higher hydrophobicity than *B. subtilis*. This was correlated with different surface properties of *P. aeruginosa*, where more proteins and polysaccharides were produced as EPS and biosurfactans. Adhesions were also dominated by electrostatic repulsion interactions, as predicted by both DLVO and xDLVO theories, due to negative charges of both interacting surfaces. Compared to *P. aeruginosa*, *B. subtilis* have to overcome a higher energy barrier when approaching SS316 surfaces. However, due to the specific properties of SS316 as conducting materials, electrostatic attraction interactions make possible for both bacteria to fall into the secondary minimum state and attach onto surfaces. In addition to electrostatic interactions, acid-base interactions via electron donor-acceptor also have significant contribution towards bacterial adhesion process, especially for *P. aeruginosa*, where attraction interactions facilitate these bacteria to overcome the energy barrier when approaching the metal surfaces.

CHAPTER 6

QUANTIFICATION OF *B. SUBTILIS* SPORE ADHESION TO STAINLESS STEEL DURING BIOFILM FORMATION

Bacterial spores are well known as a major contamination problem in many industries (Husmark and Ronner, 1992; Clement et al., 1993). Adhesion of spores onto surfaces has been identified as an important virulence factor for some species of *Bacillus,* such as *B. cereus* and *B. subtilis* (Anderson et al., 1995; Granum and Benjamin, 2003; Jullien et al., 2003). Spore adhesion also causes significant problems in pipelines where they may multiply and resporulate. (Anderson *et al.*, 1995; Scheldeman *et al.*, 2005).Since adhesion of spores onto metal surfaces has also been considered significant in biofilm formation, it is important to study the interaction between spore and metal and vegetative cells during the adhesion process. In order to inhibit and control spore and cell adhesion on surfaces, it is important to understand their adhesion mechanism.

In this chapter the morphologies and surface properties of *B. subtilis* spores were examined. Adhesion interactions between the spores and SS316 were also investigated. A theoretical approach using DLVO and extended DLVO (xDLVO) was used to quantify the interaction energies between bacteria and the metal surfaces. The effect of surface energies on spore adhesion was explained using this approach in conjunction with the direct force measurement using AFM force spectroscopy.

6. 1 Morphologies of *B. subtilis* Spores

Figure 6.1 shows both *Bacillus subtilis* spores and cells after Schaeffer-Fulton staining. The spores were stained bluish-green while the vegetative cells were stained

reddish-brown. The results from the staining experiment show that the sporulation agar indeed yielded spores. Figure 6.1a shows the vegetative cells being stained reddish-brown and Figure 6.1b shows the harvested spores being stained bluish-green.
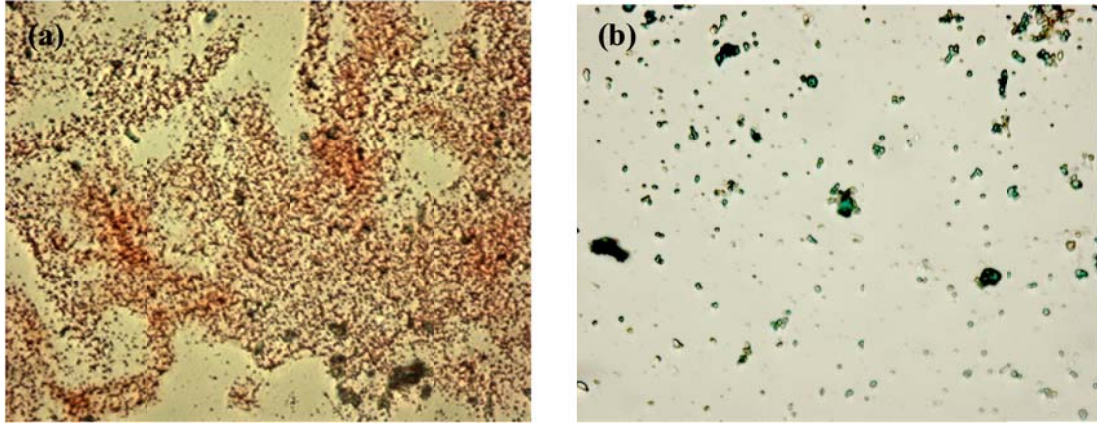
Figure 6.1 *Bacillus subtilis* morphology after Schaeffer-Fulton staining: (a) vegetative cells, and (b) spores

Morphology of the spores was further observed using scanning electron microscopy (SEM). Figure 6.2 shows SEM images of *B. subtilis* cells and spore spread onto stainless steel coupons. It was apparent that when *Bacillus* spores were formed, the shape is transformed from rod into ellipsoidal and the length is reduced from 3-5 microns to 1-2 microns.
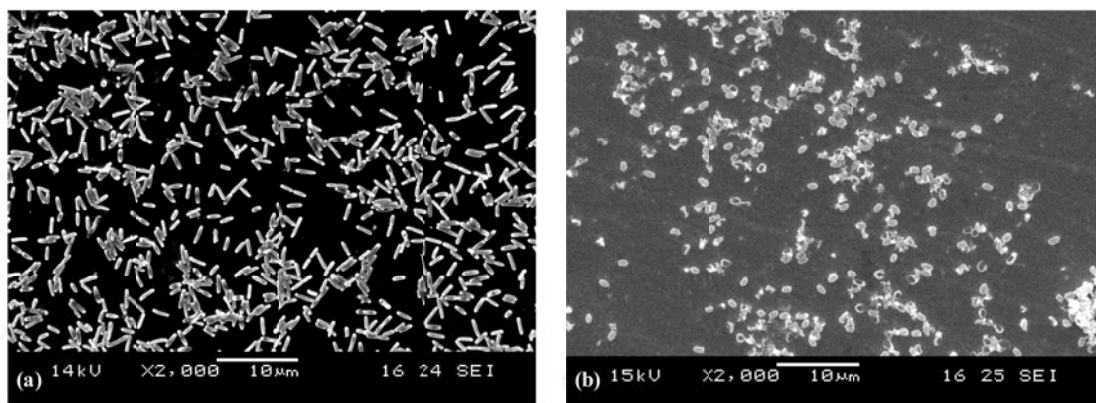
Figure 6.2 SEM Image of *B. subtilis*: (a) vegetative cells, and (b) spores

The shape and length alteration of spores is more visible when the SEM image is magnified at 10,000 times (Figure 6.3a). Morphology of the spores using AFM also revealed that the dimension of the spores (~1.7 μm) was also close to the one shown by SEM (Figure 6.3b). *Bacillus* are known to change their shape and size when transformed from vegetative cells into spores due to response of nutrient deprivation or extreme condition, such as temperature, pH, and moisture (Sargent, 1975; Bowen et al., 2002).
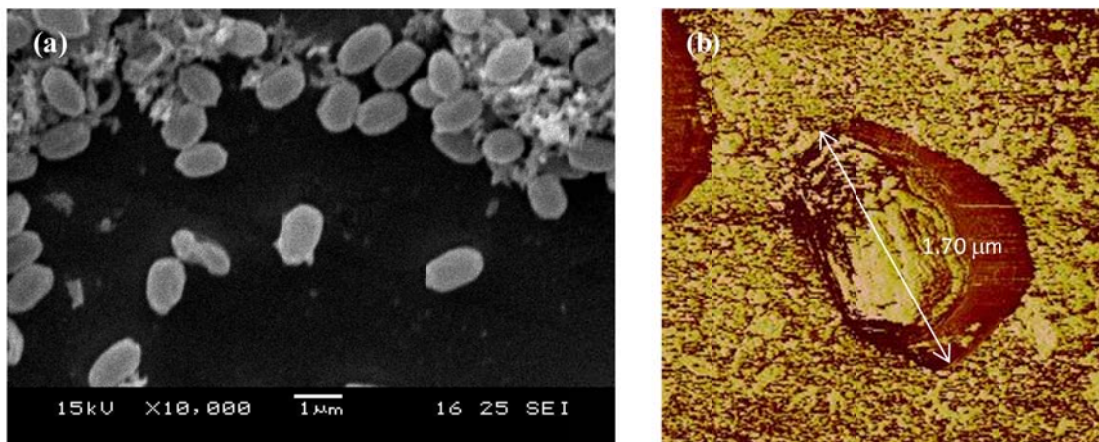
Figure 6.3 Magnified image of *B. subtilis* spores: (a) SEM at 10,000X magnification, and (b) AFM Phase Image

6. 2 *B. subtilis* Spores Surface Properties

Surface thermodynamic properties of *B. subtilis* vegetative cells and spores are determined using Young's equation (explained in Section 2.3.1). Table 6.1 shows contact angle measurement (CAM) and surface thermodynamic properties of *B. subtilis* cells and spores. Both cells and spores are found to be monopolar, i.e. the value of γ^- was at least one magnitude greater than γ^+. This shows monopolarity properties of hydrophilic surface which leads to the tendency to favor electron donation and hence result in strong acid base repulsion (Van Oss, 1993). The value of γ^- and γ^+ are comparable with other published works, where the value of γ^- and γ^+

were reported to range from 38.1 to 51.4 mJ/m^2 and 0.08 to 0.92 mJ/m^2 respectively, for *Bacillus* (Chen et al., 2010). The value of γ^- and γ^+ is influenced by different protein layers on the surfaces. It was reported that spores without certain protein coatings such as CotB and CotG will have lower γ^- and higher γ^+ values (Isticato et al., 2001; McPherson et al., 2005).

Table 6.1 Contact angles and surface thermodynamic properties of *B. subtilis* vegetative cells and spores

	Contact angle θ (°)			Zeta Potential ζ (mV)	Surface energy components (mJm^{-2})				
	θ^W	θ^{HD}	θ^{EG}		γ^+	γ^-	γ^{LW}	γ^{AB}	γ^{TOT}
Cells	29.8 ± 8.9	32.2 ± 5.8	44.7 ± 8.7	-18.9 ±0.7	0.22	72.67	23.41	7.95	104.25
Spores	50.9 ± 3.2	0	45.8 ± 1.6	-13.27 ±0.9	1.06	42.02	21.00	13.36	77.44

Acid base interaction is also related to the differences in the value between γ^+ and γ^- of the particles and that of water. For both cells and spores, the values of γ^+ were lower than that for water while values of γ^- were higher than that for water (25.5 mJm^{-2}). This indicates the surfaces have stronger affinity towards water, resulting in hydrophilic repulsive interaction with SS316 surfaces (Van Oss, 2006).

While both cells and spores were monopolar (as shown in Table 6.1) the value of γ^+ of *Bacillus* spores is greater while value of γ^- is lower than the cells. Acid base interactions are derived from the electron donating surface tension (γ^-) and electron accepting surface tension component (γ^+). From this data, we can expect that *Bacillus* cells have tendency to favor electron donation and hence result in stronger acid base repulsion than spores. However, cells have higher value of γ^{LW} compared to water

(21.8 mJm^{-2}), resulting in attraction interaction with stainless steel surfaces, while spores will have slight repulsion interaction with stainless surfaces (Van Oss, 2006).

Magnitude of electron-donor-acceptor surface energy component are also correlated with zeta potential, where surfaces with higher charges tend to have higher γ^- and lower γ^+. In this study, both *Bacillus* cells and spores have negative zeta potential (Table 6.1). Most bacterial surface possess negative surface charges, which originate from the lipopolysaccharides of the cell envelope and/or acidic functional groups on the proteins of the pili (Bayer and Sloyer Jr, 1990; Dorobantu et al., 2008). Since SS316 also have negative zeta potential (data shown in Table 5.2), this will result in electrostatic repulsion between bacterial and SS316 surfaces. However, since cells were more negatively charged than spores, cells would experience greater electrostatic repulsion.

Table 6.2 shows the equivalent radius and Hamaker constants of *B. subtilis* cells and spores. Similar to what have been shown by SEM and AFM images, measurement of equivalent radius by Zetasizer nano system revealed that spores were smaller than the vegetative cells. *Bacillus* are reported to have length size of 2.5-6.6 μm for vegetative cells (Sargent, 1975), and 1.07-1.85 μm for spores (Zandomeni et al., 2005). As explained earlier, reduction of the length occurs when the spores are formed due to unfavorable environmental condition (Bowen et al., 2002).

Table 6.2 Equivalent radius and Hamaker constant of *B. subtilis* vegetative cells and spores

	Equivalent Radius R (μm)	Hamaker Constant (A) (J x 10^{20})*
Cells	2.07 ± 0.6	1.54
Spores	1.21 ± 0.1	-0.78

*between bacteria and SS316 in water

Calculation of effective Hamaker constant (*A*) using equation 8 (Section 2.3.2) revealed negative value for *Bacillus* spores, in contrast to positive value for the vegetative cells. The Hamaker is the property of two surfaces that identify their interaction strength in the medium and depends on the dielectric properties of the surface, medium, and the cell in the case of microbial adhesion (Hermansson, 1999). Values of *A* presented in Table 6.2 are between cells/spores and stainless steel surface in the medium (water). Positive *A* values for *Bacillus* vegetative cells and spores in aqueous media has been reported between 1.38 to 7.1 x 10^{20} J (Norde and Lyklema, 1989; Chung et al., 2009). However, no information has been reported for negative A value on spores. Positive A values will result in negative interaction potential, i.e. attraction interaction, while negative value will result in repulsion interaction (Malmsten, 2003). Hamaker constant contributes to the van der Walls attractive interaction between two surfaces when immersed in the medium (Brown and Jaffé, 2005).

6. 3 Hydrophobicity Characteristic of *B. subtilis* spores

Contact angle measurement (CAM), SAT test, BATH test, and absolute hydrophobicity calculations (ΔG_{13}) based on surface energy components (Section 2.3.3) were used to assess the hydrophobicity of *B. subtilis* spores. As shown in Table 6.3 each of the hydrophobicity tests showed that both *Bacillus* spores and cells are hydrophilic, although compared to the vegetative cells, the spores exhibited significantly higher hydrophobicity.

Table 6.3 Hydrophobicity assessment of *B. subtilis* vegetative cells and spores

	CAM (^{o})	SAT (M)	BATH$_{HD}$ (%)	ΔG_{13} (mJ/m^2)
Cells	29.8 ± 8.9	2.2-4	4.98 ± 0.8	63.65

Spore	50.9 ± 3.2	2-4	12.46± 1.4	23.02

A BATH test using different hydrocarbon solvents further confirmed the higher hydrophobicity of spores. As shown in Figure 6.4 partition of spores in xylene and tetradecane was much higher compared to hexadecane. In tetradecane, spores showed much higher partitions (53.6%) compared to the vegetative cells (14%). Different affinity on surfaces in different solvents used in the BATH test has been found to be correlated with different protein components on the bacterial surfaces that interact with the solvent (Dickson and Koohmaraie, 1989).
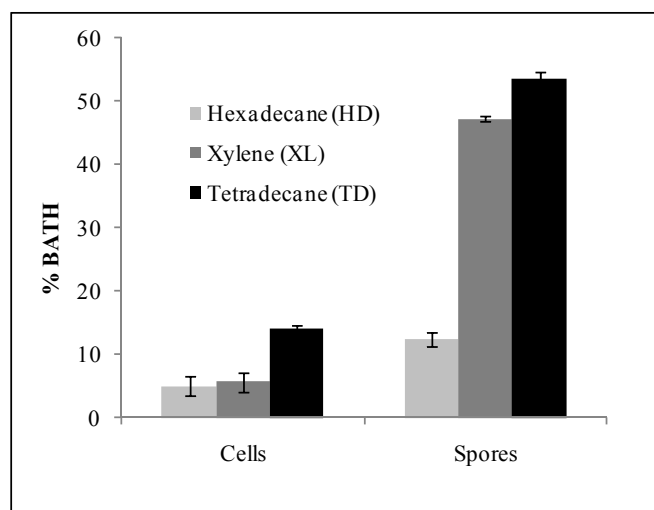
Figure 6.4 BATH partitioning of *B. subtilis* cells and spores in different hydrocarbon solvents

Higher hydrophobicity levels of spores may arise from the significantly higher amount of proteins on the spore's surfaces as a proteinaceous coat or exosporium (Warth, 1978; Murrell, 1981) when compared to the vegetative cell surfaces. *B. subtilis* are known to have peptidoglycan containing components on their vegetative cell surfaces (Doyle et al., 1984) which influence their hydrophobicity. According to the literature, the outmost layer of *B. subtilis* spores is mostly made up of a protein coat, and not exosporium (Chen et al., 2010). At least three coat proteins, CotB, CotC,

and CotG, most likely contribute to the surface hydrophobicity properties of spores (Isticato et al., 2004; Mauriello et al., 2004; Kim et al., 2005).

Since hydrophobic interactions are considered as the strongest among all long range non-covalent interactions, we may expect that during attachment onto stainless steel surfaces, *B. subtilis* spores would show greater adhesion compared to their vegetative cells. Interaction energy of the spores and vegetative cells during the adhesion process will be discussed using DLVO xDLVO theories in the following section.

6. 4 Spores and Cells Interaction based on DLVO and xDLVO Theories

Comparisons between each component of the free interaction energies for *B. subtilis* spores and vegetative cells are presented in Figure 6.5. The profile of the van der Waals free interaction energy (Figure 6.5a) shows that, with the stainless steel surface, vegetative cells have negative ΔG^{LW} implying attractive interaction, while spores have positive ΔG^{LW} implying repulsive interaction as reflected in the negative value of the Hamaker constant. In both cases, the intensity of interactions decays with separation distance and reach almost zero at beyond 8 nm.

Figure 6.5b describes the free interaction energy based on electrostatic force (ΔG^{EL}). It was found that cells have a higher energy barrier than spores, of the order of more than $1x10^3$ kT, which subsequently decays at a larger separation distance and reaches almost zero when the distance was near to 6 nm. However, at lower separation distance (~1.3 nm), the electrostatic attractive interaction of the cells become higher than the spores.
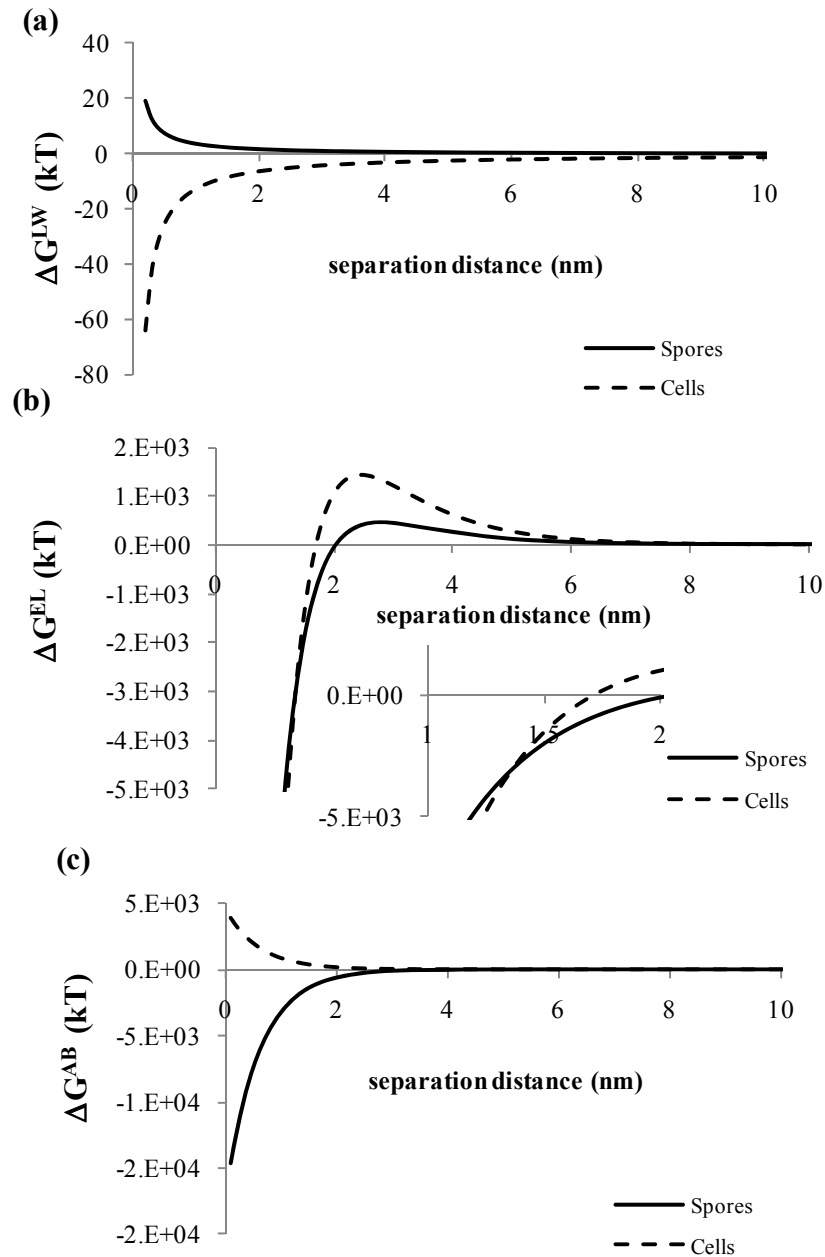
Figure 6.5 Free Interaction Energies for *B. subtilis* spores and cells: (a) van der Waals interactions, (b) electrostatic interactions, and (c) acid-base interactions

Figure 6.5c shows free interaction energy based on acid-base interaction (ΔG^{AB}). At very short range separation distance (below 2 nm) it was shown that ΔG^{AB} values were positive for vegetative cells, indicating net repulsion, and negative for spores, indicating net attraction. The influence of electrostatic interaction rapidly decreased with longer separation distance and reached almost zero at 3 nm.

The effect of each component of the interaction energies on the total energies based on DLVO and xDLVO theories for *B. subtilis* cells and spores are presented in Figure 6.6. In Figure 6.6a, it was shown that for cells, the total interaction energies were influenced mainly by electrostatic (EL) interaction only, while for spores, the effect of electrostatic (EL) and acid-base (AB) were significant to the total interaction energy (Figure 6.6b). Electrostatic double layer interactions are brought about by the repulsion of the same charge particles in aqueous medium. When particles approach the surface (i.e. the equilibrium stage), the electrostatic interaction drops drastically due to the overlap of the diffused layers (Chen and Strevett, 2003). Stainless steel SS-316 surface is more negatively charged than that of cells and spore surfaces (Table 6.1). This generates a net strong attraction at close distance (< 1 nm). As observed in Figure 6.5b and Figure 6.6, the electrostatic repulsion had a dominant contribution to the total energy barrier. This was very prevalent on the cells where the electrostatic interactions were of the same order as the total interaction energy (Figure 6.6a). In the case of spores, the electrostatic effect was dampened by attraction acid-base interaction, thus giving lower total interaction energy (Figure 6.6b). Comparable interactions have been reported between vegetative cells of *B. subtilis* with different surfaces. It was shown that the total interaction energies at neutral pH were controlled by electrostatic interactions. The magnitude of interactions were also in the order of 10^3 kT (Vijayalakshmi and Raichur, 2003). However, total interaction energies between various *Bacillus* spores were found to be lower due to strong acid-base interactions, which corroborates with the current finding (Bernardes et al., 2010; Chen et al., 2010).
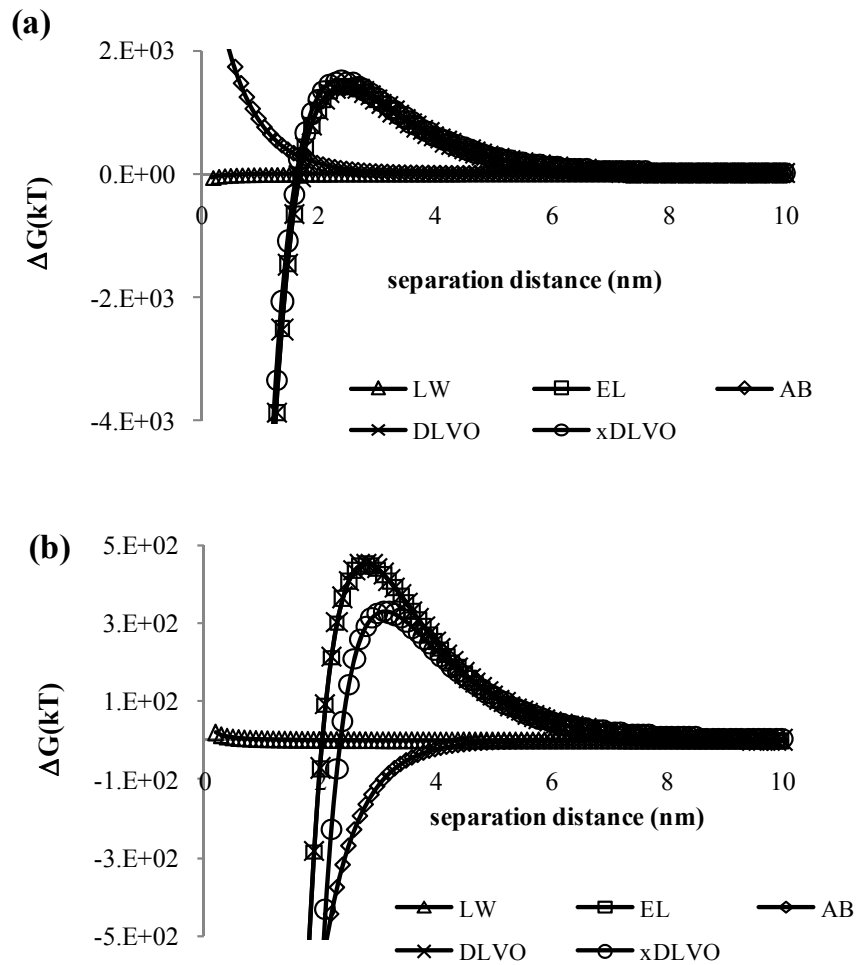
Figure 6.6 Components of total interaction energies for *B. subtilis:* (a) cells, (b) spores

Figure 6.7 compares the differences between the total interaction energies calculated from DLVO and xDLVO theories. It is observed that for the case of cells, both theories are in close agreement (Figure 6.7a), while for spores, total interaction energy from DLVO is higher than predicted by xDLVO theory (Figure 6.7b). At a separation distance greater than 5 nm, the total interaction energies calculated by DLVO and xDLVO theories are similar, both in the case of cells and spores. This was because the interactions at large separation distances are due to LW attraction between bacteria and surfaces. The secondary minima for DLVO theory was slightly lower for cells than xDLVO. The opposite was observed for spores where secondary

minimum for xDLVO is significantly lower than DLVO. Bacteria in the state of secondary minimum are reversibly attached to the surface. After moving closer to the surface, the bacteria overcome the high energy barrier. Upon overcoming this barrier, the bacteria will fall into a deep primary minimum and become irreversibly attached to the surface (Hoek and Agarwal, 2006). Cells manifested a higher energy barrier than spores, and thus it was more difficult for cells to be deposited into the primary minimum. Thus cells are predicted by both theories to have less permanent attachment compared to spores.

(a)

(b)
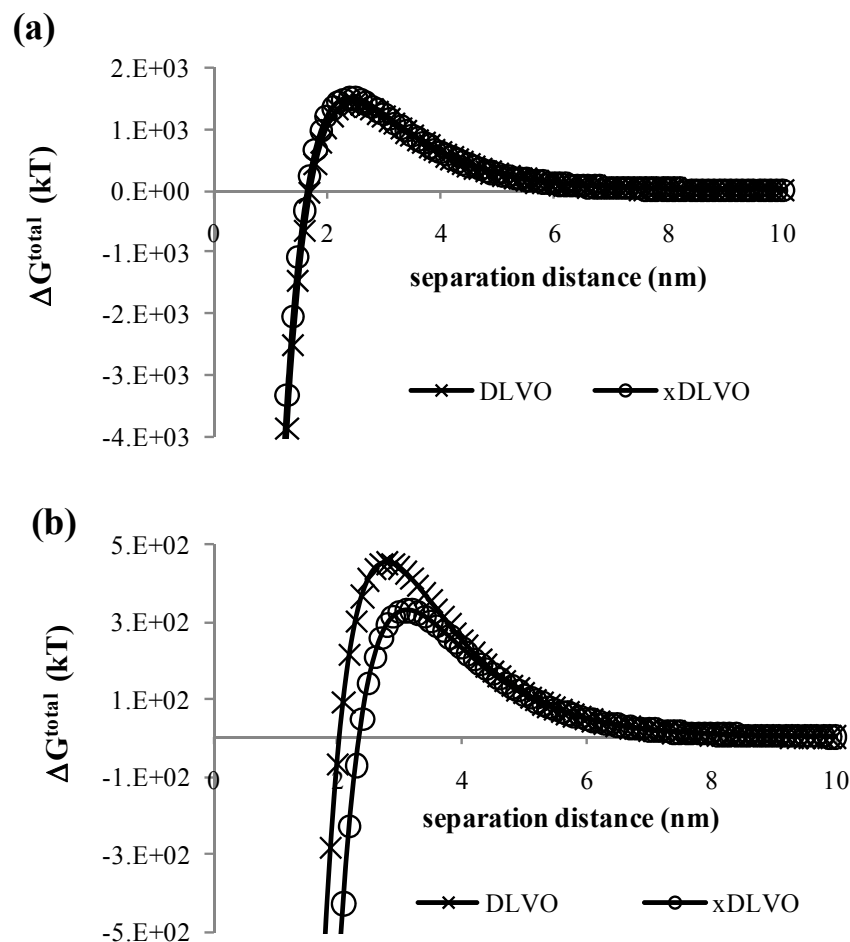
Figure 6.7 Total interaction energies for *B. subtilis:* (a) cells, (b) spores

The DLVO and xDLVO theories predicted that energy barrier for cells were very similar (Figure 6.7a). This was because ΔG^{AB} values for the cells are very small.

Thus the AB interactions have negligible effect on the total interaction energy. However, for spores, xDLVO theory predicted a smaller secondary minima and smaller energy barrier than DLVO theory (Figure 6.7b). This was because ΔG^{AB} for spores is very significant to the total interaction energy, where the interaction is attractive, thus reducing the total energy barrier. A smaller energy barrier means irreversible attachment is easier to attain.

6. 5 Infrared Spectroscopy Analysis

In order to gain deeper insight of the influence of surface properties on the adhesion mechanism, the chemical structures of *B. subtilis* cell and spore surfaces were analyzed using infrared spectroscopy. Figure 6.8 shows the spectra of both surfaces measured in the range of 4000–400 cm^{-1}, which would include the major characteristic bands pertinent for microorganisms (Schmitt and Flemming, 1998).

From this figure, it is shown that both cell and spore surfaces show similar spectra with different transmittance intensities. Broad peaks were noted in the range of 3700-3850 cm^{-1}, which may be assigned to adsorbed water molecule OH/NH group (Cornell and Schwertmann, 1996). This band can also be attributed to symmetric stretching of C-H from $-CH_3$, asymmetric C-H stretching from $-CH_2$, C-H vibration of $-CH_3$ and $-CH_2$ functional groups dominated by fatty acid chains (e.g., phospholipids), and O-H stretching of hydroxyl group and N-H stretching (Fett et al., 1995; Beech et al., 2000).
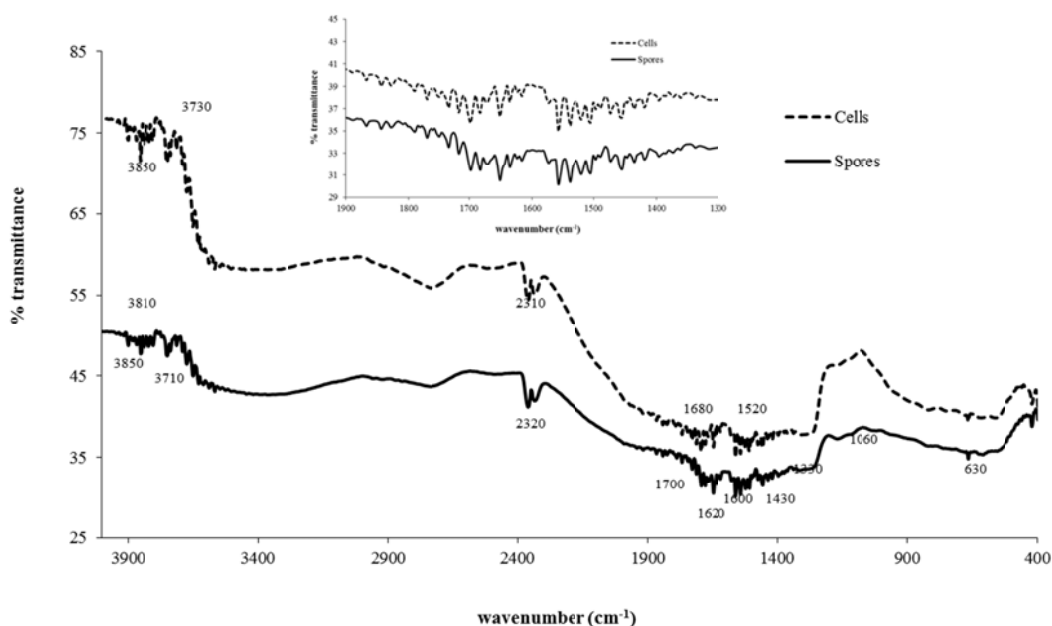
Figure 6.8 Infrared spectra of *B. subtilis* cells and spores surfaces

The FTIR spectra also indicated the presence of different functional groups of aldehydes (RCOH) (broad peaks at 1700 cm^{-1}), ketones (RCOR) (1680 cm^{-1}), carboxylic acids (RCOOH, RCOO−) (1600 cm^{-1}), carbonyl groups (CH3CO–) (1330 cm^{-1}), peptide bond (–CO– NH–) (1520 cm^{-1}), and ethers (–CH2–O–, CH3–O–, –C–O– C–) (1060 cm^{-1}) (Chen et al., 2010).

Surface thermodynamics of the bacteria are a reflection of the physicochemical properties of bacterial surfaces which are controlled by macromolecular components such as polysaccharides, proteins, and exo-polymers represented by a variety of different functional groups. It was found that hydrogen-binding groups such as RCOH and RCOO⁻ will favour electron donation (γ^-) while functional groups such as -H=CH- and >C=CH$_2$ will weaken electron donation (γ^-) (Chen and Strevett, 2003).

6. 6 AFM Force Measurement of Spores-Stainless Steel Interactions

Adhesion forces between *Bacillus* spores and SS316 surfaces were investigated using AFM force spectroscopy. Figure 6.9 shows the SEM images of AFM spore probes prepared using polydopamine, where the spores have been successfully attached to the AFM tip. The tip coated with polydopamine were found to have high affinity to bind the spores without affecting their structure (Kang and Elimelech, 2009) unlike the gluteraldehyde immobilization technique, where cross-linking of proteins and amino acids in the exocellular polymeric layer significantly influences the interaction of gluteraldehyde-treated cells (Burks et al., 2003).
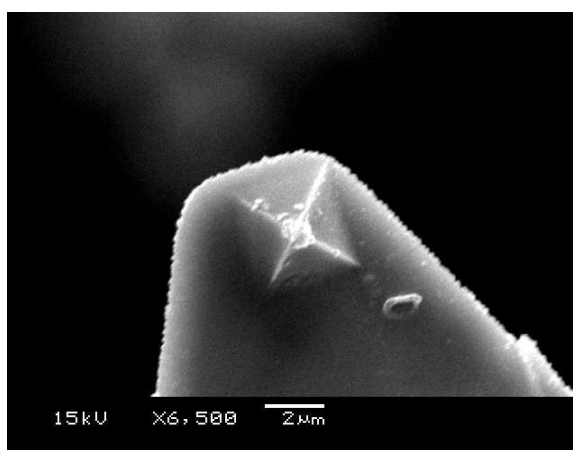
Figure 6.9 SEM Image of the spore probes on the surface of AFM tip

Force-distance curves for both bacteria are presented in Figure 6.10, each with approaching and retracting curves. A continuously increasing repulsive force is observed for both the cells and spores during the approach to metal surfaces. The interaction for cells was observed, beginning at 12 nm and reached the highest repulsive force at 1.9 nN at the cell surface (Figure 6.10a approaching line), while for the spores the interaction were observed from 15 nm from the surface and a repulsive force at 2.6 nN at the surface (Figure 6.10b approaching line) was noted.
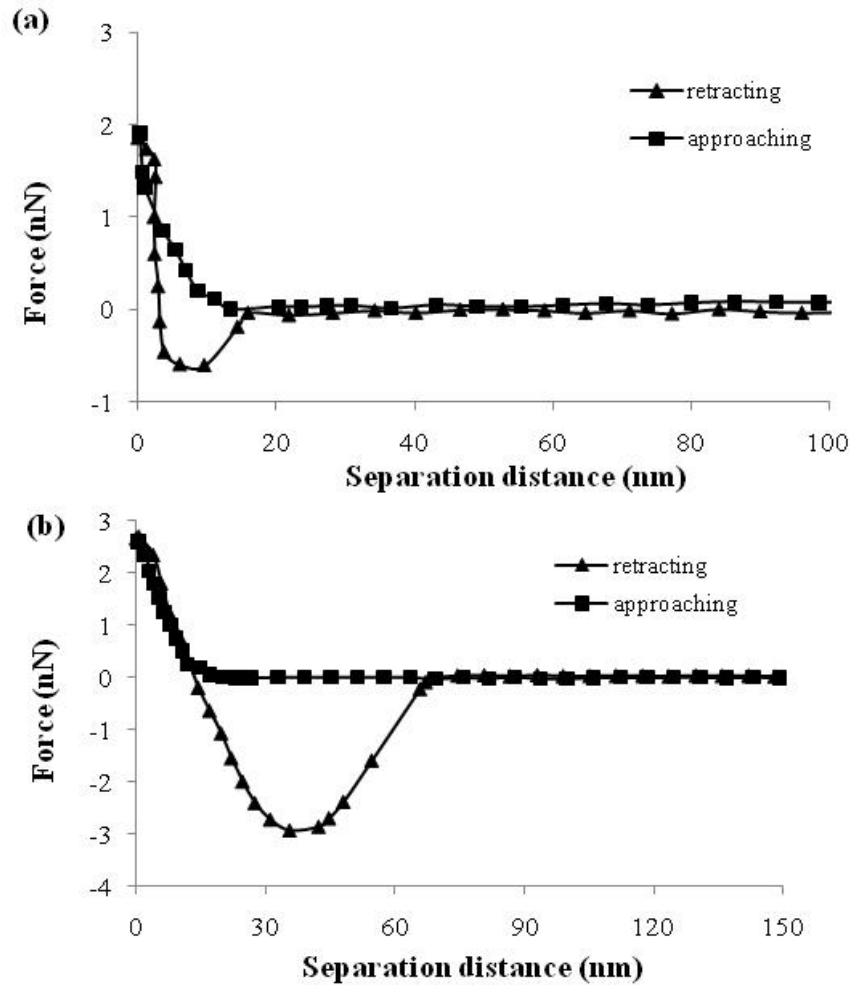
Figure 6.10 Examples AFM force-distance curves of *B. subtilis*: (a) cells; (b) spores

Van der Waals and electrostatic interactions are considered dominant in the early stages of bacterial adhesion (Rutter and Vincent, 1980). The higher repulsive forces experienced by *B. subtilis* cells were in accordance with DLVO theory which predicted that these bacteria experienced a higher energy barrier on electrostatic interaction in the very short distance

Two observations were made on the retraction curves between bacteria and spores with stainless steel. First, spores show significantly higher adhesive force (2.92 ± 0.4 nN) compared to vegetative cells (0.65 ± 0.2 nN). Second, the retraction curve between spores and stainless steel exhibited a longer separation distance before a

plateau (i.e., no interaction foces) (Figure 6.10b retracting line), while the vegetative cells show shorter separation distance (Figure 6.10a retracting line).

6. 7 Summary

In this study, surface and interaction energies based on a theoretical approach using DLVO and extended DLVO (xDLVO) theories together with AFM force measurement have been used to observe and quantify the adhesion interactions between *B. subtilis* spores and stainless steel SS316. The study revealed that compared to the vegetative cells, *B. subtilis* spores have higher affinity towards SS316 surfaces.

Physicochemical analyses have revealed that *B. subtilis* spores have higher hydrophobicity than the vegetative cells. Stronger hydrophobicity on spores is due to a significant amount of protein layers instead of peptidoglycan on the spore surfaces, enhancing the attraction interactions on the metal surfaces.

When approaching SS316 surfaces, at a very short distance, interactions between surfaces are mainly dominated by electrostatic interactions which constitute most of the total interaction energies. A larger energy barrier was faced by vegetative cells, making it more difficult to be deposited on the surfaces. On the other hand, attractive acid-base interactions facilitate spores in lowering the energy barrier and enhancing the deposition.

Stronger affinity of *B. subtilis* spores toward SS316 surfaces has also been corroborated by force measurement using AFM. Compared to its vegetative cells, *B. subtilis* spores show higher adhesion forces when retracted from SS316 surfaces. Due to various components on the surfaces such as polysaccharides, proteins, and other exo-polymers, spores establish stronger attachment on SS316 surfaces compared to their vegetative cells causing firmer biofilm formation when favorable conditions are

attained. The adhesion of spores presents more problems in biofilm control owing to their stronger attachment and persistence when the spores are formed under severe environmental conditions.

CHAPTER 7

INVESTIGATION OF EXTRACELLULAR POLYMERIC SUBSTANCES (EPS) PROPERTIES OF *P. AERUGINOSA* AND *B. SUBTILIS* AND THEIR ROLE IN BIOFILM DEVELOPMENT

In this chapter, the composition and characteristic of EPS produced by *P. aeruginosa* and *B. subtilis* from growth cultures (i.e., planktonic cells) and biofilms (i.e., sessile cells) will be elucidated by several chemical analysis techniques. Furthermore, the adhesive properties of the EPS will be observed using single molecule force spectroscopy (SMFS) using AFM to relate their composition.

7. 1 Bacterial Growth and EPS Production

Figure 7.1 and Figure 7.2 show the growth curve for *P. aeruginosa* and *B. subtilis* respectively along with their EPS production, expressed in terms of glucose, fructose, sucrose, and protein concentrations. Glucose, fructose, and sucrose are monosaccharide component of carbohydrates that are commonly found in EPS of biofilm from various *Pseudomonas* and *Bacillus* strains (Branda et al., 2005; Celik et al., 2008). The carbohydrate components are analyzed using Anthrone test (Section 3.6.4), while proteins are analyzed using Lowry test (Section 3.6.5).

Both bacterial strains exhibited about 6 hours of lag growth phase. However, *B. subtilis* enter the exponential and stationary phases of growth within a shorter time period (10 – 20 hours) than *P. aeruginosa* (15 – 22 hours). The stationary phase for *B. subtilis* was gradually followed by the death phase, while *P. aeruginosa* peaked at 22 hours briefly before entering the death phase and declining rapidly. Comparisons of

bacterial growth and EPS production for both bacteria between the exponential and stationary phase show that both bacteria have higher EPS concentrations in exponential phase, while lower EPS concentrations were found during the lag and death phases. Glucose constitutes a major component in the carbohydrate EPS from both bacteria, showing the highest concentration compared to fructose and sucrose throughout the growth. Different concentrations of monosaccharide components in the EPS largely depend on the composition of the growth medium (Grobben et al., 1996; Sheng et al., 2010). In this study, the bacteria were grown in the glucose-rich medium. Therefore, higher concentration of glucose was also found in the EPS produced during the growth.
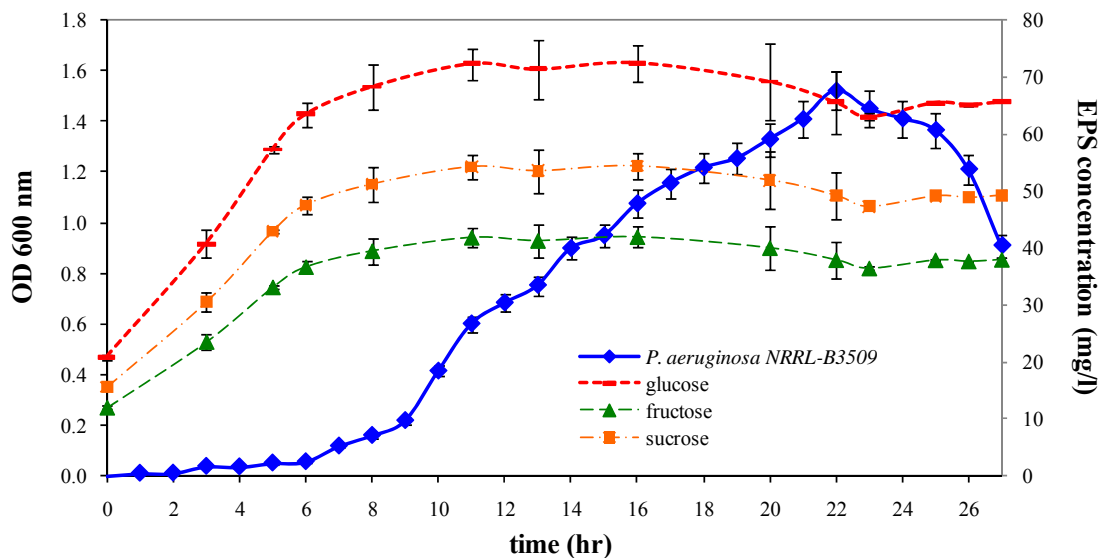
Figure 7.1 Growth curve with EPS production for *P. aeruginosa* NRRL-B3509
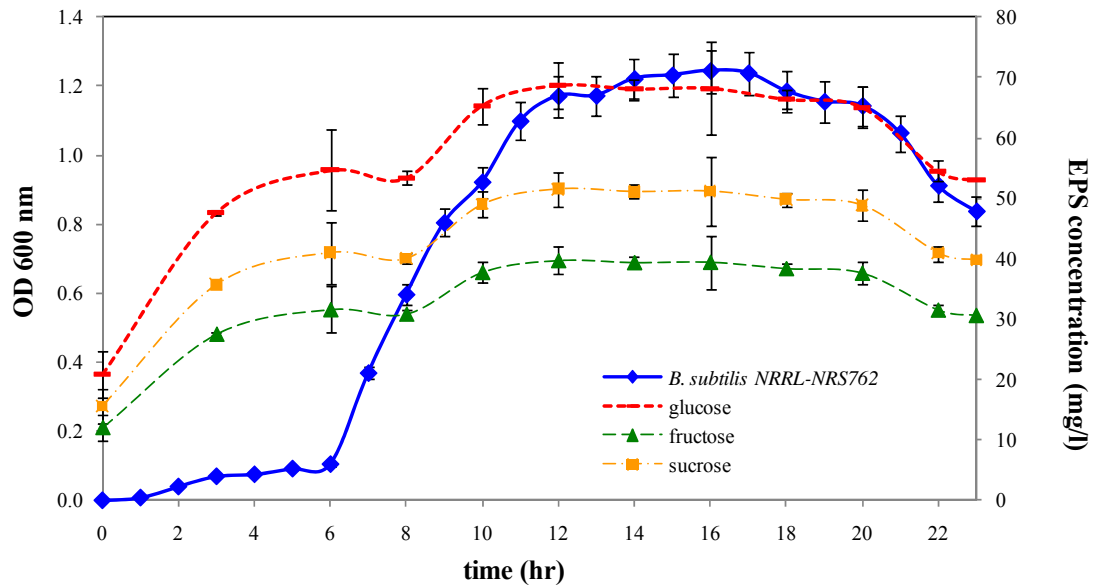
Figure 7.2 Growth curve with EPS production for *B. subtilis* NRRL-NRS762

EPS has been known to be produced by bacteria as protective barrier under conditions of starvation or extreme pH and temperatures (Knoshaug et al., 2000; Branda et al., 2005). Therefore, higher EPS production during the exponential and stationary phases could be viewed as a form of protection due to nutrient competition and depletion in the medium arising from rapid growth.

7. 2 Proteins and Carbohydrates Quantification from Bacterial Cultures and Biofilms

Figure 7.3 shows the weight of EPS in terms of total carbohydrates and total proteins for each gram of dried culture and biofilm biomass for *B. subtilis* and *P. aeruginosa*. The total carbohydrates were expressed in terms of glucose, fructose and sucrose sugars. The figure indicates that for the same bacteria, the ratio of EPS mass to dry cell mass is always higher for biofilm growth mode than planktonic growth mode. Carbohydrate components in the sessile cells are observed to be around 1.5-2.5 times that in planktonic cells, while protein components are 1.1-1.3 times. Production

of polysaccharides and protein during biofilm formation is reported to be important in supporting the biofilm cohesiveness. Hence these components are found at higher concentration in the sessile cells than in the planktonic cells (Ahimou et al., 2007b). These findings corroborate other published works which showed higher concentration of polysaccharides and protein in the biofilm EPS (Wozniak, 2003; Kives et al., 2006). It was reported that the EPS produced was not consumed as energy sources, but conferred protection to bacteria cells against adverse environmental stresses, such as nutrient depletion, extreme temperature, or antimicrobial compounds (Kim et al., 2000; Knoshaug et al., 2000). Therefore EPS production under biofilm growth mode is likely to be higher than planktonic growth mode.

Figure 7.3 also reveals that *B. subtilis* biofilm produces a higher concentration of EPS (both carbohydrates and proteins) than *P. aeruginosa*. As reported Section 4.1 and 4.2, *P. aeruginosa* formed denser biofilms than *B subtilis*. As a result, for approximately similar EPS concentration (mg/l) produced, EPS concentration expressed in mg/g dry weight biofilm will be larger in *B. subtilis* biofilm due to its lower biomass weight.
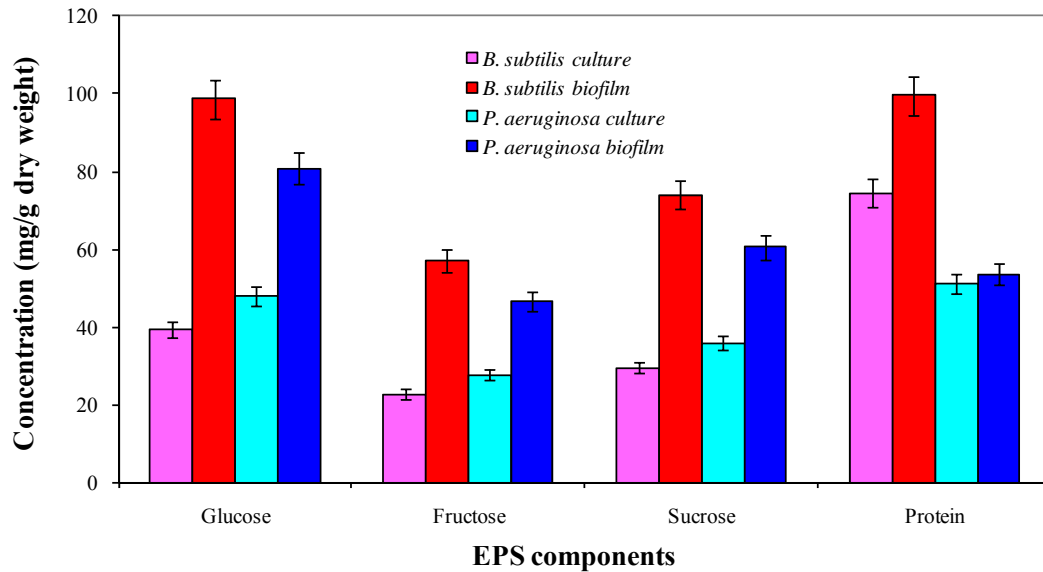
Figure 7.3 Comparison of EPS components from *B. subtilis* and *P. aeruginosa* cultures and biofilms

EPS contents of *P. aeruginosa* planktonic cells are slightly higher (approximately 10mg/g dry weight of total carbohydrate) than *B. subtilis*. On the other hand, the total protein content for planktonic *P. aeruginosa* was considerably lower; more than 20 mg/g dry weight lower than *B. subtilis* EPS. Differences in carbohydrate and protein contents in EPS could be attributed to the differing nature of the bacteria species and the types of possible EPS components produced by the bacteria (Atrih et al., 1999; Yao et al., 2002; Wozniak, 2003; Branda et al., 2006; Ryder et al., 2007). These studies suggest that *B. subtilis* EPS have higher protein content while *P. aeruginosa* EPS have higher carbohydrate content due to differences in their surface structures and metabolism, a result which is consistent with the protein and carbohydrate analysis as discussed in this section.

7. 3 EPS Elemental Composition observed using X-Ray Photoelectron Spectroscopy (XPS)

XPS was utilized to estimate the chemical and electronic state and assess the functionalities associated with carbon, nitrogen and oxygen of the extracted EPS samples. Each peak on the XPS spectra corresponds to electrons with characteristic binding energies from specific elements and the peak intensities can be used to estimate the relative elemental abundances accordingly. The XPS spectra from EPS samples are shown in Figure 7.4.
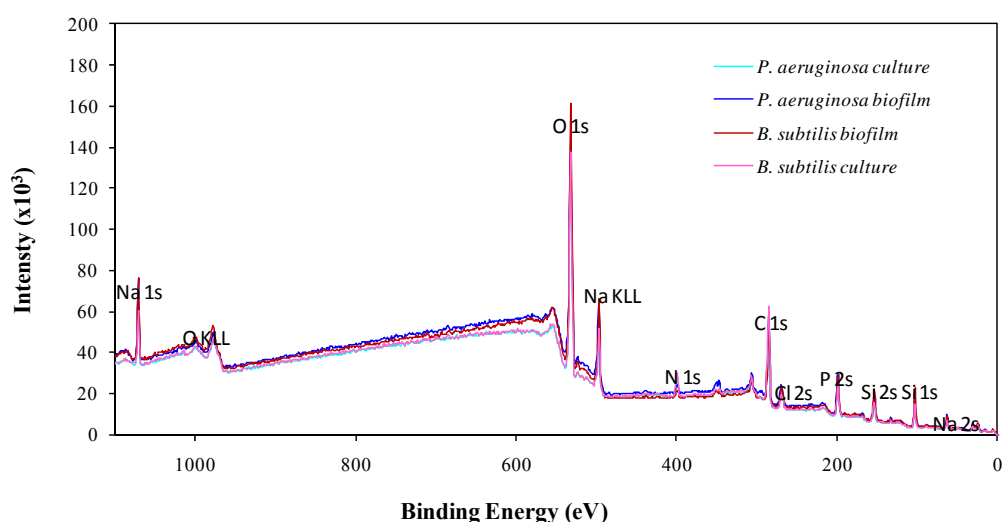
Figure 7.4 Wide scan XPS spectra of EPS samples from *B. subtilis* and *P. aeruginosa* cultures and biofilms

As depicted in Figure 7.4, the P2p peak was absent for all spectra. Absence of the P2p peak demonstrated that nucleic acids and phospholipids were below the XPS detection limit (total P < 0.1%) and there were no significant cell lysis during EPS extraction (Badireddy et al., 2010). Extraction is the most important step in determining the amount and composition of EPS accurately. A good extraction procedure should cause minimal cell lysis (Gehr and Henry, 1983). Therefore it can be concluded that any particular components detected in this study, are part of the extracellular matrix and not any intracellular polymeric component.

Investigation of the C1s, N1s and O1s spectra under high resolution scans (1eV step size) provided more information on the chemical bonding states of the elements (Omoike and Chorover, 2004; Leone et al., 2006a; Badireddy et al., 2010). The C1s spectrum was resolved into four components (Figure 7.5): (i) C–(C, H) mainly from aliphatic chains at 284.8 eV; (ii) C–(O, N) from proteins and alcohols at 286.2 eV; (iii) C=O or O–C–O as in carboxylate, carbonyl, amide, hemiacetal or acetal groups at 287.9 eV; and (iv) O=C–O from uronic acids (Badireddy et al., 2010) at 288.0 eV. Detection of uronic acids strongly indicated that compounds like MurNAc of *B. subtilis* peptidoglycan, and ManA and GulA of *P. aeruginosa* alginate were present in EPS samples (Rehm and Valla, 1997; Atrih et al., 1999).

Figure 7.5 XPS C1s spectra of EPS samples from: (a) *P. aeruginosa* cultures; (b) *P. aeruginosa* biofilms; (c) *B. subtilis* cultures; and (d) *B. subtilis* biofilms

The N1s spectrum was fitted by two peaks (Figure 7.6): (i) ≡N from amide and neutral amine groups of proteins at 399.8 eV; and (ii) ≡NH+ from charged amine groups at 400.8 eV. Both protonated and non-protonated amine were detected in biofilm and cultures are similar to other studies (Omoike and Chorover, 2004; Leone

et al., 2006a). The protonated amine site indicated the zwitter-ionic properties of EPS components. Candidates for such sites are carboxylate and/or phosphate functional groups (Leone et al., 2006a). The non-protonated amine compounds indicates that peptides were dominant in EPS samples.

Figure 7.6 XPS N1s spectra of EPS samples from: (a) *P. aeruginosa* cultures; (b) *P. aeruginosa* biofilms; (c) *B. subtilis* cultures; and (d) *B. subtilis* biofilms

The O 1s peaks were fitted into two peaks (Figure 7.7): (i) O=C as in carboxylic acid, carboxylate, carbonyl or amide functional groups at 532.2 eV; and (ii) C–O–(C, H) in alcohols, hemiacetal and acetal groups at 535.8 eV.

The atomic ratios of elements and functional groups with respect to total carbon from EPS samples are summarized in Table 7.1. From this table it is apparent that EPS from both *B. subtilis* cultures and biofilms samples have slightly higher protein content than *P. aeruginosa*, as denoted by the N/C ratio. This is similar to the trend concluded from protein and carbohydrate tests based on the Lowry and Anthrone tests. XPS analyses of bacterial surfaces found that bacterial strains with higher N/C ratios tend to have higher hydrophobicity ratings (Millsap et al., 1997;

Reid et al., 1999). Conversely, cells with higher O/C ratios tend to have higher hydrophilic ratings. The results indicate that the presence of extracellular proteinaceous materials increase the hydrophobicity of the cell surface.
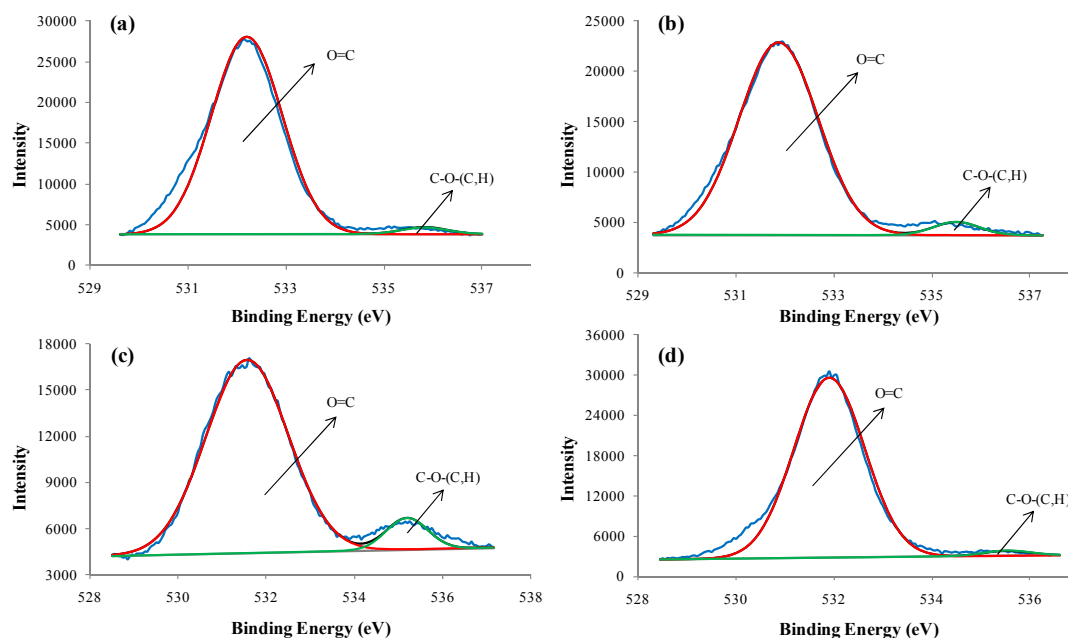
Figure 7.7 XPS O1s spectra of EPS samples from: (a) *P. aeruginosa* cultures; (b) *P. aeruginosa* biofilms; (c) *B. subtilis* cultures; and (d) *B. subtilis* biofilms

As shown in Table 7.1, EPS samples from *B. subtilis* have higher N/C ratios than *P. aeruginosa* in both growth modes. However, EPS from *P. aeruginosa* planktonic cells have higher O/C ratios, while the sessile cells have lower O/C ratio than *B. subtilis* from the same growth mode. Differences in these values might arise from different compositions of oxygen-containing chemical function on the surface of bacteria, such as oxygen in the phosphate groups and in amide function (Ahimou et al., 2007a). Values reported in Table 7.1 are comparable to XPS ratios reported for other Gram-positive and Gram-negative bacteria (Omoike and Chorover, 2004; Vermeltfoort et al., 2005; Leone et al., 2006a).

Table 7.1 Atomic ratios of elements and functional groups in EPS samples

	B. subtilis cultures	*P. aeruginosa* cultures	*B. subtilis* biofilms	*P. aeruginosa* biofilms
N/C	0.183	0.175	0.184	0.177
O/C	1.46	1.54	1.61	1.50
C–(C, H) at 284.8eV	0.36	0.28	0.39	0.29
C–(O, N) at 286.2eV	0.34	0.34	0.33	0.35
C=O, O–C–O at 287.9eV	0.21	0.29	0.20	0.28
O=C–O at 289.2eV	0.09	0.09	0.08	0.08
≡NH+/≡N	--	--	0.22	0.30

The ratio of total proteins (T_p), carbohydrates (T_c), uronic acids (T_u) and hydrocarbon-like compounds (T_{HC}) with respect to total carbon were also estimated according to the formulae proposed in other studies (Rouxhet et al., 1994; Ahimou et al., 2007a). The results are summarized in Table 7.2. This table shows no significant difference of components between biofilm and cultures from both bacteria. Rich protein content was found in EPS from all samples, followed by hydrocarbons, uronic acids, and carbohydrates.

Table 7.2 Ratios of total proteins, carbohydrates, uronic acids, and hydrocarbons to total carbons in EPS samples

Samples	Proteins $(T_p)^1$	Carbohydrates $(T_c)^2$	Uronic acids $(T_u)^3$	Hydrocarbons $(T_{HC})^4$
B. subtilis cultures	0.63	0.073	0.09	0.207
P. aeruginosa cultures	0.62	0.075	0.09	0.215
B. subtilis biofilms	0.66	0.066	0.08	0.194
P. aeruginosa biofilms	0.65	0.089	0.08	0.181

$^1T_p = 3.57(N/C)$, $^2T_c = C_{286.2eV} - (N/C) - T_u$, $^3T_u = C_{289.2eV}$, $^4T_{HC} = 1 - T_p - T_c - T_u$ (Rouxhet et al., 1994; Ahimou et al., 2007a)

7. 4 EPS Chemical Bonds and Functional Groups observed using ATR-FTIR Spectroscopy

Attenuated Total Reflection-Fourier Transform Infra-red (ATR-FTIR) Spectroscopy was used to obtain information on EPS functionalities. Figure 7.8 revealed that essentially all EPS samples showed similar spectra with different intensities; the highest absorbance intensities being shown by EPS from *P. aeruginosa* biofilms, while EPS from *B. subtilis* cultures recorded the lowest intensities.

Prominent characteristic groups of alcohols at wavelengths $1000 - 1300$ cm^{-1} and $3300 - 3500$ cm^{-1} symbolized the presence of a polyhydroxy compound – polysaccharides. Structurally, polysaccharides are composed of alcohol, aldehyde, ketone, ether and carboxylic acid functional groups. Proteins, in contrast, are associated with amine, amide and carboxylic acid functional groups. Intense absorbances for alcohol, amine and amide groups confirmed that carbohydrates and proteins are the predominant components of EPS materials.
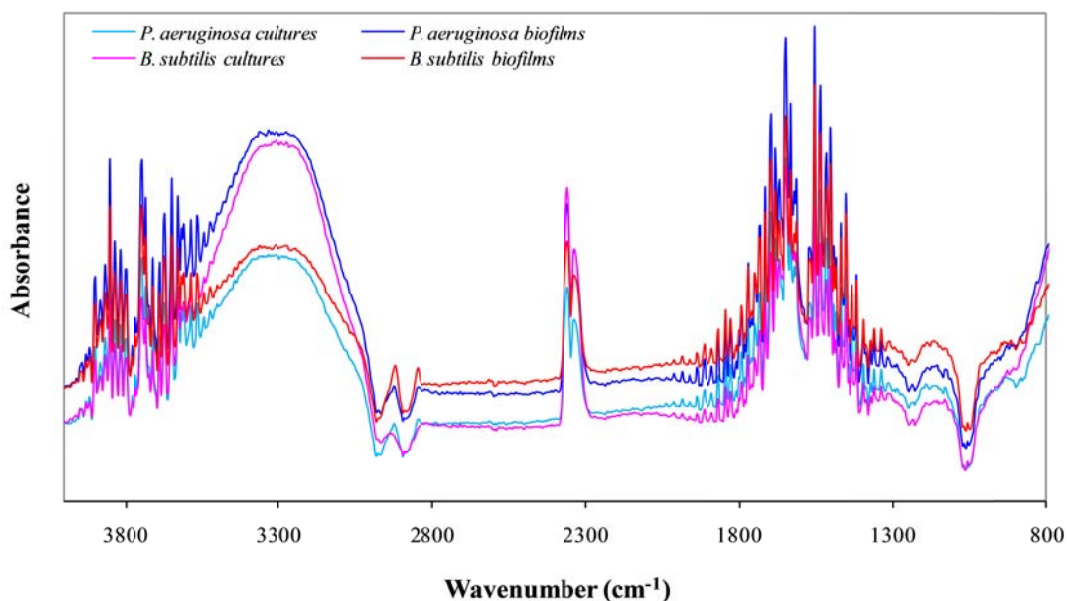
Figure 7.8 FTIR spectra of EPS samples from *B. subtilis* and *P. aeruginosa* cultures and biofilms

Broad infrared spectra in polysaccharides regions ($1000 - 1300$ cm^{-1}) are characteristic of molecules with two or three linked heterocycles in EPS samples (Gorner et al., 2003). Absorption at wavelengths around 1010 cm^{-1} showed that some polysaccharides of EPS samples encompassed D-glucose in the pyranose form. Meanwhile, the absorption at 812 cm^{-1} was due to mannose molecules. Mannose could be present in all EPS samples (Verhoef et al., 2005). Furthermore, increased absorption at 860 cm^{-1} corresponded to the presence of α-glycosidic linkages between individual glycosyl residues (Kodali et al., 2009).

The presence of amide I and II infrared bands (1540-1650 cm^{-1}) indicated that proteins within EPS samples were largely in the form of α-helix structures, although β-pleated sheets were also indicated. α-helices are one of the more prevalent secondary structures of proteins. The band at 1633cm^{-1} was specifically assigned to β-structures of protein (Badireddy et al., 2010). Based on previous tests, the absorption of *B. subtilis* EPS samples should be greater than that of *P. aeruginosa* due to its higher protein content by nature. However, the infrared spectra showed that the

absorption of *P. aeruginosa* biofilm and culture EPS samples exceeded those of *B. subtilis* biofilm and culture EPS samples in the vicinity of 1610 cm^{-1} and 1720 cm^{-1} (Figure 7.8). Intense absorption at the former region (1610 cm^{-1}) can be explained by the overlapping of the amide I band with the C–O stretching vibrational band characteristic of *P. aeruginosa* alginate polysaccharides (Silverstein et al., 1991). The increased absorption in the latter region (1720 cm^{-1}) can be inferred by the presence of o-acetylated carbohydrates common in gram-negative *P. aeruginosa* lipopolysaccharides (Badireddy et al., 2010).

Reduced absorption intensities caused by the stretching vibrations of CH_2 and CH_3 groups in the range 2850 – 2970 cm^{-1} suggested that planktonic EPS of both bacteria strains were characterized by shorter alkyl chains. Conversely, larger absorption intensities suggested that biofilm EPS were characterized by alkyl chains that were longer by at least two times. The long alkyl chains and ester functions at 1690 – 1760 cm^{-1} suggested that proteins within EPS could belong to the family of lipoproteins. Alternatively, these functionalities could have originated from fatty acid lipid components of the EPS material (Gorner et al., 2003).

7. 5 EPS Molecular Weight Distribution Analyses using Gas Permeation Chromatography (GPC)

GPC was used to determine the molecular weight distribution of the extracted EPS solutions of *B. subtilis* and *P. aeruginosa*. In this study, it was assumed that most of the polysaccharides and proteins were decomposed into smaller units via mild heating during the EPS extraction step. Therefore GPC analysis was conducted over a lower M_p range.

GPC confirmed the heterogeneity of all extracted EPS samples. The range of different molecular size fractions identified for each of the sample signified the existence of multiple sized polymeric components. EPS samples from *B. subtilis* produced a multitude of responses in the range of M_w = 206 – 911 g/mol for planktonic cultures and M_w = 207 – 925 g/mol for biofilms. Conversely, EPS samples from *P. aeruginosa* produced a multitude of responses in the range of M_w = 205 – 864 g/mol for planktonic cultures and M_w = 204 – 903 g/mol for biofilms. These results further verified that EPS produced by different bacteria species and by the same bacteria strain under different modes of growth were not compositionally identical. EPS from biofilm samples were believed to be composed of slightly higher molecular masses components or longer chain polymers. This was indicated by the slighter larger average M_w values measured for biofilm samples.

Table 7.3 shows a summary of the molecular weights and masses measured on an average basis for the four different EPS samples. Subtle variations in M_p values in Table 7.3 also highlight the distinction of EPS components between *B. subtilis* and *P. aeruginosa*.

Table 7.3 Summary of GPC data of EPS samples from *B. subtilis* and *P. aeruginosa* cultures and biofilms

Sample	M_n (g/mol)	M_w (g/mol)	M_P (g/mol)
B. subtilis cultures	337 ± 7	385 ± 14	308 ± 11
P. aeruginosa cultures	337 ± 6	385 ± 16	310 ± 5
B. subtilis biofilms	341 ± 6	392 ± 14	314 ± 8
P. aeruginosa biofilms	341 ± 4	391 ± 7	315 ± 1

M_n = weight average molecular weight, M_w = number average molecular weight, M_p = peak average molecular mass

Lower initial M_w values found for both EPS samples from *P. aeruginosa* cultures and biofilm could be related to the presence of quinonvosamine (QuiNAc)

(M_w = 205.2g/mol) which is a common acetyl sugar found in lipopolysaccharides (Wozniak, 2003). However, this was either produced in negligible amounts or entirely absent in EPS samples from *B. subtilis*. Lipopolysaccharides are therefore not a significant component in *B. subtilis* EPS.

Positive response on M_w range suggested that carbohydrates present within the EPS samples were mostly in the form of oligosaccharides. As stated previously, biopolymer breakdown have resulted from heating during extraction of EPS. Presumably, these oligosaccharides comprised up to six units of pentoses and/or their derivatives, or five units of hexoses and/or their derivatives (Leone et al., 2006b). Other oligosaccharides of *P. aeruginosa* encompassing monomers such as 3-deoxy-D-manno-octulosonic (KDO) (M_w = 238.2g/mol) and other N-acetyl sugars (most of which are of M_w = 221.2g/mol) of lipopolysaccharides (Wozniak, 2003); and ManA (M_w = 194.1g/mol) and GulA (M_w = 194.1g/mol) of alginate (Rehm and Valla, 1997) also fall in this M_w range. Specifically for EPS samples from *B. subtilis*, proteins such as short peptide chains of up to six units of GluA (M_w = 147.1g/mol) which link up together to form γ-PGA (Shih and Van, 2001), and GlcNAc (M_w = 221.2g/mol) and MurNAc (M_w = 293.0g/mol) of peptidoglycan could also be found within this M_w range.

7. 6 EPS Mass to Charge Ratio (m/z) Analyses using MALDI-TOF-MS

MALDI-TOF-MS was employed to determine the intrinsic mass-to-charge ratio (m/z) property of EPS samples used in this study. Mass spectra collected for all samples were found containing seven peaks per sample between 0.5 – 1.1 kDa, with the exception of EPS samples from *B. subtilis* biofilms which has eight peaks (Table 7.4). Selection of peaks was limited to mean signal-to-noise ratio of at least 5 to 1 to ensure reliable measurement.

Table 7.4 Identification of significant peaks in MALDI-TOF-MS Spectra

Peak	Matrix (m/z)	*B. subtilis* cultures	*P. aeruginosa* cultures	*B. subtilis* biofilms	*P. aeruginosa* biofilms
1	564.9	536.1 ± 0.1	536.0 ± 6.4	536.0 ± 9.1	514.7 ± 9.6
2	595.7	591.8 ± 0.1	564.9 ± 4.5	591.9 ± 8.2	558.4 ± 0.1
3	612.0	642.0 ± 5.9	676.0 ± 7.1	642.1 ± 6.8	612.1 ± 7.7
4	635.8	704.1 ± 0.1	730.1 ± 0.1	704.1 ± 4.5	704.2 ± 9.2
5	654.2	761.1 ± 3.0	741.1 ± 5.3	763.6 ± 4.8	764.3 ± 9.1
6	672.2	778.0 ± 9.3	846.2 ± 7.0	880.3 ± 2.3	880.5 ± 9.9
7	686.2	907.3 ± 0.057	906.3 ± 7.8	934.4 ± 0.1	1057.1 ± 0.1
8	692.0	--	--	1078.6 ± 0.1	--
9	706.9	--	--	--	--
10	806.0	--	--	--	--
11	846.1	--	--	--	--
12	864.5	--	--	--	--

MALDI-TOF mass spectrometry confirmed the finding of GPC analysis that polysaccharides and proteins present within EPS samples were mostly in the form of oligosaccharides and short chain peptides (small proteins). As shown in Table 7.4 and Figure 7.9, the two bacteria species were easily distinguishable from each other by characterizing the peaks and profiles of their respective mass spectra.

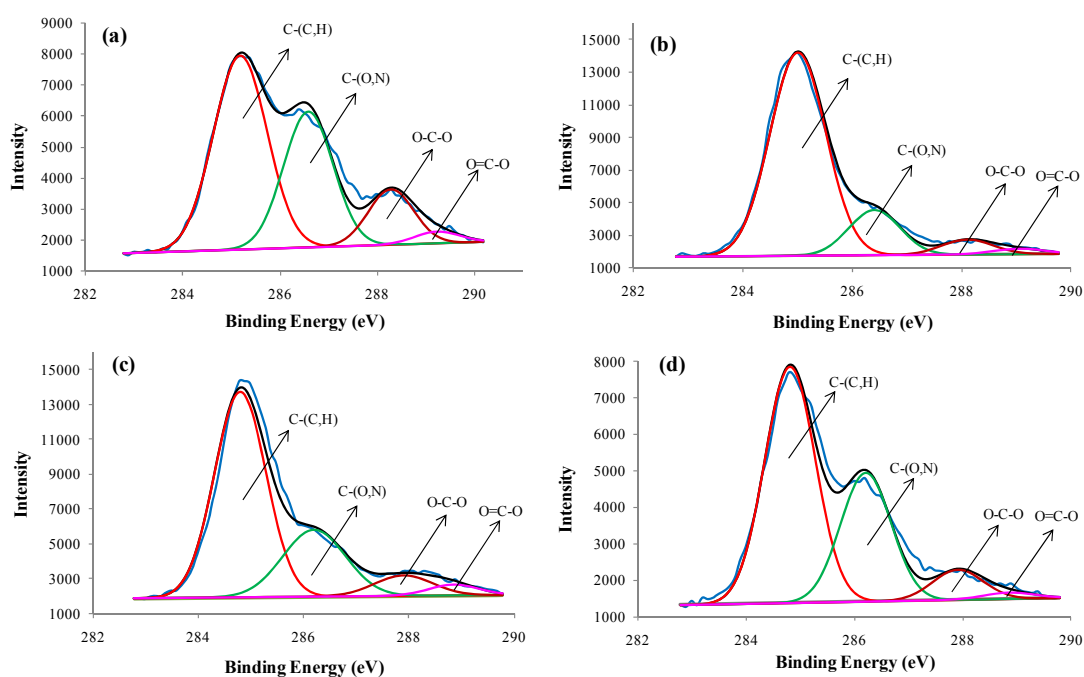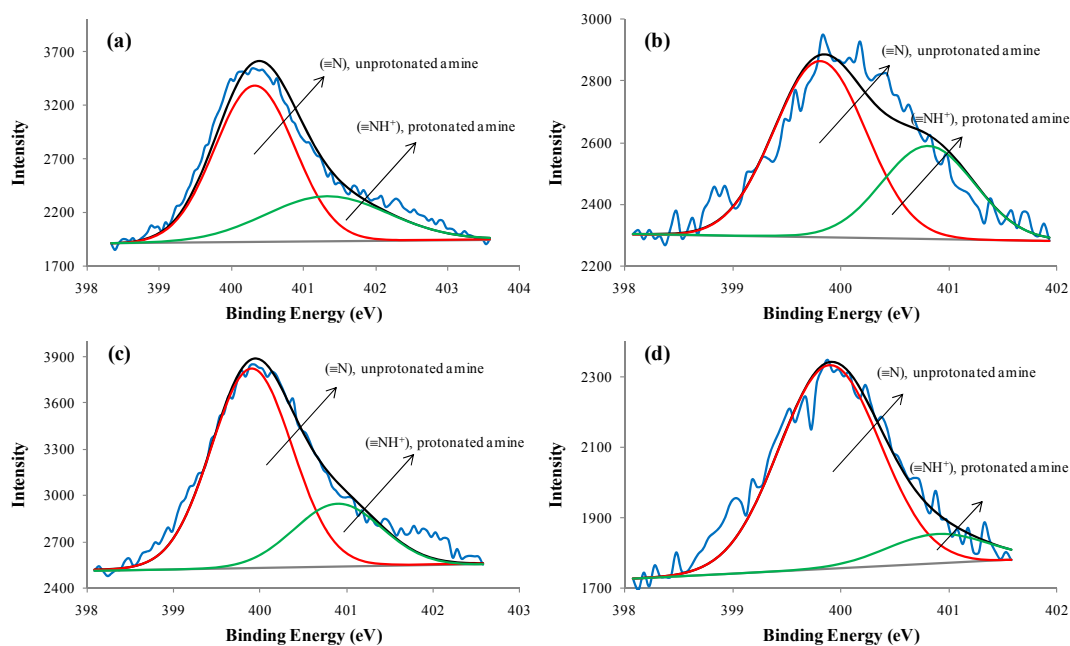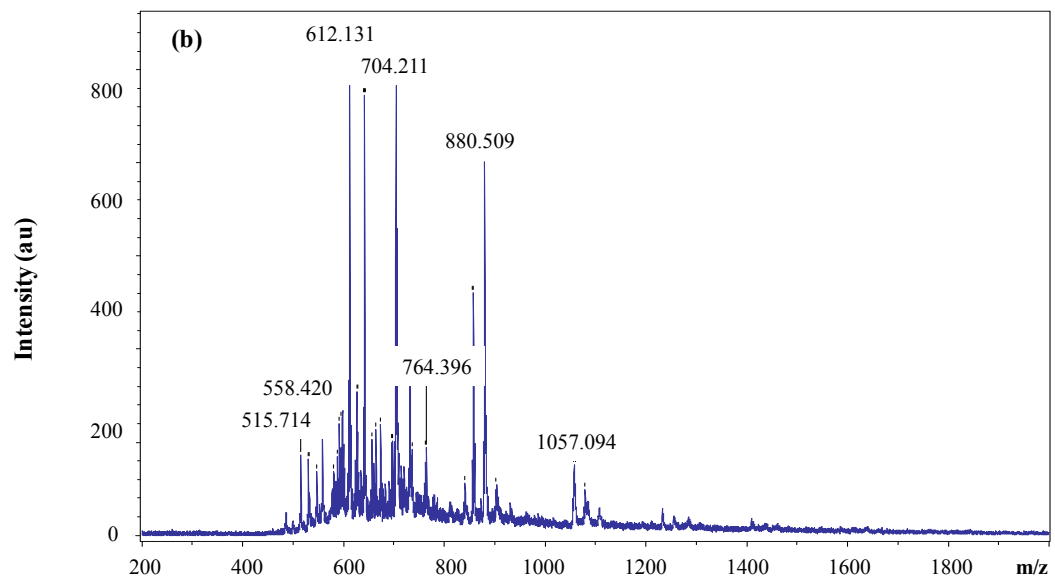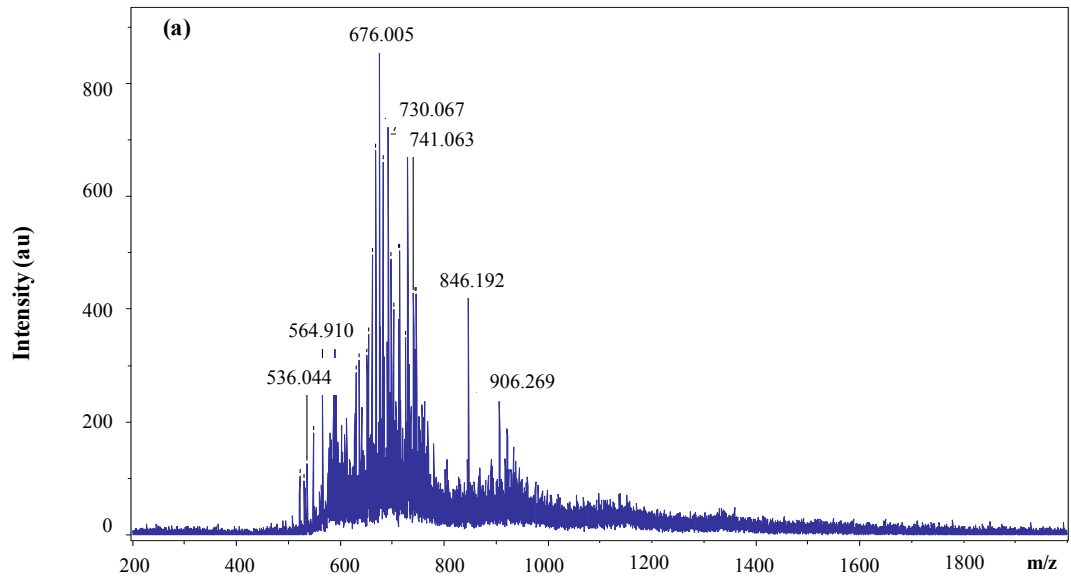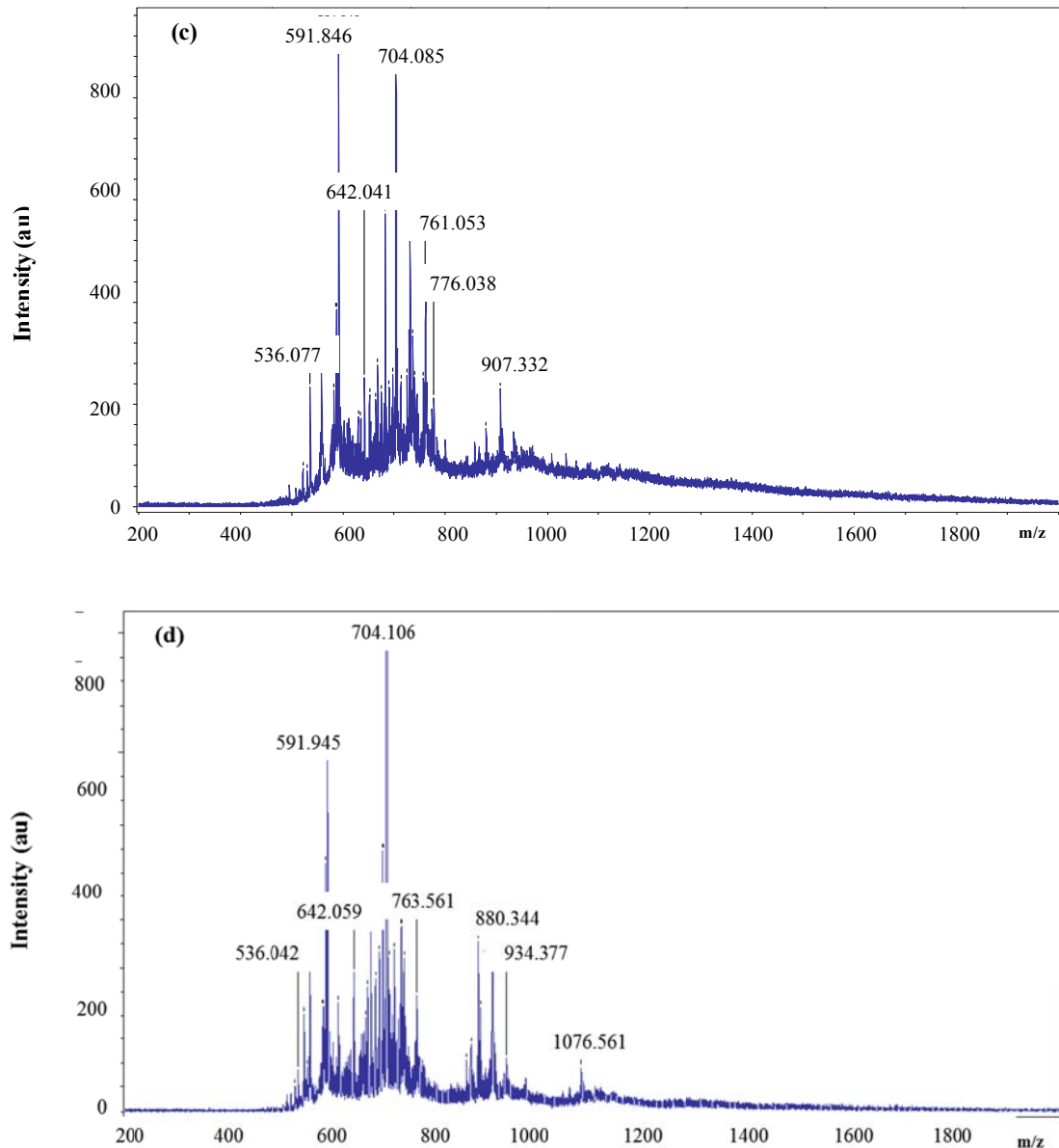**Figure 7.9** MALDI-TOF-MS spectra of EPS samples from: (a) *P. aeruginosa* cultures; (b) *P. aeruginosa* biofilms; (c) *B. subtilis* cultures; and (d) *B. subtilis* biofilms

There were no apparent differences within the range of 0.5 − 0.8 kDa in terms of the profile of the mass spectra between EPS samples from *B. subtilis* cultures and biofilms. Two particular peaks were exceptionally noticeable − 591.9 and 704.1 m/z. Beyond this range, EPS from *B. subtilis* biofilms had three unique larger molecular weight biopolymers (880.3, 934.4 and 1078.6 m/z) that were different from the cultures (907.3 m/z). In contrast, EPS from *P. aeruginosa* had more evident differences in the types of biopolymers expressed between cultures and biofilms. The

profiles of the respective spectra were considerably dissimilar. Between 0.5 – 0.74 kDa, mass spectra pointed towards EPS components of lower molecular weight for biofilm growth. However, beyond 0.74kDa, EPS components from biofilm had higher molecular weight.

These findings showed that EPS components produced by bacteria varied with the growth modes. EPS produced during planktonic growth tend to be more uniform in molecular weights, as depicted by the clustered peaks of the mass spectra over a small range of values (Figure 7.9). In contrast, EPS produced during biofilm growth were more diverse, having components with more diffused molecular weights that extended over a wider range. In addition, the types of EPS produced between different growth modes varied more greatly between *P. aeruginosa* and *B. subtilis*.

Data obtained in this study can be compared with stored bacterial mass spectra from reference libraries to predict the types of proteins or carbohydrates (Sauer and Kliem, 2010). Short peptide chains of GluA arising from γ-PGA of *B. subtilis* could have accounted for peaks 591.8, 591.9 (four units) and 880.3 m/z (six units). The characteristic m/z ratios of *P. aeruginosa* reflected the absence of GluA as an EPS component. Ratio of m/z showing 536.1, 907.3, and 1078.6 could indicate that the oligosaccharides in *B. subtilis* were composed of hexoses (three, five or six units) or other hexose derivatives. Likewise, 536.0 and 906.3 m/z ratios reflected that the oligosaccharides in *P. aeruginosa* were composed of hexoses or other hexose derivates (three or five units). These short chain oligosaccharides could perhaps involved glucose, mannose and galactose monosaccharides that make up the Psl or Pel carbohydrates. Alternatively, it could reflect the minor amounts of xylose or arabinose detected in some *P. aeruginosa* strains. Other derivatives of Psl and Pel

carbohydrates linked with hexose sugars could have also accounted for close by m/z ratios such as 558.4 and 1057.1.

Lastly, 764.3 m/z value of EPS samples from *P. aeruginosa* biofilms might be the result of ManA and GulA (four units in total linked together), which constitute the alginate polysaccharide. Other studies have reported that alginate is required for attachment to surfaces (Mai et al., 1993) and formation of thick and three dimensional biofilms (Nivens et al., 2001; Hay et al., 2009). Since biofilms were not formed in planktonic culture suspensions, ManA and GulA were probably not significantly expressed and reflected in the mass spectrum of EPS samples from *P. aeruginosa* cultures. However, alginate was not totally absent from these samples as the O=C–O functionality detected via XPS confirmed the presence of uronic acid enrichment in the planktonic culture samples.

7. 7 Single Molecule Force Spectroscopy (SMFS) using Atomic Force Microscope (AFM)

In this section, AFM force volume measurements were made to explore the diversity and adhesive properties of EPS on the bacteria cell surfaces. This will help in understanding the roles of EPS in cell adhesion and aggregation. The conformational and nano-mechanical properties (adhesion and extension) of individual EPS or exopolymers on the microbial cell surface are made possible with this analysis.

SMFS with polydopamine-functionalized AFM tips revealed major differences in EPS properties of the two bacteria strains. The adhesion force histograms (Figure 7.10) revealed that *P. aeruginosa* exhibited higher mean forces (162.00 ± 98.02 pN) than *B. subtilis* (114.80 ± 55.15 pN). The distribution of the adhesion histogram for *P. aeruginosa* was broader, falling over the range of 50-550

pN, unlike for *B. subtilis* which was concentrated in the range 50–400 pN. Adhesion force with the highest frequency in *P. aeruginosa* (Figure 7.10a) correspond to single mannose interactions. The mean binding force of 162 pN measured for *P. aeruginosa* corresponds to the simultaneous detection of two mannose or glucose residues Specific rupture force of mannose or glucose complexes on the surface of a living yeast cell has been reported to be in the range of 75 to 200 pN (Gad et al., 1997). The presence of mannose and/or glucose residues could have arisen from Pel and Psl polysaccharides present within *P. aeruginosa* EPS (Ryder et al., 2007). Since mannose and glucose interactions were more strongly detected than other interactions, these mannose- or glucose-rich polysaccharides most likely constituted the predominant components of EPS samples from *P. aeruginosa*.
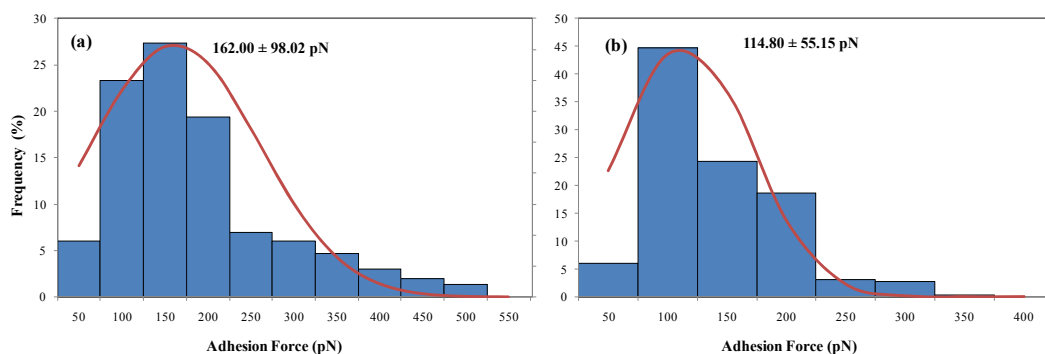
Figure 7.10 Adhesion force histogram (n=300) for : (a) *P. aeruginosa*; and (b) *B. subtilis*

Three-dimensional maps were also presented to further visualize the differences in polymer properties of the two bacteria strains (Figure 7.11 and Figure 7.12). Comparison of both figures demonstrated that while polysaccharides and proteins were homogeneously distributed on the cell surfaces for both bacteria, the exo-biopolymers were clearly more extended and more adhesive on *P. aeruginosa*. Most of the polymers of *P. aeruginosa* were extended within 400 nm to 1200 nm in length and exhibited adhesion forces of 60 pN to 175 pN (Figure 7.11). Longer

extension lengths denoted that the biopolymers were longer in length and more capable of stretching. Enhanced adhesion forces could have resulted from the detection of multiple polydopamine–biopolymer interactions or biopolymers with a greater adhesive nature.
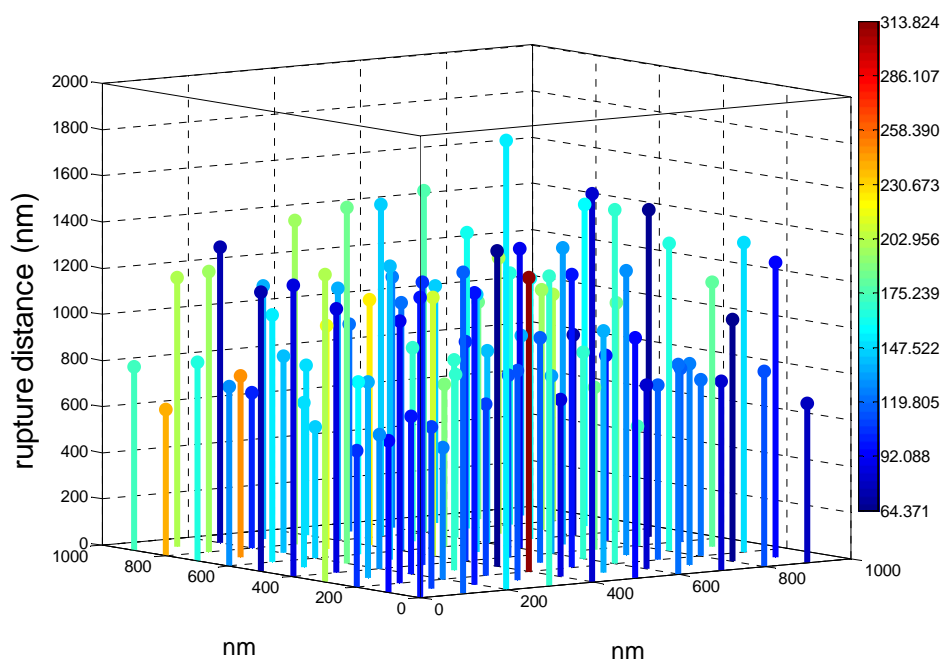
Figure 7.11 Three-dimensional reconstructed maps of polymer properties for *P. aeruginosa* by combining adhesion force values (expressed as false colors) and rupture distances (expressed as z level) measured at different x, y locations

Smaller adhesion forces ranging from 30 pN up to 150 pN and moderate rupture distances between 100 nm and 400 nm were observed on *B. subtilis*. Despite this, a small minority (< 10%) of adhesive force measured for *B. subtilis* were in the range of 300 pN to 500 pN (Figure 7.12). These data confirmed that the stretched polymers on different bacteria were not only of different nature, as deduced from the previous analyses, but also possessed different mechanical properties. Hence, this suggested the possibility of the aggregation or adhesive properties of EPS being correlated to the types of components present within the EPS.
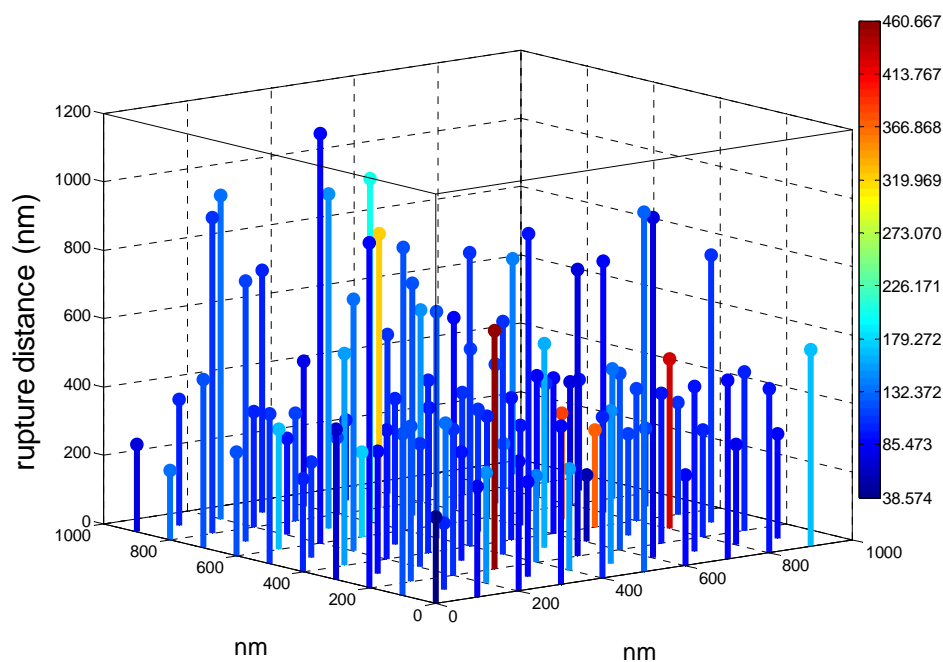
Figure 7.12 Three-dimensional reconstructed maps of polymer properties for *B. subtilis* by combining adhesion force values (expressed as false colors) and rupture distances (expressed as z level) measured at different x, y locations

7. 8 General Discussion

Anthrone and Lowry tests provided a relative estimate of the total carbohydrate and protein contents respectively, within the EPS samples. XPS and ATR-FTIR assessed the major elemental and electronic state, chemical bonds and functional groups of the EPS samples, while GPC and MALDI-TOF-MS allowed for the identification of specific EPS components based on the characteristic mass profiles. In addition, probing of the distribution and mechanical properties of the exo-biopolymers of interest were made possible with the use of AFM force measurements. All these analytical methods offered different yet complementary approaches toward elucidating the compositional, conformational and adhesive characteristics of EPS produced by *P. aeruginosa* NRRL-B3509 and *B. subtilis* NRRL-NRS762.

A comparison of the results from different analysis provided much evidence that the type of EPS produced varied with the bacterial growth modes. Firstly, sessile

cells produced 1.1 − 2.5 times greater quantities of EPS in terms of total carbohydrate and protein than their planktonic cells on a dry cell mass basis, as shown in the Anthrone and Lowry tests. This is because EPS are produced to offer protection against non-ideal growth conditions under biofilm growth and not as energy sources under planktonic growth. Secondly, the compositions of planktonic and biofilm EPS are dissimilar, as revealed by ATR and GPC. EPS from biofilms had higher concentrations of carbohydrates and proteins which also have higher molecular masses than EPS associated with the planktonic cells. Thirdly, MALDI-TOF and SMFS results showed that EPS produced under planktonic and sessile growth were structurally distinct. Shorter peptide chains and oligosaccharides were predominantly present in EPS produced from planktonic growth. In contrast, longer protein chains and polysaccharides characterized sessile growth.

The occurrence of long alkyl chains and ester functions found in EPS from biofilms also suggests the possibility of lipoproteins or lipid components which were absent or insignificant in EPS from cultures. Nonetheless, there were insignificant variations in the major chemical bonds and functional groups present within EPS from both modes of growth. Lastly, AFM showed that EPS samples from biofilms were more adhesive than the one from cultures.

The differences between EPS samples from cultures and biofilms particularly for *B. subtilis* NRRL-NRS762, were not significant. MALDI-TOF-MS confirmed the presence of a number of similar components in the EPS from both sample types. For *P. aeruginosa* NRRL-B3509, however, there were more pronounced differences between the components of EPS samples from cultures and biofilms, as revealed in the MALDI-TOF mass spectra.

Moreover, it was shown that the appearance of alginate in EPS samples from cultures could have been reduced, as ManA and GulA were not expressed and reflected in the spectrum. Since there is a distinct correlation between the appearance of mucoid phenotype and the overproduction of alginate (Ryder et al., 2007), the reduced production of alginate could have accounted for the less mucoid appearance observed in culture samples as compared to biofilm samples.

The elements, types of functional groups and chemical bonds revealed by the various analytical techniques can be used to piece together the monomers and resultant polymers present within the EPS samples of *B. subtilis* and *P. aeruginosa*. Evidence in this study indicated the presence of γ-PGA and peptidoglycan in *B. subtilis* NRRL-NRS762. Short peptide chains of GluA as revealed by GPC and MALDI-TOF-MS possibly constituted γ-PGA. However, it was not possible to deduce the exact molecular weight of the γ-PGA due to polymer breakdown during the extraction of the EPS. It has been reported that γ-PGA derived from microorganisms have molecular weights ranging from 10kDa to over 1000kDa (Ashiuchi and Misono, 2002).

The O=C–O functionality detected in *B. subtilis* samples and GPC mass profiles was consistent with the occurrence of MurNAc and GlcNAc compounds. Peptidoglycan has been reported to be made up of alternating β-1,4-linked GlcNAc and MurNAc substituted with peptide side chains. These are mostly tripeptides with uncross-linked, but form tripeptide tetrapeptide when peptide side chains are cross-linked by the free amino group of mesodiaminopimelic acid and carboxylic acid group of D-Ala (Atrih and Foster, 1999). Detection of oligosaccharides of hexoses or their derivatives could have corresponded to the short chains of alternating MurNAc and GlcNAc units. The short peptide chains of peptidoglycan could have also

accounted for some of the low molecular mass peaks detected in GPC and MALDI-TOF-MS analyses.

Lipopolysaccharides, alginate, Pel and Psl carbohydrates are more prevalent components of EPS from *P. aeruginosa* NRRL-B3509. Minor amounts of xylose and arabinose have also been detected Previous studies have revealed that xylose and arabinose were not found in lipopolysaccharides, alginate, Pel and Psl carbohydrates of *P. aeruginosa* (Rehm and Valla, 1997; Wozniak, 2003; Friedman and Kolter, 2004). Xylose and arabinose monosaccharides could have originated from other less predominant polysaccharides in the EPS samples. Identified o-acetylated carbohydrates, QuiNAc, KDO and mannose compounds were also representative of lipopolysaccharides existence in EPS samples from this bacteria. The presence of uronic acids as revealed by XPS, overlapping of the amide I band with the C–O stretching vibrational band by ATR and mass profiles of ManA and GulA, were characteristic of alginate. Remarkably, extensive detection of mannose- and glucose-rich polysaccharides confirmed that both Pel and Psl were detected in *P. aeruginosa* NRRL-B3509.

The spectroscopic studies revealed that EPS produced by *P. aeruginosa* has higher carbohydrates but lower protein content than *B. subtilis*. Colorimetric assays showed the total carbohydrates to be approximately 10mg/g dry weight higher and the total proteins to be approximately 20mg/g dry weight lower. These results, together with AFM force measurements, suggest that polysaccharides, rather than proteins, play a crucial role in determining the adhesive nature of bacterial EPS. These could possibly explain the larger magnitude of the adhesion forces detected for *P. aeruginosa* EPS samples, as opposed to the much reduced adhesion forces for *B. subtilis* EPS samples.

It was shown that compounds that bind to or disrupt carbohydrates decreased the adherence of *P. fragi* to stainless steel. However, compounds specific for proteins had little effect on adherence (Herald and Zotolla, 1989). Further support for polysaccharides, rather than proteins, being involved in the adhesion process has earlier been published. Lipopolysaccharides and alginate polysaccharides of *P. aeruginosa* have been shown to be important components influencing initial surface attachment (Mai et al., 1993; Shi and Zhu, 2009). The presence of o-acetylated carbohydrates on the lipopolysaccharides is believed to a play critical role in cell aggregation and adhesion (Nivens et al., 2001; Sutherland, 2001; Tielen et al., 2005). Similarly, the Psl polysaccharide of *P. aeruginosa* promotes cell-surface and intercellular interactions (Ma et al., 2006). Pel polysaccharide, however, has indirect correlations to adhesive functions as it is required for the maintenance of a mature biofilm structure (Friedman and Kolter, 2004). Likewise, alginate reportedly plays a role in the formation of thick and three-dimensional mature biofilms (Nivens et al., 2001; Hay et al., 2009).

The discrepancy in the adhesive properties of EPS measured in this study might have arisen from the differences in the conformations between polysaccharides and proteins present within the EPS. The different types of bindings that exist between different monomers (monosaccharides versus amino acids) can influence the structure of EPS, and hence, their adhesive properties (Poulsen, 1999). The absence of exopolysaccharides in the biofilm matrix of *B. subtilis* has been reported to be correlated with their roles in cellular adhesion and structural maintenance (Branda et al., 2005). It was also found that γ-PGA protein production is linked with enhancement of cellular adherence to surfaces (Stanley and Lazazzera, 2005). However, a later study using wild strains bearing mutations in the genes responsible

for γ-PGA synthesis concluded that γ-PGA did not contribute significantly to bacterial adhesion (Branda et al., 2006). Differences in the structures of polysaccharides and proteins could also affect the hydrophobicity or hydrophilicity of the EPS layer. A hydrophobic molecule would rather exist in another hydrophobic environment than in a hydrophilic environment and vice versa (Palmer et al., 2007). Hence, hydrophobic or hydrophilic effects have widely been suggested to influence the adherence of cells to surfaces (Hood and Zottola, 1995).

In addition, the lengths of exopolymers were observed to be correlated to their adhesion strengths. With increasing polymer length, there is a possibility of a greater number of side chains that can form bridges and complexes with the surface (Palmer et al., 2007) or entrap cells and cause cellular aggregation. This explains the more extended and more adhesive polymers probed on the surface of *P. aeruginosa* cells. It might also explain why biofilm adherence was much stronger than planktonic cell adherence for the same species, since EPS from biofilms were characterized by much longer proteins and carbohydrate compounds.

Greater awareness of the compositional, conformation and adhesive properties of EPS components and insights into how these properties might be correlated can be derived from this study. A better understanding of the mechanism of bacterial attachment and the various factors influencing this process can be exploited to enhance existing beneficial biofilm systems and bio-remediation systems and/or control detrimental bio-fouling and biotransfer potential. Most importantly, exopolysaccharides have been identified as one of the prime EPS components, besides proteins, that confer adherence properties to the bacteria and biofilm matrices. Hence, these exopolysaccharides can serve as active targets for controlling or removing bacterial biofilm formations.

7. 9 Summary

The present study has provided further insights into identifying the compositional and conformational properties of extracellular polymeric substances (EPS) produced by planktonic and biofilm cells of *B. subtilis* and *P. aeruginosa*. XPS, ATR-FTIR, GPC and MALDI-TOF-MS analyses provided detailed examination of the differences in chemistry of the respective exopolymers. It was established that EPS produced by the two different species were chemically dissimilar. More proteinaceous compounds, such as γ-PGA and peptidoglycan, were present in EPS from *B. subtilis*. Conversely, EPS from *P. aeruginosa* were characterized by greater carbohydrate components like lipopolysaccharides, alginate, Pel and Psl polysaccharides. The relative proportions of polysaccharides and/or proteins constituents and associated functional group chemistry, however, varied with the growth mode of the bacteria.

AFM was then used to probe the adhesive nature of EPS produced by the bacteria by using Single Molecule Force Spectroscopy (SMFS). The idea that compositional differences could influence the adhesive properties of EPS was investigated. *P. aeruginosa* exhibited a mean force of 162.00 ± 98.02 pN while *B. subtilis* exhibited a mean force of 114.80 ± 55.15 pN. Comparison of the two bacterial species indicated that the presence of polysaccharides in the EPS layer promoted the adhesion strength of the EPS. Proteins in EPS had lesser adherence effects. On the other hand, comparison of the two growth modes for the same bacterial strain indicated that greater EPS production and enhanced cellular adhesion are associated with biofilm growth. Therefore, characterization of EPS has provided a better understanding of their major properties and their roles in cellular adhesion and biofilm formation.

CHAPTER 8

CONCLUSIONS AND RECOMMENDATIONS

8. 1 Conclusions

This research investigated the surface properties and interactions between two bacteria, *P. aeruginosa* NRRL-B3509 and *B. subtilis* NRRL-NRS762, and stainless steel SS316, and their relation during adhesion process in biofilm formation. Biofilm formed by both bacteria were characterized and compared. Physicochemical analyses and theoretical approaches using DLVO and extended DLVO were used to explain the interactions and factors involved during adhesion process. Atomic force microscopy (AFM) was also used to quantify the adhesion forces between bacteria and SS316. Various chemical analyses and single molecule force spectroscopy (SMFS) were also employed to investigate the composition and adhesive properties of EPS secreted by both bacteria.

For both bacterial strains, biofilms were established within 24 hours. However, SEM observation showed that the biofilm formed by *P. aeruginosa* NRRL- B3509 were denser compared to *B. subtilis* NRRL-NRS762. One possible cause for this phenomenon is that *P. aeruginosa* showed higher specific growth rate than *B. subtilis*. *P. aeruginosa* grew and replicated faster, resulting in higher competition for utilizing the nutrient in the medium. Since biofilm formation is one of the defensive ways of microorganisms surviving a lack of nutrient, more of the bacterial cell of this strain become sessile and form biofilm. The second possible cause is related to the nature of cell surface properties of each microbial strain. *B. subtilis* shows a more negative zeta potential than *P. aeruginosa*, and thus, the stability of *B. subtilis* in the medium suspensions is higher than *P. aeruginosa*, and is comparatively less likely to attach to

the metal surface. This is confirmed by CFU counts and dry weight of biofilm, which were lower for *B. subtilis*. Monitoring the surface of the biofilm using FTIR spectroscopy also revealed that *P. aeruginosa* NRRL-B3509 produced more EPS which contain protein, which act as adhesive in the attachment process. This results in *P. aeruginosa* forming thicker and denser than biofilm of *B. subtilis*. As both strains are commonly found in the industries, concerns about biofilm formation would be higher with *P. aeruginosa*, since initial attachment is a crucial step in biofilm formation. This series of experiments also showed the likelihood of *P. aeruginosa* and *B. subtilis* to establish biofilm and become persistent in the environment.

A direct approach via AFM force measurement and theoretical approach using surface interaction energies combined with DLVO and xDLVO theories has been used to interpret the interactions between these two bacteria and SS316 metal surfaces. Higher affinity was shown by *P. aeruginosa* when the adhesion force was measured using AFM. Average adhesion forces of bacterial cell probes on SS316 surface in 10mM PBS buffer (pH 7.2) with surface delays varying from 0 to 60 seconds were 3.84 - 8.53 nN and 0.65 – 1.44 nN for *P. aeruginosa* and *B. subtilis* respectively. Due to bond maturation and protein interaction between the bacterial surfaces and the metal, stronger forces became more prominent with longer surface delays. Physicochemical analyses have revealed that *P. aeruginosa* is more hydrophobic than *B. subtilis*. This correlated well with different surface properties of *P. aeruginosa*, where more proteins and polysaccharides were produced as EPS and biosurfactant. Adhesions were also dominated by electrostatic repulsion interactions, as predicted by both DLVO and xDLVO theories, due to negative charges of both interacting surfaces. Compared to *P. aeruginosa*, *B. subtilis* have to overcome a higher energy barrier when approaching SS316 surfaces. However, as a conducting

material, SS316 can generate image charges in the opposite of sign with charges from approaching bacteria. This causes electrostatic attractive interaction between bacteria and metal surfaces, which makes it possible for both bacteria to fall into the secondary minimum state and attach onto surfaces. In addition to electrostatic interactions, acid-base interactions via electron donor-acceptor also contributed significantly towards bacterial adhesion, especially for *P. aeruginosa*, where attraction interactions facilitate the bacteria to overcome the energy barrier when approaching the metal surface.

Surface and interaction energies based on a theoretical approach using DLVO and xDLVO theories together with AFM force measurement have also been used to observe and quantify the adhesion interactions between *B. subtilis* spores and stainless steel SS316. The study revealed that, compared to vegetative cells, *B. subtilis* spores showed higher affinity towards SS316 surfaces. Physicochemical analyses have revealed that *B. subtilis* spores have higher hydrophobicity than the vegetative cells. Stronger hydrophobicity on spores is due to the significant amount of protein layers (instead of peptidoglycan) on the spore surfaces, thus enhancing the attraction interactions on the metal surfaces. When approaching SS316 surfaces, at a very short distance, interactions between surfaces are mainly dominated by electrostatic interactions which constitute most of the total interaction energies. A larger energy barrier was faced by vegetative cells, making it more difficult to be deposited on the surfaces. On the other hand, attractive acid-base interactions facilitate spores in lowering the energy barrier and enhancing the deposition. Stronger affinity of *B. subtilis* spores toward SS316 surfaces were also corroborated by force measurement using AFM. Compared to its vegetative cells, *B. subtilis* spores showed higher adhesion forces (2.92 ± 0.4 nN) when retracted from SS316 surfaces compared to the

vegetative cells (0.65 ± 0.2 nN). Due to various components on the surfaces such as polysaccharides, proteins, and other exo-polymers, spores establish stronger attachment on SS316 surfaces compared to their vegetative cells, thus causing firmer biofilm adhesion under favorable conditions. The presence of spores is thus more problematic in biofilm control due to stronger attachment and its persistence under environmental conditions which favor the development of spores.

The composition and characteristic of EPS produced by *P. aeruginosa* and *B. subtilis* from both growth cultures and biofilms have also been elucidated using several techniques for chemical analysis. XPS, ATR-FTIR, GPC and MALDI-TOF-MS analyses provided detailed examination of the differences in chemistry of the respective exopolymers. It was established that EPS produced by the two different species were chemically dissimilar. More proteinaceous compounds, such as γ-PGA and peptidoglycan, were present in EPS from *B. subtilis*. Conversely, EPS from *P. aeruginosa* were characterized by greater carbohydrate components such as lipopolysaccharides, alginate, Pel and Psl polysaccharides. The relative proportions of polysaccharides and/or protein constituents and associated functional group chemistry, however, varied with the growth mode of the bacteria. AFM was then used to probe the adhesive nature of EPS produced by the bacteria by using Single Molecule Force Spectroscopy (SMFS). The idea that compositional differences could influence the adhesive properties of EPS was investigated. *P. aeruginosa* exhibited a mean force of 162.00 ± 98.02 pN while *B. subtilis* exhibited a mean force of 114.80 ± 55.15 pN. Comparison of the two bacterial species indicated that the presence of polysaccharides in the EPS layer promoted the adhesion strength of the EPS. Proteins in EPS had lesser adherence effects. On the other hand, comparison of the two growth

modes for the same bacterial strain indicated that greater EPS production and enhanced cellular adhesion are associated with biofilm growth.

8. 2 Recommendations

The surface interactions and surface properties of two bacteria related to their ability to adhere and form biofilm on stainless steel SS316 have been studied. Experiments with AFM force spectroscopy using viable bacterial probes to quantify the bacterial-metal interaction forces in nano-scale have been made and the composition and the adhesive properties of EPS found on the bacterial surfaces elucidated. A contribution has been made to the understanding of both the cell surface properties and the structure-function relationship between bacteria and stainless steel SS316 surface during the adhesion process. From this knowledge, more effective and efficient biofilm control can be developed based on specific properties of biofilm forming bacteria.

However, the work has been limited to the initial bacteria-metal interaction during the adhesion process. As such it does not consider factors that influence biofilm accumulation. Since biofilm formation is a complex process, further study on surface-structure relationship and interactions during subsequent processes, such as maturation and detachment, will give a better understanding of biofilm formation mechanism. Such knowledge would be very beneficial in biofilm control.

In this study, interactions of bacteria on metal surfaces during the adhesion process have been limited to stainless steel surfaces. Stainless steel was chosen as it is commonly utilized in the food-processing industries. However various other surfaces have also been reported to be used in this kind of environment, such as plastics, rubbers, or other polymers. A study of the properties and interactions of these surfaces with bacteria will be of added value, since specific surfaces are likely to create

different conditions for bacterial attachment, and hence require specific control technology.

Interactions of bacteria on the stainless steel surfaces in this study were investigated in a static system. Natural adhesion and biofilm formation commonly occur in non-static flow-through system, such as in the pipelines and heat exchangers. The flow rate of the fluid is expected to have a significant effect on the bacterial adhesion on the metal surfaces and subsequent biofilm formation. Slow flow rate would facilitate the biofilm growth and accumulation, while a high flow rate would induce detachment. Hence, it is important to investigate the relationship between the flow rate, the hydrodynamics, and the interactions of bacteria-metal surfaces.

Lastly, biofilm formation involve a consortium of bacteria which may give rise to more complex process and impact than in pure culture systems. A cooperative role between aerobic and anaerobic bacteria often occurs, as well as metabolic compound production and utilization from one bacterium to another. This relationship among bacteria thus renders complexity in adhesion and biofilm formation. Since this study is limited to the interactions between pure culture bacteria and metal surfaces, more study is required to investigate the interactions between mixed cultures and surfaces to reflect the natural biofilm phenomenon.

8. 3 Limitations

It is important to realize that there are several limitations in this research work. In this study, we used one of the most established theoretical approaches, the DLVO theory, to predict interactions between the bacteria and metal surfaces. Although widely used in various systems involving living microorganisms, the accuracy of the theory is still debatable. The DLVO theory and thermodynamic approach in calculating the adhesion energy may be relevant in bacterial adhesion, i.e. at different

separation distances between cell surface and substratum surface. Accuracy may be increased by using the extended DLVO theory which incorporates the hydrophobicity/ hydration effect as described in acid-base interaction in addition of van der Waals and electrostatic interactions. It must be emphasized that biological systems are dynamic, and biological changes in sessile bacteria, as compared its planktonic cells, made it impossible to fully explain microbial adhesion by only this theoretical approach. The theory nonetheless helps in focusing the research framework and forms the basis for further study.

Although the polydopamine wet adhesive technique was used to glue a single bacterium on the AFM tips, SEM figures showed that the bacterium is not attached precisely on the tip's apex. It is likely that different position of the bacteria on the tip may influence the accuracy of the force measurement (to varying degrees) due to the different magnitude of interactions experienced by the bacteria and the metal surfaces. This limitation may be overcome by incorporating an optical microscope to visually improve the attachment so that the bacteria may be more precisely attached on the tip's apex. In addition, reliability and reproducibility of force measurements can be improved by using more cell probes for the same bacteria and system in the computation of the average adhesion forces.

The hydrophilic nature of the surfaces of both the microorganisms also influences the adhesion force measurements, especially under changing moisture condition (or humidity). Hydrophilic surfaces tend to greater interaction (i.e. higher adhesion) at higher humidity, due to water penetration into the surface pores via capillary forces, thus enhancing the interaction between surfaces. Moisture also influence bacterial surface thermodynamics, depending on the characteristics of the outer membrane. Gram-negative bacteria contain high lipid and low peptidoglycan

content on their outer membrane, causing the surface properties to be easily influenced by moisture contents of the surrounding environments. On the other hand, Gram-positive bacteria are high in peptidoglycan, making them more resistant to the surrounding environment.

Further improvement may be made on the characterization of the EPS. In this study, separation, purification of the components of the EPS and its identification was not attempted, and only a generalization of the different possible parts that assumed from various chemical and surface characterizations. Since the current study has found that EPS of the two model bacteria consisted mainly of polysaccharides and proteins, the next step would be analyzes of components of polysaccharides and proteins, particularly specific components that have significant influence on adhesion. Polysaccharides may be analyzed and identified using techniques methods such as gas-liquid chromatography and HPLC, while proteins analysis may be performed using gel electrophoresis, liquid chromatography, or DNA microarray.

XPS results in EPS characterization should also to be treated with caution since peak deconvolutions in XPS are highly subjective. Moreover, XPS data showed that differences in protein and carbohydrates content on four EPS types are not significant, hence cannot fully support the conclusions obtained.

REFERENCES

Abu-Lail, N.I., Camesano, T.A., (2002). Elasticity of *Pseudomonas putida* KT2442 surface polymers probed with single-molecule force microscopy. Langmuir 18(10), 4071-4081.

Abu-Lail, N.I., Camesano, T.A., (2003a). Polysaccharide properties probed with atomic force microscopy. Journal of Microscopy 212(3), 217-238.

Abu-Lail, N.I., Camesano, T.A., (2003b). Role of lipopolysaccharides in the adhesion, retention, and transport of *Escherichia coli* JM109. Environmental Science and Technology 37(10), 2173-2183.

Ahimou, F., Boonaert, C.J.P., Adriaensen, Y., Jacques, P., Thonart, P., Paquot, M., Rouxhet, P.G., (2007a). XPS analysis of chemical functions at the surface of *Bacillus subtilis*. Journal of Colloid and Interface Science 309(1), 49-55.

Ahimou, F., Denis, F.A., Touhami, A., Dufrene, Y.F., (2002). Probing microbial cell surface charges by atomic force microscopy. Langmuir 18(25), 9937-9941.

Ahimou, F., Paquot, M., Jacques, P., Thonart, P., Rouxhet, P.G., (2001). Influence of electrical properties on the evaluation of the surface hydrophobicity of *Bacillus subtilis*. Journal of Microbiological Methods 45(2), 119-126.

Ahimou, F., Semmens, M.J., Haugstad, G., Novak, P.J., (2007b). Effect of protein, polysaccharide, and oxygen concentration profiles on biofilm cohesiveness. Applied and Environmental Microbiology 73(9), 2905-2910.

Al-Awadhi, H., Al-Hasan, R.H., Sorkhoh, N.A., Salamah, S., Radwan, S.S., (2003). Establishing oil-degrading biofilms on gravel particles and glass plates. International Biodeterioration and Biodegradation 51(3), 181-185.

Al-Zahrani, A.R.A., Idris, G., (2010). Biological treatment of hydrocarbon contaminants: petroleum hydrocarbon uptake by *Pseudomonas alkanolytica*. Journal of King Abdulaziz University : Engineering Sciences 21(1), 39-53.

Allison, D.G., Sutherland, I.W., (1987). The role of exopolysaccharides in adhesion of freshwater bacteria. Journal of General Microbiology 133(5), 1319-1327.

Alsteens, D., Dupres, V., Mc Evoy, K., Wildling, L., Gruber, H.J., Dufrene, Y.F., (2008). Structure, cell wall elasticity, and polysaccharide properties of living yeast cells, as probed by AFM. Nanotechnology 19(384005), 1-9.

Anderson, A., Ronner, U., Granum, P., (1995). What problems does the food industry have with the spore forming pathogens Bacillus cereus and Clostrirliuni perfringens. International Journal of Food Microbiology, 145-157.

Anderson, L., Unger, F.M., (1983). *Bacterial lipopolysaccharides: structure, synthesis, and biological activities*. American Chemical Society.

Ankolekar, C., Labbe, R.G., (2009). Physical characteristics of spores of food-associated isolates of the *Bacillus cereus* group. Applied and Environmental Microbiology 76(3), 982-984.

Anwar, H., Dasgupta, M.K., Costerton, J.W., (1990). Testing the susceptibility of bacteria in biofilms to antibacterial agents. Antimicrobial Agents and Chemotherapy 34(11), 2043-2046.

Anwar, H., Strap, J.L., Costerton, J.W., (1992). Eradication of biofilm cells of *Staphylococcus aureus* with tobramycin and cephalexin. Canadian Journal of Microbiology 38(7), 618-625.

Ashiuchi, M., Misono, H., (2002). Biochemistry and molecular genetics of poly-gamma-glutamate synthesis. Applied Microbiology and Biotechnology 59(1), 9-14.

Atrih, A., Bacher, G., Allmaier, G., Williamson, M.P., Foster, S.J., (1999). Analysis of peptidoglycan structure from vegetative cells of *Bacillus subtilis* 168 and role of PBP 5 in peptidoglycan maturation. Journal of Bacteriology 181(13), 3956-3966.

Atrih, A., Foster, S.J., (1999). The role of peptidoglycan structure and structural dynamics during endospore dormancy and germination. Antonie Van Leeuwenhoek 75(4), 299-307.

Augustin, M., Ali-Vehmas, T., Atroshi, F., (2004). Assessment of enzymatic cleaning agents and disinfectants against bacterial biofilms. Journal of Pharmacy and Pharmaceutical Science 7(1), 55-64.

Azeredo, J., Visser, J., Oliveira, R., (1999). Exopolymers in bacterial adhesion: interpretation in terms of DLVO and XDLVO theories. Colloids and Surfaces B: Biointerfaces 14(1-4), 141-148.

Badireddy, A.R., Chellam, S., Gassman, P.L., Engelhard, M.H., Lea, A.S., Rosso, K.M., (2010). Role of extracellular polymeric substances in bioflocculation of activated sludge microorganisms under glucose-controlled conditions. Water Research 44(15), 4505-4516.

Bakke, R., Trulear, M.G., Robinson, J.A., Characklis, W.G., (1984). Activity of *Pseudomonas aeruginosa* in biofilms: Steady state. Biotechnology and Bioengineering 26(12), 1418-1424.

Basson, A., Flemming, L.A., Chenia, H.Y., (2008). Evaluation of adherence, hydrophobicity, aggregation, and biofilm development of *Flavobacterium johnsoniae*-like isolates. Microbial Ecology 55(1), 1-14.

Bayer, M.E., Sloyer Jr, J.L., (1990). The electrophoretic mobility of Gram-positive and Gram-negative bacteria. Journal of General Microbiology 136(5), 867-874.

Beech, I.B., Gaylarde, C.C., (1999). Recent advances in the study of biocorrosion: an overview. Revista de Microbiologia 30(3), 117-190.

Beech, I.B., Gubner, R., Zinkevich, V., Hanjangsit, L., Avci, R., (2000). Characterisation of conditioning layers formed by exopolymeric substances of *Pseudomonas* NCIMB 2021 on surfaces of AISI 316 stainless steel. Biofouling 16(2), 93-104.

Beech, I.B., Smith, J.R., Steele, A.A., Penegar, I., Campbell, S.A., (2002). The use of atomic force microscopy for studying interactions of bacterial biofilms with surfaces. Colloids and Surfaces B: Biointerfaces 23(2-3), 231-247.

Benoit, M., Gabriel, D., Gerisch, G., Gaub, H.E., (2000). Discrete interactions in cell adhesion measured by single-molecule force spectroscopy. Nature Cell Biology 2(6), 313-317.

Bento, F.M., Camargo, F.A., Okeke, B.C., Frankenberger Jr, W.T., (2005). Diversity of biosurfactant producing microorganisms isolated from soils contaminated with diesel oil. Microbiological Research 160(3), 249-255.

Bernardes, P.C., Andrade, N.J., Ferreira, S.O., Sa, J.P.N., Araujo, E.A., Delatorre, D.M.Z., Luiz, L.M.P., (2010). Assessment of hydrophobicity and roughness of stainless steel adhered by an isolate of *Bacillus cereus* from a dairy plant. Brazilian Journal of Microbiology 41(4), 984-992.

Beveridge, T., Graham, L., (1991). Surface layers of bacteria. Microbiology and Molecular Biology Reviews 55(4), 684-705.

Binnig, G., Quate, C.F., Gerber, C., (1986). Atomic force microscope. Physical Review Letters 56(9), 930-933.

Blackman, I.C., Frank, J.F., (1996). Growth of *Listeria monocytogenes* as a biofilm on various food-processing surfaces. Journal of Food Protection 59(8), 827-831.

Blaschek, H.P., Wang, H.H., Agle, M.E., (2007). *Biofilms in the Food Environment.* Blackwell Publishers Iowa.

Boks, N.P., Busscher, H.J., Van Der Mei, H.C., Norde, W., (2008). Bond-strengthening in *Staphylococcal* adhesion to hydrophilic and hydrophobic surfaces using atomic-force microscopy. Langmuir 24(22), 12990-12994.

Bond, P.L., Smriga, S.P., Banfield, J.F., (2000). Phylogeny of microorganisms populating a thick, subaerial, predominantly lithotrophic biofilm at an extreme acid mine drainage site. Applied and Environmental Microbiology 66(9), 3842-3849.

Bosecker, K., (1997). Bioleaching: metal solubilization by microorganisms. FEMS Microbiology Reviews 20(3-4), 591-604.

Bowen, W.R., Fenton, A.S., Lovitt, R.W., Wright, C.J., (2002). The measurement of *Bacillus mycoides* spore adhesion using atomic force microscopy, simple counting methods, and a spinning disk technique. Biotechnology and Bioengineering 79(2), 170-179.

Bowen, W.R., Lovitt, R.W., Wright, C.J., (2000). Direct quantification of *Aspergillus niger* spore adhesion to mica in air using an atomic force microscope. Colloids and Surfaces A: Physicochemical and Engineering Aspects 173(1-3), 205-210.

Bowen, W.R., Lovitt, R.W., Wright, C.J., (2001). Atomic force microscopy study of the adhesion of *Saccharomyces cerevisiae*. Journal of Colloid and Interface Science 237(1), 54-61.

Boyd, A., Chakrabarty, A.M., (1995). Pseudomonas aeruginosa biofilms: Role of the alginate exopolysaccharide. Journal of Industrial Microbiology 15(3), 162-168.

Branda, S.S., Chu, F., Kearns, D.B., Losick, R., Kolter, R., (2006). A major protein component of the *Bacillus subtilis* biofilm matrix. Molecular Microbiology 59(4), 1229-1238.

Branda, S.S., Vik, A., Friedman, L., Kolter, R., (2005). Biofilms: the matrix revisited. Trends in Microbiology 13(1), 20-26.

Brant, J., Childress, A., (2002). Membrane-colloid interactions: comparison of extended DLVO predictions with AFM force measurements. Environmental Engineering Science 19(6), 413-427.

Bremer, P.J., Fillery, S., McQuillan, A.J., (2006). Laboratory scale Clean-In-Place (CIP) studies on the effectiveness of different caustic and acid wash steps on the removal of dairy biofilms. International Journal of Food Microbiology 106(3), 254-262.

Brown, D.G., Jaffé, P.R., (2005). Effects of Nonionic Surfactants on the Cell Surface Hydrophobicity and Apparent Hamaker Constant of a Sphingomonas sp. Environmental Science & Technology 40(1), 195-201.

Burks, G.A., Velegol, S.B., Paramonova, E., Lindenmuth, B.E., Feick, J.D., Logan, B.E., (2003). Macroscopic and nanoscale measurements of the adhesion of bacteria with varying outer layer surface composition. Langmuir 19(6), 2366-2371.

Busscher, H., Van de Belt-Gritter, B., Van der Mei, H., (1995). Implications of microbial adhesion to hydrocarbons for evaluating cell surface hydrophobicity 1. Zeta potentials of hydrocarbon droplets. Colloids and Surfaces B: Biointerfaces 5(3-4), 111-116.

Busscher, H.J., Norde, W., Sharma, P.K., van der Mei, H.C., (2010). Interfacial re-arrangement in initial microbial adhesion to surfaces. Current Opinion in Colloid & Interface Science 15(6), 510-517.

Butt, H., Jaschke, M., Ducker, W., (1995). Measuring surface forces in aqueous electrolyte solution with the atomic force microscope. Bioelectrochemistry and Bioenergetics 38(1), 191-201.

Camesano, T.A., Liu, Y., Datta, M., (2007). Measuring bacterial adhesion at environmental interfaces with single-cell and single-molecule techniques. Advances in Water Resources 30(6-7), 1470-1491.

Camesano, T.A., Logan, B.E., (2000). Probing Bacterial Electrosteric Interactions Using Atomic Force Microscopy. Environmental Science & Technology 34(16), 3354-3362.

Cao, N., Du, J., Chen, C., Gong, C.S., Tsao, G.T., (1997). Production of fumaric acid by immobilized *Rhizopus* using rotary biofilm contactor. Applied Biochemistry and Biotechnology 63(1), 387-394.

Carpentier, B., Chassaing, D., (2004). Interactions in biofilms between *Listeria monocytogenes* and resident microorganisms from food industry premises. International Journal of Food Microbiology 97(2), 111-122.

Celik, G.Y., Aslim, B., Beyatli, Y., (2008). Characterization and production of the exopolysaccharide (EPS) from *Pseudomonas aeruginosa* G1 and *Pseudomonas putida* G12 strains. Carbohydrate Polymers 73(1), 178-182.

Chan-Blanco, Y., Bonilla-Leiva, A., Velazquez, A., (2003). Using banana to generate lactic acid through batch process fermentation. Applied Microbiology and Biotechnology 63(2), 147-152.

Characklis, W., Nevimons, M., Picologlou, B., (1981). Influence of fouling biofilms on heat transfer. Heat Transfer Engineering 3(1), 23-37.

Chen, G., Driks, A., Tawfiq, K., Mallozzi, M., Patil, S., (2010). *Bacillus anthracis* and *Bacillus subtilis* spore surface properties and transport. Colloids and Surfaces B: Biointerfaces 76(2), 512-518.

Chen, G., Strevett, K.A., (2003). Microbial surface thermodynamics and interactions in aqueous media. Journal of Colloid and Interface Science 261(2), 283-290.

Cheung, H., Sun, S., Sreedhar, B., Ching, W., Tanner, P., (2000). Alterations in extracellular substances during the biofilm development of Pseudomonas aeruginosa on aluminium plates. Journal of Applied Microbiology 89(1), 100-106.

Chin, C., Yiacoumi, S., Tsouris, C., (2002). Influence of metal ion sorption on colloidal surface forces measured by atomic force microscopy. Environmental Science and Technology 36(3), 343-348.

Christenson, H., Claesson, P., (2001). Direct measurements of the force between hydrophobic surfaces in water. Advances in Colloid and Interface Science 91(3), 391-436.

Chung, E., Kweon, H., Yiacoumi, S., Lee, I., Joy, D.C., Palumbo, A.V., Tsouris, C., (2009). Adhesion of spores of *Bacillus thuringiensis* on a planar surface. Environmental Science and Technology 44(1), 290-296.

Clement, J.A., Martin, S.G., Porter, R., Butt, T.M., Beckett, A., (1993). Germination and the role of extracellular matrix in adhesion of urediniospores of *Uromyces viciae-fabae* to synthetic surfaces. Mycological Research 97(5), 585-593.

Cloete, T.E., Jacobs, L., (2001). Surfactants and the attachment of *Pseudomonas aeruginosa* to 3CR12 stainless steel and glass. Water SA 27(1), 21–26.

Coetser, S.E., Cloete, T.E., (2005). Biofouling and biocorrosion in industrial water systems. Critical Reviews in Microbiology 31(4), 213-232.

Cornell, R.M., Schwertmann, U., (1996). *The iron oxides: Structure, properties, reactions, occurrences, and uses*. VCG-Weinheim Germany.

Costerton, J., Stewart, P., Greenberg, E., (1999). Bacterial biofilms: a common cause of persistent infections. Science 284(5418), 1318-1322.

Costerton, J.W., Anwar, H., (1994). *Pseudomonas aeruginosa*: The microbe and pathogen. Infectious Disease and Therapy Series 12, 1-17.

Costerton, J.W., Cheng, K.J., Geesey, G.G., Ladd, T.I., Nickel, J.C., Dasgupta, M., Marrie, T.J., (1987). Bacterial biofilms in nature and disease. Annual Review of Microbiology 41, 435-464.

Costerton, J.W., Lewandowski, Z., Caldwell, D.E., Korber, D.R., Lappin-Scott, H.M., (1995). Microbial biofilms. Annual Reviews in Microbiology 49(1), 711-745.

Cramton, S.E., Gerke, C., Schnell, N.F., Nichols, W.W., Gotz, F., (1999). The intercellular adhesion (ica) locus is present in *Staphylococcus aureus* and is required for biofilm formation. Infection and Immunity 67(10), 5427-5433.

Daims, H., Nielsen, J.L., Nielsen, P.H., Schleifer, K.H., Wagner, M., (2001). In situ characterization of *Nitrospira*-like nitrite-oxidizing bacteria active in wastewater treatment plants. Applied and Environmental Microbiology 67(11), 5273-5284.

Davies, D., Parsek, M., Pearson, J., Iglewski, B., Costerton, J., Greenberg, E., (1998a). The involvement of cell-to-cell signals in the development of a bacterial biofilm. Science 280(5361), 295.

Davies, D.G., Parsek, M.R., Pearson, J.P., Iglewski, B.H., Costerton, J.W., Greenberg, E.P., (1998b). The involvement of cell-to-cell signals in the development of a bacterial biofilm. Science 280(5361), 295-298.

Desai, J.D., Banat, I.M., (1997). Microbial production of surfactants and their commercial potential. Microbiology and Molecular Biology Reviews 61(1), 47-64.

Dickson, J.S., Koohmaraie, M., (1989). Cell surface charge characteristics and their relationship to bacterial attachment to meat surfaces. Applied and Environmental Microbiology 55(4), 832-836.

Dong, Y.H., Gusti, A.R., Zhang, Q., Xu, J.L., Zhang, L.H., (2002). Identification of quorum-quenching N-acyl homoserine lactonases from *Bacillus* species. Applied and Environmental Microbiology 68(4), 1754.

Dorobantu, L.S., Bhattacharjee, S., Foght, J.M., Gray, M.R., (2008). Atomic force microscopy measurement of heterogeneity in bacterial surface hydrophobicity. Langmuir 24(9), 4944-4951.

Dosti, B., Zeydim, Z.G., Greene, A.K., (2005). Effectiveness of ozone, heat and chlorine for destroying common food spoilage bacteria in synthetic media and biofilms. International Journal of Dairy Technology 58(1), 19-24.

Doyle, R.J., Nedjat-Haiem, F., Singh, J.S., (1984). Hydrophobic characteristics of *Bacillus* spores. Current Microbiology 10(6), 329-332.

Ducker, W., Senden, T., Pashley, R., (1991). Direct measurement of colloidal forces using an atomic force microscope. Nature 353(6341), 239-241.

Dufrene, Y., (2002). Atomic force microscopy, a powerful tool in microbiology. Journal of Bacteriology 184(19), 5205-5213.

Dufrêne, Y., (2008). Towards nanomicrobiology using atomic force microscopy. Nature Reviews Microbiology 6(9), 674-680.

Dufrene, Y.F., (2004). Using nanotechniques to explore microbial surfaces. Nature Reviews Microbiology 2(6), 451-460.

Dufrene, Y.F., Boonaert, C.J.P., Gerin, P.A., Asther, M., Rouxhet, P.G., (1999). Direct probing of the surface ultrastructure and molecular interactions of dormant and germinating spores of *Phanerochaete chrysosporium*. Journal of Bacteriology 181(17), 5350-5354.

Dunstall, G., Rowe, M.T., Wisdom, G.B., Kilpatrick, D., (2005). Effect of quorum sensing agents on the growth kinetics of *Pseudomonas spp.* of raw milk origin. Journal of Dairy Research 72(03), 276-280.

Eginton, P., Gibson, H., Holah, J., Handley, P., Gilbert, P., (1995). The influence of substratum properties on the attachment of bacterial cells. Colloids and Surfaces B: Biointerfaces 5(3-4), 153-159.

Egli, K., Bosshard, F., Werlen, C., Lais, P., Siegrist, H., Zehnder, A., Van der Meer, J., (2003). Microbial composition and structure of a rotating biological contactor biofilm treating ammonium-rich wastewater without organic carbon. Microbial Ecology 45(4), 419-432.

El Masry, M.H., Hassouna, M.S., El Rakshy, N., Mousa, I., (1995). Bacterial populations in the biofilm and non biofilm components of a sand filter used in water treatment. FEMS Microbiology Letters 131(3), 263-269.

Ernst, R.K., Yi, E.C., Guo, L., Lim, K.B., Burns, J.L., Hackett, M., Miller, S.I., (1999). Specific lipopolysaccharide found in cystic fibrosis airway *Pseudomonas aeruginosa*. Science 286(5444), 1561.

Faille, C., Jullien, C., Fontaine, F., Bellon-Fontaine, M.N., Slomianny, C., Benezech, T., (2002). Adhesion of *Bacillus* spores and *Escherichia* coli cells to inert surfaces: role of surface hydrophobicity. Canadian Journal of Microbiology 48(8), 728-738.

Fang, H.H.P., Xu, L.C., Chan, K.Y., (2002). Effects of toxic metals and chemicals on biofilm and biocorrosion. Water Research 36(19), 4709-4716.

Fett, W.F., Wells, J.M., Cescutti, P., Wijey, C., (1995). Identification of exopolysaccharides produced by fluorescent pseudomonads associated with commercial mushroom (*Agaricus bisporus*) production. Applied and Environmental Microbiology 61(2), 513-517.

Fletcher, M., Marshall, K.C., (1982). Bubble contact angle method for evaluating substratum interfacial characteristics and its relevance to bacterial attachment. Applied and Environmental Microbiology 44(1), 184-192.

Flint, S., Palmer, J.S., Bloemen, K., Brooks, J., Crawford, R., (2001). The growth of *Bacillus stearothermophilus* on stainless steel. Journal of Applied Microbiology 90(2), 151-157.

Francius, G., Alsteens, D., Dupres, V., Lebeer, S., De Keersmaecker, S., Vanderleyden, J., Gruber, H.J., Dufrene, Y.F., (2009). Stretching polysaccharides on live cells using single molecule force spectroscopy. Nature Protocols 4(6), 939-946.

Francius, G., Lebeer, S., Alsteens, D., Wildling, L., Gruber, H.J., Hols, P., Keersmaecker, S., Vanderleyden, J., Dufrene, Y.F., (2008). Detection, localization, and conformational analysis of single polysaccharide molecules on live bacteria. ACS Nano 2(9), 1921-1929.

Francolini, I., Donelli, G., (2010). Prevention and control of biofilm based medical device related infections. FEMS Immunology & Medical Microbiology 59(3), 227-238.

Friedman, L., Kolter, R., (2004). Genes involved in matrix formation in *Pseudomonas aeruginosa* PA14 biofilms. Molecular Microbiology 51(3), 675-690.

Fritz, M., Radmacher, M., Petersen, N., Gaub, H.E., (1994). Visualization and identification of intracellular structures by force modulation microscopy and drug induced degradation. Journal of Vacuum Science and Technology B: Microelectronics and Nanometer Structures 12(3), 1526-1529.

Gad, M., Itoh, A., Ikai, A., (1997). Mapping cell wall polysaccharides on living microbial cells using Atomic Force Microscopy. Cell Biology International 21(11), 697-706.

Gehr, R., Henry, J., (1983). Removal of extracellular material techniques and pitfalls. Water Research 17(12), 1743-1748.

Giffel, M., Wagendorp, A., Herrewegh, A., Driehuis, F., (2002). Bacterial spores in silage and raw milk. Antonie Van Leeuwenhoek 81(1), 625-630.

Gorner, T., de Donato, P., Ameil, M.H., Montarges-Pelletier, E., Lartiges, B.S., (2003). Activated sludge exopolymers: separation and identification using size exclusion chromatography and infrared micro-spectroscopy. Water Research 37(10), 2388-2393.

Gottenbos, B., Busscher, H., Van Der Mei, H., Nieuwenhuis, P., (2002a). Pathogenesis and prevention of biomaterial centered infections. Journal of Materials Science: Materials in Medicine 13(8), 717-722.

Gottenbos, B., van der Mei, H.C., Klatter, F., Nieuwenhuis, P., Busscher, H.J., (2002b). In vitro and in vivo antimicrobial activity of covalently coupled quaternary ammonium silane coatings on silicone rubber. Biomaterials 23(6), 1417-1423.

Granum, P.E., Benjamin, C., (2003). BACILLUS: Food Poisoning, *Encyclopedia of Food Sciences and Nutrition*. Academic Press, Oxford, pp. 365-371.

Grasso, D., Smets, B.F., Strevett, K.A., Machinist, B.D., Van Oss, C.J., Giese, R.F., Wu, W., (1996). Impact of physiological state on surface thermodynamics and adhesion of *Pseudomonas aeruginosa*. Environmental Science and Technology 30(12), 3604-3608.

Grobben, G.J., Smith, M.R., Sikkema, J., de Bont, J.A.M., (1996). Influence of fructose and glucose on the production of exopolysaccharides and the activities of enzymes involved in the sugar metabolism and the synthesis of sugar nucleotides in *Lactobacillus delbrueckii subsp. bulgaricus* NCFB 2772. Applied Microbiology and Biotechnology 46(3), 279-284.

Guina, T., Purvine, S.O., Yi, E.C., Eng, J., Goodlett, D.R., Aebersold, R., Miller, S.I., (2003). Quantitative proteomic analysis indicates increased synthesis of a quinolone by *Pseudomonas aeruginosa* isolates from cystic fibrosis airways. Proceedings of the National Academy of Sciences of the United States of America 100(5), 2771-2776.

Hall-Stoodley, L., Stoodley, P., (2002). Developmental regulation of microbial biofilms. Current Opinion in Biotechnology 13(3), 228-233.

Hancock, I., Poxton, I., (1988). *Bacterial cell surface techniques*. John Wiley & Sons.

Hay, I.D., Remminghorst, U., Rehm, B.H.A., (2009). MucR, a novel membrane-associated regulator of alginate biosynthesis in *Pseudomonas aeruginosa*. Applied and Environmental Microbiology 75(4), 1110-1120.

Helke, D.M., Somers, E.B., Wong, A.C.L., (1993). Attachment of *Listeria monocytogenes* and *Salmonella typhimurium* to stainless steel and Buna-N in the presence of milk and individual milk components. Journal of Food Protection 56(6), 479-484.

Helm, D., Naumann, D., (1995). Identification of some bacterial cell components by FT IR spectroscopy. FEMS Microbiology Letters 126(1), 75-79.

Herald, P.J., Zotolla, E.A., (1989). Effect of various agents upon the attachment of *Pseudomonas fragi* to stainless steel. Journal of Food Science 54(2), 461-464.

Hermansson, M., (1999). The DLVO theory in microbial adhesion. Colloids and Surfaces B: Biointerfaces 14(1-4), 105-119.

Hoek, E., Agarwal, G., (2006). Extended DLVO interactions between spherical particles and rough surfaces. Journal of Colloid and Interface Science 298(1), 50-58.

Hood, S.K., Zottola, E.A., (1995). Biofilms in food processing. Food Control 6(1), 9-18.

Hood, S.K., Zottola, E.A., (1997). Growth media and surface conditioning influence the adherence of *Pseudomonas fragi, Salmonella typhimurium, and Listeria monocytogenes* cells to stainless steel. Journal of Food Protection 60(9), 1034-1037.

Husmark, U., Ronner, U., (1990). Forces involved in adhesion of *Bacillus cereus* spores to solid surfaces under different environmental conditions. Journal of Applied Bacteriology 69(4), 557-562.

Husmark, U., Ronner, U., (1992). The influence of hydrophobic, electrostatic and morphologic properties on the adhesion of *Bacillus* spores. Biofouling 5(4), 335-344.

Isticato, R., Cangiano, G., Tran, H.T., Ciabattini, A., Medaglini, D., Oggioni, M.R., De Felice, M., Pozzi, G., Ricca, E., (2001). Surface display of recombinant proteins on *Bacillus subtilis* spores. Journal of Bacteriology 183(21), 6294.

Isticato, R., Esposito, G., Zilhao, R., Nolasco, S., Cangiano, G., De Felice, M., Henriques, A.O., Ricca, E., (2004). Assembly of multiple CotC forms into the *Bacillus subtilis* spore coat. Journal of Bacteriology 186(4), 1129-1135.

Ito, T., Sugita, K., Okabe, S., (2004). Isolation, characterization, and in situ detection of a novel chemolithoautotrophic sulfur-oxidizing bacterium in wastewater biofilms growing under microaerophilic conditions. Applied and Environmental Microbiology 70(5), 3122.

Jolley, J.G., Geesey, G.G., Hankins, M.R., Wright, R.B., Wichlacz, P.L., (1988). Auger electron spectroscopy and x ray photoelectron spectroscopy of the biocorrosion of copper by gum arabic, bacterial culture supernatant and *Pseudomonas atlantica* expolymer. Surface and Interface Analysis 11(6 7), 371-376.

Jucker, B., Zehnder, A., Harms, H., (1998). Quantification of polymer interactions in bacterial adhesion. Environ. Sci. Technol 32(19), 2909-2915.

Jullien, C., Bénézech, T., Carpentier, B., Lebret, V., Faille, C., (2003). Identification of surface characteristics relevant to the hygienic status of stainless steel for the food industry. Journal of Food Engineering 56(1), 77-87.

Jung, S.H., Park, D., Park, J.H., Kim, Y.M., Ha, K.S., (2010). Molecular imaging of membrane proteins and microfilaments using atomic force microscopy. Experimental & Molecular Medicine 42(9), 597.

Kang, S., Elimelech, M., (2009). Bioinspired single bacterial cell force spectroscopy. Langmuir 25(17), 9656-9659.

Katsikogianni, M., Missirlis, Y., (2004). Concise review of mechanisms of bacterial adhesion to biomaterials and of techniques used in estimating bacteria-material interactions. European Cells and Materials 8, 37-57.

Kim, D.S., Thomas, S., Fogler, H.S., (2000). Effects of pH and trace minerals on long-term starvation of *Leuconostoc mesenteroides*. Applied and Environmental Microbiology 66(3), 976-981.

Kim, J., Lee, C., Kim, B., (2005). Spore-displayed streptavidin: a live diagnostic tool in biotechnology. Biochemical and Biophysical Research Communications 331(1), 210-214.

Kives, J., Guadarrama, D., Orgaz, B., Rivera-Sen, A., Vazquez, J., SanJose, C., (2005). Interactions in biofilms of *Lactococcus lactis ssp. cremoris* and *Pseudomonas fluorescens* cultured in cold UHT milk. Journal of Dairy Science 88(12), 4165-4171.

Kives, J., Orgaz, B., San Jose, C., (2006). Polysaccharide differences between planktonic and biofilm-associated EPS from *Pseudomonas fluorescens* B52. Colloids and Surfaces B: Biointerfaces 52(2), 123-127.

Knoshaug, E.P., Ahlgren, J.A., Trempy, J.E., (2000). Growth associated exopolysaccharide expression in *Lactococcus lactis subspecies cremoris* Ropy352. Journal of Dairy Science 83(4), 633-640.

Kodali, V.P., Das, S., Sen, R., (2009). An exopolysaccharide from a probiotic: Biosynthesis dynamics, composition and emulsifying activity. Food Research International 42(5-6), 695-699.

Konig, D.P., Perdreau-remington, F., Rutt, J., Sto berger, P., Hilgers, R.D., Plum, G., (1998). Slime production of *Staphylococcus epidermidis*: Increased bacterial adherence and accumulation onto pure titanium. Acta Orthopaedica 69(5), 523-526.

Kumar, C.G., Anand, S.K., (1998). Significance of microbial biofilms in food industry: a review. International Journal of Food Microbiology 42(1-2), 9-27.

Kuyukina, M.S., Ivshina, I.B., Serebrennikova, M.K., Krivorutchko, A.B., Podorozhko, E.A., Ivanov, R.V., Lozinsky, V.I., (2009). Petroleum-contaminated water treatment in a fluidized-bed bioreactor with immobilized *Rhodococcus* cells. International Biodeterioration and Biodegradation 63(4), 427-432.

Lazarova, V., Manem, J., (1995). Biofilm characterization and activity analysis in water and wastewater treatment. Water Research 29(10), 2227-2245.

Lederberg, J., (2000). *Pseudomonas. Encyclopedia of Microbiology*. Academic Press, San Diego.

Leone, L., Loring, J., Sjoberg, S., Persson, P., Shchukarev, A., (2006a). Surface characterization of the Gram-positive bacteria *Bacillus subtilis*-an XPS study. Surface and Interface Analysis 38(4), 202-205.

Leone, S., Molinaro, A., Alfieri, F., Cafaro, V., Lanzetta, R., Donato, A.D., Parrilli, M., (2006b). The biofilm matrix of *Pseudomonas sp.* OX1 grown on phenol is mainly constituted by alginate oligosaccharides. Carbohydrate Research 341(14), 2456-2461.

Li, Q.S., Lee, G.Y.H., Ong, C.N., Lim, C.T., (2008). AFM indentation study of breast cancer cells. Biochemical and Biophysical Research Communications 374(4), 609-613.

Li, X., Yan, Z., Xu, J., (2003). Quantitative variation of biofilms among strains in natural populations of *Candida albicans*. Microbiology 149(2), 353-362.

Lim, C.T., Zhou, E.H., Li, A., Vedula, S.R.K., Fu, H.X., (2006). Experimental techniques for single cell and single molecule biomechanics. Materials Science and Engineering: C 26(8), 1278-1288.

Lindahl, M., Faris, A., Wadström, T., Hjertén, S., (1981). A new test based on `salting out' to measure relative hydrophobicity of bacterial cells. Biochimica et Biophysica Acta (BBA) - General Subjects 677(3-4), 471-476.

Liu, Y., Zhao, Q., (2005). Influence of surface energy of modified surfaces on bacterial adhesion. Biophysical chemistry 117(1), 39-45.

Lower, S.K., Hochella, M.F., Jr., Beveridge, T.J., (2001). Bacterial recognition of mineral surfaces: Nanoscale interactions between *Shewanella* and alpha -FeOOH. Science 292(5520), 1360-1363.

Ma, L., Jackson, K.D., Landry, R.M., Parsek, M.R., Wozniak, D.J., (2006). Analysis of *Pseudomonas aeruginosa* conditional Psl variants reveals roles for the Psl

polysaccharide in adhesion and maintaining biofilm structure postattachment. Journal of Bacteriology 188(23), 8213-8221.

Mai, G.T., McCormack, J.G., Seow, W.K., Pier, G.B., Jackson, L.A., Thong, Y.H., (1993). Inhibition of adherence of mucoid *Pseudomonas aeruginosa* by alginase, specific monoclonal antibodies, and antibiotics. Infection and Immunity 61(10), 4338-4343.

Malmsten, M., (2003). *Biopolymers at interfaces*. Marcel Dekker Inc, New York.

Marcotte, L., Kegelaer, G., Sandt, C., Barbeau, J., Lafleur, M., (2007). An alternative infrared spectroscopy assay for the quantification of polysaccharides in bacterial samples. Analytical Biochemistry 361(1), 7-14.

Marin, M., Pedregosa, A., Laborda, F., (1996). Emulsifier production and microscopical study of emulsions and biofilms formed by the hydrocarbon-utilizing bacteria *Acinetobacter calcoaceticus* MM5. Applied Microbiology and Biotechnology 44(5), 660-667.

Markwell, M.A.K., Haas, S.M., Bieber, L.L., Tolbert, N.E., (1978). A modification of the Lowry procedure to simplify protein determination in membrane and lipoprotein samples* 1. Analytical Biochemistry 87(1), 206-210.

Mauriello, E.M.F., Duc, L.H., Isticato, R., Cangiano, G., Hong, H.A., Felice, M.D., Ricca, E., Cutting, S.M., (2004). Display of heterologous antigens on the *Bacillus subtilis* spore coat using CotC as a fusion partner. Vaccine 22(9-10), 1177-1187.

Mayer, C., Moritz, R., Kirschner, C., Borchard, W., Maibaum, R., Wingender, J., Flemming, H.-C., (1999). The role of intermolecular interactions: studies on model systems for bacterial biofilms. International Journal of Biological Macromolecules 26(1), 3-16.

McPherson, D.C., Kim, H., Hahn, M., Wang, R., Grabowski, P., Eichenberger, P., Driks, A., (2005). Characterization of the *Bacillus subtilis* spore morphogenetic coat protein CotO. Journal of Bacteriology 187(24), 8278-8290.

Mei, L., van der Mei, H.C., Ren, Y., Norde, W., Busscher, H.J., (2009). Poisson analysis of *Streptococcal* bond strengthening on stainless steel with and without a salivary conditioning film. Langmuir 25(11), 6227-6231.

Meyer, B., (2003). Approaches to prevention, removal and killing of biofilms. International Biodeterioration & Biodegradation 51(4), 249-253.

Midelet, G., Carpentier, B., (2004). Impact of cleaning and disinfection agents on biofilm structure and on microbial transfer to a solid model food. Journal of Applied Microbiology 97(2), 262-270.

Millsap, K.W., Reid, G., Van der Mei, H.C., Busscher, H.J., (1997). Cluster analysis of genotypically characterized *Lactobacillus* species based on physicochemical cell surface properties and their relationship with adhesion to hexadecane. Canadian Journal of Microbiology 43(3), 284-291.

Molina-Bolivar, J., Galisteo-Gonzalez, F., Hidalgo-Alvarez, R., (1999). The role played by hydration forces in the stability of protein-coated particles: non-classical DLVO behaviour. Colloids and Surfaces B: Biointerfaces 14(1-4), 3-17.

Monroe, D., (2007). Looking for chinks in the armor of bacterial biofilms. Plos Biology 5(11), e307.

Mozes, N., Handley, P.S., Busscher, H.J., Rouxhet, P.G., (1991). *Microbial cell surface analysis : structural and physicochemical methods*. John Wiley & Sons.

Müller, D.J., Dufrêne, Y.F., (2008). Atomic force microscopy as a multifunctional molecular toolbox in nanobiotechnology. Nature Nanotechnology 3(5), 261-269.

Murrell, W., (1981). Biophysical studies on the molecular mechanisms of spore heat resistance and dormancy. Sporulation and germination. American Society for Microbiology, Washington, DC, 64-77.

Myers, D., Meyers, D., (1991). *Surfaces, interfaces, and colloids: principles and applications*. VCH New York.

Nikaido, H., (2003). Molecular basis of bacterial outer membrane permeability revisited. Microbiology and Molecular Biology Reviews 67(4), 593.

Nivens, D.E., Ohman, D.E., Williams, J., Franklin, M.J., (2001). Role of alginate and its o-acetylation in formation of *Pseudomonas aeruginosa* microcolonies and biofilms. Journal of Bacteriology 183(3), 1047-1057.

Norde, W., Lyklema, J., (1989). Protein adsorption and bacterial adhesion to solid surfaces: a colloid-chemical approach. Colloids and Surfaces 38(1), 1-13.

Obuekwe, C.O., Al-Jadi, Z.K., Al-Saleh, E.S., (2007). Sequential hydrophobic partitioning of cells of *Pseudomonas aeruginosa* gives rise to variants of increasing cell-surface hydrophobicity. FEMS Microbiology Letters 270(2), 214-219.

Oliveira, R., (1997). Understanding Adhesion: A Means for Preventing Fouling. Experimental Thermal and Fluid Science 14, 316-322.

Olsson, A.L.J., van der Mei, H.C., Busscher, H.J., Sharma, P.K., (2010). Novel analysis of bacterium−substratum bond maturation measured using a quartz crystal microbalance. Langmuir 26(13), 11113-11117.

Omoike, A., Chorover, J., (2004). Spectroscopic study of extracellular polymeric substances from *Bacillus subtilis*: aqueous chemistry and adsorption effects. Biomacromolecules 5(4), 1219-1230.

Ong, Y.L., Razatos, A., Georgiou, G., Sharma, M.M., (1999). Adhesion forces between *E. coli* bacteria and biomaterial surfaces. Langmuir 15(8), 2719-2725.

Palmer, J., Flint, S., Brooks, J., (2007). Bacterial cell attachment, the beginning of a biofilm. Journal of Industrial Microbiology and Biotechnology 34(9), 577-588.

Park, S.I., Daeschel, M.A., Zhao, Y., (2004). Functional properties of antimicrobial lysozyme chitosan composite films. Journal of Food Science 69(8), 215-221.

Parkar, S., Flint, S., Brooks, J., (2004). Evaluation of the effect of cleaning regimes on biofilms of thermophilic bacilli on stainless steel. Journal of Applied Microbiology 96(1), 110-116.

Pashley, R., Karaman, M., Craig, V., Kohonen, M., (1998). Use of the light-lever technique for the measurement of colloidal forces. Colloids and Surfaces A: Physicochemical and Engineering Aspects 144(1-3), 1-8.

Peng, J.S., Tsai, W.C., Chou, C.C., (2001). Surface characteristics of *Bacillus cereus* and its adhesion to stainless steel. International Journal of Food Microbiology 65(1-2), 105-111.

Pereira, A., Mendes, J., Melo, L.F., (2008). Using nanovibrations to monitor biofouling. Biotechnology and Bioengineering 99(6), 1407-1415.

Pijanowska, A., Kaczorek, E., Chrzanowski, Olszanowski, A., (2007). Cell hydrophobicity of *Pseudomonas spp.* and *Bacillus spp.* bacteria and hydrocarbon biodegradation in the presence of Quillaya saponin. World Journal of Microbiology and Biotechnology 23(5), 677-682.

Poulsen, L.V., (1999). Microbial Biofilm in Food Processing. Lebensmittel-Wissenschaft und-Technologie 32(6), 321-326.

Pruthi, V., Cameotra, S.S., (1997). Rapid identification of biosurfactant-producing bacterial strains using a cell surface hydrophobicity technique. Biotechnology Techniques 11(9), 671-674.

Rasmussen, T.B., Skindersoe, M.E., Bjarnsholt, T., Phipps, R.K., Christensen, K.B., Jensen, P.O., Andersen, J.B., Koch, B., Larsen, T.O., Hentzer, M., (2005). Identity and effects of quorum-sensing inhibitors produced by *Penicillium* species. Microbiology 151(5), 1325.

Razatos, A., Ong, Y., Boulay, F., Elbert, D., Hubbell, J., Sharma, M., Georgiou, G., (2000). Force measurements between bacteria and poly (ethylene glycol)-coated surfaces. Langmuir 16(24), 9155-9158.

Rehm, B., Valla, S., (1997). Bacterial alginates: biosynthesis and applications. Applied Microbiology and Biotechnology 48(3), 281-288.

Reid, G., Bialkowska-Hobrzanska, H., van der Mei, H.C., Busscher, H., (1999). Correlation between genetic, physico-chemical surface characteristics and adhesion of four strains of *Lactobacillus*. Colloids and Surfaces B: Biointerfaces 13(2), 75-81.

Rijnaarts, H., Norde, W., Bouwer, E., Lyklema, J., Zehnder, A., (1995). Reversibility and mechanism of bacterial adhesion. Colloids and Surfaces B: Biointerfaces 4(1), 5-22.

Rogers, J., Dowsett, A.B., Dennis, P.J., Lee, J.V., Keevil, C.W., (1994). Influence of plumbing materials on biofilm formation and growth of *Legionella pneumophila* in potable water systems. Applied and Environmental Microbiology 60(6), 1842.

Rosmaninho, R., Santos, O., Nylander, T., Paulsson, M., Beuf, M., Benezech, T., Yiantsios, S., Andritsos, N., Karabelas, A., Rizzo, G., (2007). Modified stainless steel surfaces targeted to reduce fouling-Evaluation of fouling by milk components. Journal of Food Engineering 80(4), 1176-1187.

Rouxhet, P., Mozes, N., Dengis, P., Dufrêne, Y., Gerin, P., Genet, M., (1994). Application of X-ray photoelectron spectroscopy to microorganisms. Colloids and Surfaces B: Biointerfaces 2(1-3), 347-369.

Rutter, P., Vincent, B., (1980). The adhesion of microorganisms to surfaces: physico-chemical aspects. Microbial adhesion to surfaces, 79-92.

Ryder, C., Byrd, M., Wozniak, D.J., (2007). Role of polysaccharides in *Pseudomonas aeruginosa* biofilm development. Current Opinion in Microbiology 10(6), 644-648.

Ryu, J., Beuchat, L., (2005). Biofilm formation and sporulation by *Bacillus cereus* on a stainless steel surface and subsequent resistance of vegetative cells and spores to chlorine, chlorine dioxide, and a peroxyacetic acid–based sanitizer. Journal of Food Protection 68(12), 2614-2622.

Sand, W., Gerke, T., Hallmann, R., Schippers, A., (1995). Sulfur chemistry, biofilm, and the (in) direct attack mechanism - a critical evaluation of bacterial leaching. Applied Microbiology and Biotechnology 43(6), 961-966.

Sargent, M.G., (1975). Control of cell length in *Bacillus subtilis*. Journal of Bacteriology 123(1), 7-19.

Sauer, S., Kliem, M., (2010). Mass spectrometry tools for the classification and identification of bacteria. Nature Reviews Microbiology 8(1), 74-82.

Scheldeman, P., Pil, A., Herman, L., De Vos, P., Heyndrickx, M., (2005). Incidence and diversity of potentially highly heat-resistant spores isolated at dairy farms. Applied and Environmental Microbiology 71(3), 1480-1494.

Schmitt, J., Flemming, H.C., (1998). FTIR-spectroscopy in microbial and material analysis. International Biodeterioration & Biodegradation 41(1), 1-11.

Schreiber, D.R., Millero, F.J., Gordon, A.S., (1990). Production of an extracellular copper-binding compound by the heterotrophic marine bacterium *Vibrio alginolyticus*. Marine Chemistry 28(4), 275-284.

Schwermer, C.U., Lavik, G., Abed, R.M.M., Dunsmore, B., Ferdelman, T.G., Stoodley, P., Gieseke, A., De Beer, D., (2008). Impact of nitrate on the structure and function of bacterial biofilm communities in pipelines used for injection of seawater into oil fields. Applied and Environmental Microbiology 74(9), 2841.

Setlow, P., (2006). Spores of *Bacillus subtilis*: their resistance to and killing by radiation, heat and chemicals. Journal of Applied Microbiology 101(3), 514-525.

Sheng, G., Yu, H., Li, X., (2010). Extracellular polymeric substances (EPS) of microbial aggregates in biological wastewater treatment systems: A review. Biotechnology Advances.

Sheng, X., Ting, Y.P., Pehkonen, S.O., (2007). Force measurements of bacterial adhesion on metals using a cell probe atomic force microscope. Journal of Colloid and Interface Science 310(2), 661-669.

Sheng, X., Ting, Y.P., Pehkonen, S.O., (2008). The influence of ionic strength, nutrients and pH on bacterial adhesion to metals. Journal of Colloid and Interface Science 321(2), 256-264.

Shi, X., Zhu, X., (2009). Biofilm formation and food safety in food industries. Trends in Food Science & Technology 20(9), 407-413.

Shih, I.L., Van, Y.T., (2001). The production of poly-([gamma]-glutamic acid) from microorganisms and its various applications. Bioresource Technology 79(3), 207-225.

Silverstein, R.M., Webster, F.X., Kiemle , D., (1991). *Spectrometric Identification of Organic Compounds* (5 ed). John Wiley & Sons Inc.

Simoes, M., Simoes, L.C., Vieira, M.J., (2010). A review of current and emergent biofilm control strategies. LWT-Food Science and Technology 43(4), 573-583.

Smith, J.L., Fratamico, P.M., Novak, J.S., (2004). Quorum sensing: a primer for food microbiologists. Journal of Food Protection 67(5), 1053-1070.

Socrates, G., (2004). *Infrared and Raman characteristic group frequencies: tables and charts*. John Wiley & Sons Inc.

Speers, J., Gilmour, A., (1985). The influence of milk and milk components on the attachment of bacteria to farm dairy equipment surfaces. Journal of Applied Microbiology 59(4), 325-332.

Splendiani, A., Livingston, A.G., Nicolella, C., (2006). Control of membrane attached biofilms using surfactants. Biotechnology and Bioengineering 94(1), 15-23.

Stanley, N.R., Lazazzera, B.A., (2005). Defining the genetic differences between wild and domestic strains of *Bacillus subtilis* that affect poly dl glutamic acid production and biofilm formation. Molecular Microbiology 57(4), 1143-1158.

Strevett, K.A., Chen, G., (2003). Microbial surface thermodynamics and applications. Research in microbiology 154(5), 329-335.

Sutherland, I.W., (2001). Biofilm exopolysaccharides: A strong and sticky framework. Microbiology 147(1), 3-9.

Tamagnini, L.M., Gonzalez, R.D., (1997). Bacteriological stability and growth kinetics of *Pseudomonas aeruginosa* in bottled water. Journal of Applied Microbiology 83(1), 91-94.

Tauveron, G., Slomianny, C., Henry, C., Faille, C., (2006). Variability among *Bacillus cereus* strains in spore surface properties and influence on their ability to contaminate food surface equipment. International Journal of Food Microbiology 110(3), 254-262.

Thouvenin, M., Langlois, V., Briandet, R., Langlois, J., Guerin, P., Peron, J., Haras, D., Vallee-Rehel, K., (2003). Study of erodable paint properties involved in antifouling activity. Biofouling 19(3), 177-186.

Tielen, P., Strathmann, M., Jaeger, K.E., Flemming, H.C., Wingender, J., (2005). Alginate acetylation influences initial surface colonization by mucoid *Pseudomonas aeruginosa*. Microbiological research 160(2), 165-176.

Trachoo, N., (2003). Biofilms and the food industry. Biofilms 25(6), 808.

Tsibouklis, J., Stone, M., (2000). Inhibiting bacterial adhesion onto surfaces: the non-stick coating approach. International journal of adhesion and adhesives 20(2), 91-96.

Tsuneda, S., Aikawa, H., Hayashi, H., Yuasa, A., Hirata, A., (2003). Extracellular polymeric substances responsible for bacterial adhesion onto solid surface. FEMS Microbiology Letters 223(2), 287-292.

Ubbink, J., Schär-Zammaretti, P., (2005). Probing bacterial interactions: integrated approaches combining atomic force microscopy, electron microscopy and biophysical techniques. Micron 36(4), 293-320.

van der Aa, B.C., Michel, R.M., Asther, M., Torrez Zamora, M., Rouxhet, P.G., Dufrene, Y.F., (2001). Stretching cell surface macromolecules by atomic force microscopy. Langmuir 17(11), 3116-3119.

van der Mei, H., van de Belt-Gritter, B., Busscher, H., (1995). Implications of microbial adhesion to hydrocarbons for evaluating cell surface hydrophobicity 2. Adhesion mechanisms. Colloids and Surfaces B: Biointerfaces 5(3-4), 117-126.

van der Mei, H.C., Weerkamp, A.H., Busscher, H.J., (1987). A comparison of various methods to determine hydrophobic properties of streptococcal cell surfaces. Journal of Microbiological Methods 6(5), 277-287.

van Loosdrecht, M.C., Norde, W., Zehnder, A.J., (1990). Physical chemical description of bacterial adhesion. Journal of Biomaterials Applications 5(2), 91-106.

Van Oss, C.J., (1993). Acid-base interfacial interactions in aqueous media. Colloids and Surfaces A: Physicochemical and Engineering Aspects 78, 1-49.

Van Oss, C.J., (1995). Hydrophobicity of biosurfaces--Origin, quantitative determination and interaction energies. Colloids and Surfaces B: Biointerfaces 5(3-4), 91-110.

Van Oss, C.J., (1997). Hydrophobicity and hydrophilicity of biosurfaces. Current opinion in colloid & interface science 2(5), 503-512.

Van Oss, C.J., (2006). *Interfacial forces in aqueous media* (2nd ed). CRC Press, New York.

Vanhaecke, E., Remon, J.P., Moors, M., Raes, F., De Rudder, D., Van Peteghem, A., (1990). Kinetics of *Pseudomonas aeruginosa* adhesion to 304 and 316-L stainless steel: Role of cell surface hydrophobicity. Applied and Environmental Microbiology 56(3), 788-795.

Velegol, S., Logan, B., (2004). Contributions of bacterial surface polymers, electrostatics, and cell elasticity to the shape of AFM force curves. Langmuir 20(9), 3820.

Verhoef, R., Schols, H.A., Blanco, A., Siika-Aho, M., Ratto, M., Buchert, J., Lenon, G., Voragen, A.G.J., (2005). Sugar composition and FT-IR analysis of exopolysaccharides produced by microbial isolates from paper mill slime deposits. Biotechnology and Bioengineering 91(1), 91-105.

Vermeltfoort, P.B.J., van Kooten, T.G., Bruinsma, G.M., Hooymans, A.M.M., van der Mei, H.C., Busscher, H.J., (2005). Bacterial transmission from contact lenses to porcine corneas: an ex vivo study. Investigative Ophthalmology and Visual science 46(6), 2042-2046.

Vijayalakshmi, S., Raichur, A., (2003). The utility of *Bacillus subtilis* as a bioflocculant for fine coal. Colloids and Surfaces B: Biointerfaces 29(4), 265-275.

Villena, G.K., Venkatesh, L., Yamazaki, A., Tsuyumu, S., Gutiérrez-Correa, M., (2009). Initial intracellular proteome profile of *Aspergillus niger* biofilms. Rev. peru. biol 16(1), 101-108.

Vladkova, T., (2009). Surface modification approach to control biofouling. Marine and Industrial Biofouling 23, 135-163.

Warth, A., (1978). Molecular structure of the bacterial spore. Advances in microbial physiology 17, 1-45.

Weng, Y.M., Chen, M.J., Chen, W., (1999). Antimicrobial food packaging materials from poly (ethylene-co-methacrylic acid). Lebensmittel-Wissenschaft und-Technologie 32(4), 191-195.

Whitehead, K.A., Colligon, J., Verran, J., (2004). The production of surfaces of defined topography and chemistry for microbial retention studies, using ion beam sputtering technology. International Biodeterioration & Biodegradation 54(2-3), 143-151.

Wingender, J., Neu, T.R., Flemming, H.C., (1999). What are bacterial extracellular polymeric substances. Microbial Extracellular Polymeric Substances, 1–19.

Wozniak, D.J., (2003). Alginate is not a significant component of the extracellular polysaccharide matrix of PA14 and PAO1 *Pseudomonas aeruginosa* biofilms. Proceedings of the National Academy of Sciences 100(13), 7907-7912.

Wright, C.J., Armstrong, I., (2006). The application of atomic force microscopy force measurements to the characterisation of microbial surfaces. Surface and Interface Analysis 38(11), 1419-1428.

Wright, C.J., Shah, M.K., Powell, L.C., Armstrong, I., (2010). Application of AFM from microbial cell to biofilm. Scanning 32(3), 134-149.

Wu, P.J., Livermore, D.M., (1990). Response of chemostat cultures of *Pseudomonas aeruginosa* to carbapenems and other Î²-lactams. Journal of Antimicrobial Chemotherapy 25(6), 891-902.

Wu, Y., Xie, Q., Zhou, A., Zhang, Y., Nie, L., Yao, S., Mo, X., (2000). Detection and analysis of *Bacillus subtilis* growth with piezoelectric quartz crystal impedance based on starch hydrolysis. Analytical Biochemistry 285(1), 50-57.

Xu, W., Mulhern, P., Blackford, B., Jericho, M., Firtel, M., Beveridge, T., (1996). Modeling and measuring the elastic properties of an archaeal surface, the sheath of *Methanospirillum hungatei*, and the implication of methane production. Journal of Bacteriology 178(11), 3106-3112.

Yao, X., Walter, J., Burke, S., Stewart, S., Jericho, M.H., Pink, D., Hunter, R., Beveridge, T.J., (2002). Atomic force microscopy and theoretical considerations of surface properties and turgor pressures of bacteria. Colloids and Surfaces B: Biointerfaces 23(2-3), 213-230.

Zandomeni, R.O., Fitzgibbon, J.E., Carrera, M., Steubing, E., Rogers, J.E., Sagripanti, J.L., (2005). Spore Size Comparison Between Several *Bacillus* Species. Geo-Centers Inc Aberdeen Proving Ground MD.

Zhang, Y., Miller, R.M., (1994). Effect of a *Pseudomonas rhamnolipid* biosurfactant on cell hydrophobicity and biodegradation of octadecane. Applied and Environmental Microbiology 60(6), 2101-2106.

Zhong, H., Zeng, G., Yuan, X.Z., Fu, H., Huang, G.H., Ren, F.Y., (2007). Adsorption of dirhamnolipid on four microorganisms and the effect on cell surface hydrophobicity. Applied Microbiology and Biotechnology 77(2), 447-455.

Ziegler, S., Ackermann, S., Majzlan, J., Gescher, J., (2009). Matrix composition and community structure analysis of a novel bacterial pyrite leaching community. Environmental Microbiology 11(9), 2329-2338.

Zlatanova, J., Lindsay, S.M., Leuba, S.H., (2000). Single molecule force spectroscopy in biology using the atomic force microscope. Progress in Biophysics and Molecular Biology 74(1-2), 37-61.

Zobell, C.E., (1943). The effect of solid surfaces upon bacterial activity. Journal of Bacteriology 46(1), 39.

APPENDIX A OPTICAL DENSITY AND CELL ENUMERATION OF BACTERIA

A. 1. Optical density and pH measurement of *P. aeruginosa*

Time (h)	No	OD	OD avg	SD	pH	pH avg	SD
1	1	0.055	0.0551	0.0004	7.22	7.21	0.01
	2	0.0548			7.20		
	3	0.0556			7.22		
3	1	0.0714	0.0649	0.0060	7.23	7.23	0.02
	2	0.0639			7.21		
	3	0.0595			7.24		
6	1	0.1028	0.1136	0.0097	7.28	7.28	0.03
	2	0.1164			7.30		
	3	0.1216			7.25		
10	1	0.1967	0.1856	0.0129	7.25	7.25	0.01
	2	0.1887			7.24		
	3	0.1715			7.26		
16	1	0.3041	0.2716	0.0296	7.24	7.24	0.03
	2	0.246			7.27		
	3	0.2648			7.21		
24	1	0.7848	0.7952	0.0091	7.30	7.30	0.02
	2	0.7991			7.28		
	3	0.8017			7.31		
27	1	0.7509	0.7501	0.0308	7.30	7.29	0.02
	2	0.7804			7.27		
	3	0.7189			7.31		
30	1	0.7628	0.7655	0.0121	7.19	7.20	0.02
	2	0.755			7.22		
	3	0.7788			7.20		
33	1	0.6123	0.6058	0.0286	7.19	7.19	0.03
	2	0.6306			7.16		
	3	0.5746			7.22		

A. 2. Optical density and pH measurement of *B. subtilis*

Time (h)	No	OD	OD avg	SD	pH	pH avg	SD
1	1	0.0481	0.0476	0.0007	7.20	7.20	0.02
	2	0.048			7.19		
	3	0.0468			7.22		
3	1	0.0913	0.0925	0.0011	7.19	7.19	0.02
	2	0.0928			7.20		
	3	0.0934			7.17		
6	1	0.1043	0.1178	0.0123	7.20	7.20	0.03
	2	0.1208			7.22		
	3	0.1283			7.17		
10	1	0.1421	0.1495	0.0074	7.17	7.17	0.03
	2	0.1496			7.20		
	3	0.1569			7.15		
16	1	0.1543	0.1456	0.0089	7.12	7.12	0.03
	2	0.1458			7.10		
	3	0.1366			7.15		
24	1	0.1039	0.1119	0.0140	7.01	7.00	0.03
	2	0.1038			7.02		
	3	0.1281			6.97		

A. 3. CFU count of planktonic cells of *P. aeruginosa*

Time (h)	Colony no.	Dilution factor	Spreading volume (μL)	CFU/mL	CFU Avg	SD
1	31	4	200	1.55E+06	1.93E+06	340342.9643
	44	4	200	2.20E+06		
	41	4	200	2.05E+06		
3	46	5	200	2.30E+07	2.40E+07	8046738.47
	33	5	200	1.65E+07		
	65	5	200	3.25E+07		
6	113	5	200	5.65E+07	6.62E+07	11579435.8
	126	5	200	6.30E+07		
	158	5	200	7.90E+07		
10	64	6	200	3.20E+08	3.70E+08	44440972.09
	77	6	200	3.85E+08		
	81	6	200	4.05E+08		
16	59	6	100	5.90E+08	6.17E+08	122202018.5
	75	6	100	7.50E+08		
	51	6	100	5.10E+08		

24	85	6	100	8.50E+08	8.80E+08	79372539.33
	97	6	100	9.70E+08		
	82	6	100	8.20E+08		
27	95	6	100	9.50E+08	9.07E+08	83864970.84
	96	6	100	9.60E+08		
	81	6	100	8.10E+08		
30	84	6	100	8.40E+08	8.57E+08	47258156.26
	91	6	100	9.10E+08		
	82	6	100	8.20E+08		
33	72	6	100	7.20E+08	6.90E+08	36055512.75
	70	6	100	7.00E+08		
	65	6	100	6.50E+08		

A. 4. CFU count of planktonic cells of *B. subtilis*

Time (h)	Colony no.	Dilution factor	Spreading volume (μL)	CFU/mL	CFU avg	SD
1	105	2	100	1.05E+05	1.08E+05	11789.82612
	121	2	100	1.21E+05		
	98	2	100	9.80E+04		
3	102	3	100	1.02E+06	1.02E+06	95043.84953
	93	3	100	9.30E+05		
	112	3	100	1.12E+06		
6	153	3	100	1.53E+06	1.51E+06	25166.11478
	148	3	100	1.48E+06		
	151	3	100	1.51E+06		
10	154	3	100	1.54E+06	1.52E+06	96090.23537
	161	3	100	1.61E+06		
	142	3	100	1.42E+06		
16	198	3	100	1.98E+06	1.86E+06	120000
	186	3	100	1.86E+06		
	174	3	100	1.74E+06		
24	169	3	100	1.69E+06	1.61E+06	92915.73243
	151	3	100	1.51E+06		
	164	3	100	1.64E+06		

A. 5. CFU count of sessile cells of *P. aeruginosa*

Time (h)	Colony no.	Dilution factor	Spreading volume (mL)	CFU/mL	CFU/mL	SD
1	159	3	100	1.59E+06	1.53E+06	127410.099
	138	3	100	1.38E+06		
	161	3	100	1.61E+06		

3	532	3	100	5.32E+06	5.28E+06	287460.1422
	497	3	100	4.97E+06		
	554	3	100	5.54E+06		
6	68	4	100	6.80E+06	6.83E+06	251661.1478
	71	4	100	7.10E+06		
	66	4	100	6.60E+06		
10	56	4	100	5.60E+06	5.83E+06	776745.3465
	67	4	100	6.70E+06		
	52	4	100	5.20E+06		
16	55	4	100	5.50E+06	5.90E+06	781024.9676
	68	4	100	6.80E+06		
	54	4	100	5.40E+06		
24	61	4	100	6.10E+06	6.23E+06	513160.1439
	68	4	100	6.80E+06		
	58	4	100	5.80E+06		

A. 6. CFU count of sessile cells of *B. subtilis*

Time (h)	Colony no.	Dilution factor	Spreading volume (mL)	CFU/mL	CFU/mL	SD
1	33	1	100	3.30E+03	3.23E+03	404.1451884
	28	1	100	2.80E+03		
	36	1	100	3.60E+03		
3	44	1	100	4.40E+03	4.50E+03	556.7764363
	40	1	100	4.00E+03		
	51	1	100	5.10E+03		
6	52	1	100	5.20E+03	5.30E+03	754.9834435
	46	1	100	4.60E+03		
	61	1	100	6.10E+03		
10	56	1	100	5.60E+03	5.57E+03	550.7570547
	50	1	100	5.00E+03		
	61	1	100	6.10E+03		
16	74	1	100	7.40E+03	7.33E+03	404.1451884
	69	1	100	6.90E+03		
	77	1	100	7.70E+03		
24	89	1	100	8.90E+03	8.73E+03	568.6240703
	81	1	100	8.10E+03		
	92	1	100	9.20E+03		

A. 7. Biofilm dry weight of *P. aeruginosa*

Time (h)	No	Before (g)	After (g)	Biofilm (g)	Average (g)	SD
1	1	0.5338	0.5332	0.0006	0.0005	0.0002
	2	0.5266	0.5263	0.0003		
	3	0.5244	0.5239	0.0005		
3	1	0.5353	0.5336	0.0017	0.0016	0.0004
	2	0.5162	0.515	0.0012		
	3	0.5279	0.526	0.0019		
6	1	0.529	0.5271	0.0019	0.0017	0.0002
	2	0.5283	0.5267	0.0016		
	3	0.6153	0.6138	0.0015		
10	1	0.5362	0.5344	0.0018	0.0024	0.0007
	2	0.5277	0.5246	0.0031		
	3	0.5267	0.5244	0.0023		
16	1	0.5243	0.5214	0.0029	0.0026	0.0006
	2	0.6163	0.6133	0.003		
	3	0.5354	0.5334	0.002		
24	1	0.5102	0.508	0.0022	0.0024	0.0003
	2	0.5322	0.53	0.0022		
	3	0.5256	0.5229	0.0027		

A. 7. Biofilm dry weight of *B. subtilis*

Time	No	Before (g)	After (g)	Biofilm (g)	Average (g)	SD
1	1	0.5245	0.5243	0.0002	0.0003	0.0001
	2	0.524	0.5237	0.0003		
	3	0.5353	0.535	0.0003		
3	1	0.5338	0.5335	0.0003	0.0003	0.0001
	2	0.5234	0.5231	0.0003		
	3	0.6109	0.6105	0.0004		
6	1	0.5284	0.528	0.0004	0.0004	0.0001
	2	0.534	0.5335	0.0005		
	3	0.5285	0.5281	0.0004		
10	1	0.6111	0.6105	0.0006	0.0004	0.0002
	2	0.5235	0.5232	0.0003		
	3	0.523	0.5226	0.0004		
16	1	0.5325	0.5319	0.0006	0.0006	0.0001
	2	0.5279	0.5274	0.0005		
	3	0.5276	0.527	0.0006		

24	1	0.5187	0.5175	0.0012	0.0010	0.0002
	2	0.6187	0.6177	0.001		
	3	0.5251	0.5242	0.0009		

APPENDIX B HYDROPHOBICITY TEST

B. 1. Contact Angle Measurement of *P. aeruginosa*

Water (W)		Ethylene Glycol (EG)		Formamide (FM)	
LHS	RHS	LHS	RHS	LHS	RHS
48.8	51.6	43.6	46.7	44.5	46.4
50	52.2	48.5	48	34.7	35.9
50.9	51.8	42.7	45.5	32.7	33.4
46.7	46.6	50.4	50.5	42.4	40.1
32.1	28.6	49	48.9	38.7	34.7
33.8	37.3	51.2	54.7	46.6	47
37.6	39	47.1	47.8	47.3	52.6
38.2	47.3	46.9	47.2	42.1	36.7
40.3	41.9	51.3	57.2	43.2	43.5
41.3	37.8	43.3	39.1	54.5	54.6
52.6	51.2	41.4	42.2	53.1	55.3
52.9	51	40.9	40.9	44.9	45.5
62	62.3	41.2	40.4	47.4	48.4
57	58.4	44.8	44.7	48.2	45.7
56.9	66	41.1	39.8	57.9	59.1
53.1	54	58.4	59.4	60	58.2
52.2	53.5	49.5	51.2	AVERAGE	
43	40.4	50.3	53.2	46.10	
49	49	AVERAGE		STD	
AVERAGE		47.19		7.86	
47.85		STD			
STD		5.35			
8.68					

B. 2. Contact Angle Measurement of *B. subtilis*

Water (W)		Ethylene Glycol (EG)		Hexadecane (HD)		Formamide (FM)	
LHS	RHS	LHS	RHS	LHS	RHS	LHS	RHS
30.4	31.4	44.2	41.7	31.4	30.9	`27.5	45.2
21.1	20.3	38.3	44.1	34.3	27.9	46.8	45.3
22.8	31.2	32	39.5	28.1	36	35.7	`23.7
19.7	`18.7	32	30.7	38.7	36	45.9	45.9
19	`16.2	39.5	36.1	42.8	39.7	50.4	47.5
26.4	25.9	56.1	54	40.2	35.9	`58.8	`55.6
44.4	47.9	`21.8	`21.8	28.5	26.8	28.9	`21.4
34.5	29.8	43.8	45.4	32.9	31.5	`6.6	37.9
26	27.4	48.6	47.2	30.7	31.5	38.6	29.1

`17.1	`15.9	55.7	52.1	32.9	32	28.9	`22.2
20.3	26.5	54.2	58.6	39	42	`19.7	`17.1
25.2	21	33.8	`27.3	33.4	33.8	AVERAGE	
`18.4	`17.9	33.8	40.6	`19.5	`18.7	40.47	
`18.1	23.2	45.7	47.2	`15.1	`15.9	STD	
24	28	53	54.2	26.8	24	7.76	
42.6	46.6	37.3	34.1	21.9	23.9		
44.2	45.7	51.4	47.7	30.1	31.2		
28.3	29.7	53.8	50.3	24	26.20		
AVERAGE		57.8	`61.9	42.1	40.9		
29.78		56.1	50.2	27.5	25.9		
STD		30.2	36.3	28.1	48.7		
8.94		36.5	56.5	30.2	30.9		
		39.3	48.6	28.4	36		
		35.5	32.2	37.1	34.7		
		42.6	56.7	24.4	22.9		
		AVERAGE		28.1	25.5		
		44.68		32.4	38.7		
		STD		28.6	33.8		
		8.70		25.9	33.7		
				33.8	38.3		
				AVERAGE			
				32.17			
				STD			
				5.83			

B. 3. Contact Angle Measurement of SS 316

Water (W)		Ethylene Glycol (EG)		Hexadecane (HD)		Formamide (FM)	
LHS	RHS	LHS	RHS	LHS	RHS	LHS	RHS
91	90.6	80.4	55.6	16.6	16.6	48.1	48.3
86	86.7	71.8	73	21	21.6	40.1	40.3
82.6	80.5	73.9	73.7	28.6	28.6	51.4	59.1
93.6	92.3	69.9	72.8	9.5	9.6	50.5	47.6
92.1	92.4	67.9	70.1	7.2	7.2	55.7	54.3
93.4	93.1	60.1	60.7	10.8	10.8	50.3	48.9
94.1	93.9	62.6	63.9	20.5	21.5	51.2	51.8
91.7	90.8	62.4	64.8	7.8	9.1	58.6	54.1
97.6	97.2	58.2	58.4	8	8	56.4	59.5
89.9	90	57.9	62.8	AVERAGE		57.8	57.7
94.6	94.8	58.8	58.8	14.61		51.7	51.4
85.5	84.7	62.8	65	STD		AVERAGE	
84.6	84.5	55.1	60.2	7.38		52.04	
78	77.9	57.6	59.6			STD	

87.7	83.8	58.8	58			5.35	
80.5	79.1	57.9	54.3				
78	78.8	50.7	53.9				
79.6	79.3	50.5	50.9				
79.2	80.7	43.3	43.2				
84.8	83.9	54.2	49.4				
83.1	82.5	40.8	42.4				
AVERAGE		**AVERAGE**					
86.79		59.69					
STD		**STD**					
6.11		9.57					

B. 4. Contact Angle Measurement of spores

Water (W)		Ethylene Glycol (EG)	
LHS	**RHS**	**LHS**	**RHS**
54.8	55.5	44.4	45.1
49.5	48.7	44.5	46.9
49.1	50.7	47.5	48.2
45.4	52.9	45.5	45.3
51.2	52.9	45.8	45.6
47.6	51.8	42.5	42.7
48	46.8	45.5	46
55.7	58.8	45.6	45.8
49.3	51.8	46.8	46.8
51.2	50	48	48.1
49.18	49.99	**AVERAGE**	
AVERAGE		45.83	
50.95		**STD**	
STD		1.58	
3.20			

B. 5. BATH Test of *P. aeruginosa*

Hexadecane (HD)				
Ao	**A1**	**%**	**Average**	**STD**
1.0299	0.9004	12.57		
1.0299	0.9121	11.44	12.29	0.8
1.0299	0.8975	12.86		
Xylene (XL)				
Ao	**A1**	**%**	**Average**	**STD**
1.0331	0.8951	13.36		
1.0331	0.9096	11.95	13.42	1.5
1.0331	0.8786	14.95		

Tetradecane (TD)				
Ao	**A1**	**%**	**Average**	**STD**
1.132	0.9838	13.09		
1.132	0.9987	11.78	11.58	1.6
1.132	1.0204	9.86		

B. 6. BATH Test of *B. subtilis*

Hexadecane (HD)				
Ao	**A1**	**%**	**Average**	**STD**
0.9457	0.9047	4.34		
0.9457	0.8901	5.88	4.98	0.8
0.9457	0.901	4.73		
Xylene (XL)				
Ao	**A1**	**%**	**Average**	**STD**
1.0688	1.0005	6.39		
1.0688	1.0231	4.28	5.62	1.2
1.0688	1.0026	6.19		
Tetradecane (TD)				
Ao	**A1**	**%**	**Average**	**STD**
1.0688	0.9202	13.90		
1.0688	0.923	13.64	13.95	0.3
1.0688	0.9159	14.31		

B. 7. BATH Test of Spores

Hexadecane (HD)				
Ao	**A1**	**%**	**Average**	**STD**
0.9626	0.8579	10.88		
0.9626	0.8344	13.32	12.46	1.4
0.9626	0.8358	13.17		
Xylene (XL)				
Ao	**A1**	**%**	**Average**	**STD**
1.0222	0.5583	45.38		
1.0222	0.5228	48.86	47.22	1.7
1.0222	0.5374	47.43		
Tetradecane (TD)				
Ao	**A1**	**%**	**Average**	**STD**
1.0222	0.494	51.67		
1.0222	0.4502	55.96	53.55	2.2
1.0222	0.4801	53.03		

B. 5. Emulsification Index

	B	M	T	EI (%)	Ave	STD
24 h						
blank	1.6	0	1.6	0.00		
P. aeruginosa	1.4	1.5	0.3	46.88	**44.79**	**3.6**
	1.5	1.5	0.2	46.88		
	1.5	1.3	0.4	40.63		
B. Subtilis	1.6	0.4	1.2	12.50	**11.46**	**1.8**
	1.6	0.4	1.2	12.50		
	1.6	0.3	1.3	9.38		
Spore	1.6	0.4	1.2	12.50	**13.54**	**1.8**
	1.5	0.5	1.2	15.63		
	1.6	0.4	1.2	12.50		
48 h						
blank	1.6	0	1.6	0.00		
P. aeruginosa	1.3	1.6	0.3	50.00	**48.96**	**1.8**
	1.6	1.5	0.1	46.88		
	1.4	1.6	0.2	50.00		
B. Subtilis	1.6	0.5	1.1	15.63	**15.63**	**0.0**
	1.6	0.5	1.1	15.63		
	1.6	0.5	1.1	15.63		
Spore	1.6	0.5	1.1	15.63	**16.67**	**1.8**
	1.5	0.6	1.1	18.75		
	1.6	0.5	1.1	15.63		
72 h						
blank	1.6	0	1.6	0.00		
P. aeruginosa	1.5	1.5	0.2	46.88	**48.96**	**1.8**
	1.6	1.6	0	50.00		
	1.6	1.6	0	50.00		
B. Subtilis	1.6	0.6	1	18.75	**16.67**	**1.8**
	1.6	0.5	1.1	15.63		
	1.6	0.5	1.1	15.63		
Spore	1.5	0.5	1.2	15.63	**18.75**	**3.1**
	1.5	0.7	1	21.88		
	1.5	0.6	1.1	18.75		

APPENDIX C MEASUREMENT OF SURFACE AND INTERACTION ENERGY COMPONENTS

C. 1. Zeta Potentials of SS316

No	pH	pH Std.	ZP [mV]	ZP Std. [mV]	ZP [V]
1	4.201	9.53E-04	-208.6	1.376	-0.209
2	4.22	7.73E-04	-211.6	2.719	-0.212
3	4.66	1.27E-04	-248.4	2.584	-0.248
4	5.105	0.002292	-275.6	1.757	-0.276
5	5.591	0.004126	-300	1.14	-0.300
6	6.11	0.007496	-315.2	2.672	-0.315
7	6.654	0.006504	-327.6	2.012	-0.328
8	7.254	0.007087	-335.4	3.548	-0.335
9	7.775	0.01351	-340	3.174	-0.340
10	8.195	0.008464	-346.2	3.737	-0.346
11	8.608	0.005077	-350.7	2.786	-0.351
12	9.027	0.003132	-354.7	1.821	-0.355

C. 2. Zeta Potentials of *P. aeruginosa*

No	ZP (mV)	ZP (V)
1	-13.2	-0.013
2	-12.2	-0.012
3	-12.5	-0.013
4	-13.1	-0.013
5	-12.3	-0.012
6	-12.9	-0.013
7	-13.2	-0.013
8	-11.8	-0.012
9	-12.3	-0.012
10	-12	-0.012
11	-10.4	-0.010
12	-13.1	-0.013
	Average	
	-12.42	-0.012
	STD	
	0.803	0.001

C. 3. Zeta Potentials of *B. subtilis*

No	ZP (mV)	ZP (V)
1	-19.3	-0.019
2	-18.4	-0.018
3	-17.5	-0.018
4	-18.3	-0.018
5	-17.8	-0.018
6	-18	-0.018
7	-17.1	-0.017
8	-18.5	-0.019
9	-17.4	-0.017
10	-17.5	-0.018
11	-18.7	-0.019
12	-18.6	-0.019
	Average	
	-18.09	-0.018
	STD	
	0.650	0.001

C. 4. Zeta Potentials of Spores

No	ZP (mV)	ZP (V)
1	-12.5	-0.013
2	-12.6	-0.013
3	-13	-0.013
4	-12.4	-0.012
5	-14.9	-0.015
6	-13.5	-0.014
7	-14.5	-0.015
8	-13.7	-0.014
9	-13.3	-0.013
10	-13.4	-0.013
11	-11.8	-0.012
12	-13.6	-0.014
	Average	
	-13.27	-0.013
	STD	
	0.882	0.001

C. 5. Equivalent radius of *P. aeruginosa*

No	Size (d.nm)		radius (um)		
1	1786	**Average**	0.89	**Average**	
2	1441	**1488.50**	0.72	**0.74**	um
3	1617	**STD**	0.81	**STD**	
4	1284	**185.63**	0.64	**0.09**	
5	1465		0.73		
6	1338		0.67		

C. 6. Equivalent radius of *B. subtilis*

No	Size (d.nm)	Average	radius (um)	Average	
2	5113	**4133.63**	2.56	**2.07**	um
3	4414	**STD**	2.21	**STD**	
4	6298	**1136.49**	3.15	**0.57**	
5	3101		1.55		
6	3800		1.90		
8	3112		1.56		
9	3086		1.54		
10	4145		2.07		

C. 7. Equivalent radius of Spores

No	Size (d.nm)		radius (um)		
1	2232	**Average**	1.12	**Average**	
2	2634	**2429.50**	1.32	**1.21**	um
3	2747	**STD**	1.37	**STD**	
4	2265	**212.10**	1.13	**0.11**	
5	2391		1.20		
6	2308		1.15		

APPENDIX D EPS CHARACTERIZATION

D. 1. Growth and EPS Production of *P. aeruginosa*

	OD		Lowry	
time (h)	average	stdev	time	Protein
0.00	0.00	0.01	0.00	0.89
1.00	0.01	0.00	1.00	0.83
2.00	0.01	0.00	2.00	0.72
3.00	0.04	0.01	3.00	0.89
4.00	0.03	0.01	4.00	0.91
5.00	0.05	0.01	5.00	0.73
6.00	0.06	0.00	6.00	0.80
7.00	0.12	0.01	7.00	0.78
8.00	0.16	0.01	8.00	0.84
9.00	0.22	0.02	9.00	0.77
10.00	0.41	0.01	10.00	0.86
11.00	0.60	0.00	11.00	0.81
12.00	0.68	0.02	12.00	0.80
13.00	0.75	0.05	13.00	0.76
14.00	0.90	0.02	14.00	0.75
15.00	0.95	0.01	15.00	1.19
16.00	1.07	0.01	16.00	0.88
17.00	1.16	0.01	17.00	0.81
18.00	1.22	0.01	18.00	0.85
19.00	1.25	0.01	19.00	0.82
20.00	1.33	0.02	20.00	1.00
21.00	1.41	0.04	21.00	0.88
22.00	1.52	0.03	22.00	0.84
23.00	1.45	0.03	23.00	0.98
24.00	1.41	0.01	24.00	0.79
25.00	1.36	0.01	25.00	0.73
26.00	1.21	0.02	26.00	0.71
27.00	0.91	0.03	27.00	0.65

	Anthrone			stdev		
time (h)	glucose	fructose	sucrose	glucose	fructose	sucrose
0.00	20.83	12.05	15.63			
3.00	40.74	23.56	30.56	0.43	0.25	0.32
5.00	57.27	33.12	42.95	2.42	1.40	1.81
6.00	63.42	36.68	47.57	0.58	0.33	0.43

8.00	68.27	39.48	51.20	2.06	1.19	1.55
11.00	72.33	41.83	54.25	3.97	2.30	2.98
13.00	71.37	41.27	53.53	2.76	1.60	2.07
16.00	72.49	41.92	54.37	5.11	2.96	3.83
20.00	69.18	40.01	51.89	3.23	1.87	2.42
22.00	65.56	37.91	49.17	6.76	3.91	5.07
23.00	63.02	36.45	47.27	5.48	3.17	4.11
25.00	65.49	37.87	49.11	0.62	0.36	0.47
26.00	65.13	37.66	48.84	0.18	0.10	0.13
27.00	65.64	37.96	49.23	0.19	0.11	0.14

D. 2. Growth and EPS Production of *B. subtilis*

	OD		Lowry	
time (h)	average	stdev	time	Protein
0.00	0.00	0.00	0.00	0.89
1.00	0.01	0.00	1.00	0.87
2.00	0.04	0.01	2.00	0.83
3.00	0.07	0.01	3.00	0.89
4.00	0.08	0.00	4.00	0.92
5.00	0.09	0.01	5.00	0.95
6.00	0.10	0.00	6.00	1.01
7.00	0.37	0.00	7.00	0.95
8.00	0.60	0.01	8.00	0.90
9.00	0.80	0.01	9.00	0.89
10.00	0.92	0.01	10.00	0.90
11.00	1.10	0.04	11.00	0.91
12.00	1.17	0.01	12.00	0.89
13.00	1.17	0.01	13.00	0.89
14.00	1.22	0.01	14.00	1.05
15.00	1.23	0.00	15.00	0.86
16.00	1.24	0.01	16.00	0.83
17.00	1.24	0.00	17.00	0.85
18.00	1.18	0.01	18.00	0.92
19.00	1.15	0.01	19.00	0.90
20.00	1.14	0.01	20.00	0.92
21.00	1.06	0.04	21.00	0.92
22.00	0.91	0.03	22.00	0.93
23.00	0.84	0.01	23.00	0.91

	Anthrone			stdev		
time	glucose	fructose	sucrose	glucose	fructose	sucrose
0.00	20.83	12.05	15.63			

3.00	47.62	27.54	35.71	3.76	2.17	2.82
6.00	54.65	31.60	40.98	0.49	0.28	0.36
8.00	53.38	30.87	40.03	6.72	3.89	5.04
10.00	65.35	37.80	49.02	1.11	0.64	0.83
12.00	68.72	39.74	51.54	2.98	1.72	2.23
14.00	68.14	39.41	51.10	3.81	2.20	2.85
16.00	68.25	39.47	51.19	1.44	0.84	1.08
18.00	66.42	38.41	49.81	7.69	4.45	5.77
20.00	65.12	37.66	48.84	1.43	0.83	1.07
22.00	54.53	31.53	40.90	3.41	1.97	2.56
23.00	52.99	30.65	39.74	1.71	0.99	1.28

D. 3. Carbohydrate and Protein

		B. subtilis				*P. aeruginosa*			
		Culture		Biofilm		Culture		Biofilm	
		Conc (mg/l)	Conc (mg/mg)	Conc (mg/l)	Conc (mg/mg)	Conc (mg/l)	Conc (mg/mg)	Conc (mg/l)	Conc (mg/mg)
1.00	Glucose	15.20	23.39	36.18	109.64	29.61	40.56	21.19	66.23
	Fructose	8.79	13.52	20.92	63.41	17.12	23.46	12.26	38.30
	Sucrose	11.40	17.54	27.14	82.23	22.21	30.42	15.90	49.67
	Protein	50.40	77.53	58.10	176.05	46.08	63.12	17.02	53.20
2.00	Glucose	44.28	68.12	34.22	103.70	38.06	52.13	31.65	98.89
	Fructose	25.61	39.39	19.79	59.97	22.01	30.15	18.30	57.19
	Sucrose	33.21	51.09	25.67	77.78	28.54	39.10	23.73	74.17
	Protein	46.44	71.45	20.01	60.65	33.18	45.45	17.59	54.96
3.00	Glucose	17.51	26.94	27.38	82.98	37.41	51.25	24.67	77.08
	Fructose	10.13	15.58	15.84	47.99	21.63	29.64	14.27	44.58
	Sucrose	13.14	20.21	20.54	62.23	28.06	38.43	18.50	57.81
	Protein	48.45	74.54	20.59	62.38	32.71	44.80	16.76	52.37
ave	Glucose	25.66	39.48	32.59	98.77	35.03	47.98	25.84	80.74
	Fructose	14.84	22.83	18.85	57.12	20.26	27.75	14.94	46.69
	Sucrose	19.25	29.61	24.45	74.08	26.27	35.99	19.38	60.55
	Protein	48.43	74.51	32.90	99.69	37.32	51.12	17.12	53.51
stdev	Glucose		24.86		14.00		6.44		16.63
	Fructose		14.38		8.10		3.72		9.62
	Sucrose		18.65		10.50		4.83		12.48
	Protein		3.04		1.22		10.40		1.32